DESIGN ISSUES IN THE NEXT GENERATION WAVELENGTH DIVISION MULTIPLEXED OPTICAL NETWORK

SURENDRAKUMAR RICHARD PRAMOD

A thesis submitted to
The Faculty of Graduate and Postdoctoral studies
in conformity with the requirements for the degree of
Doctor of Philosophy (PhD)
degree in Electrical Engineering

Ottawa-Carleton Institute for Electrical and Computer Engineering
School of Information Technology and Engineering
University of Ottawa
Ottawa, Ontario, Canada

© Surendrakumar Richard Pramod, Ottawa, Canada, 2007

Library and Archives Canada

Published Heritage Branch

395 Wellington Street
Ottawa ON K1A 0N4
Canada

Bibliothèque et Archives Canada

Direction du Patrimoine de l'édition

395, rue Wellington
Ottawa ON K1A 0N4
Canada

Your file Votre référence
ISBN: 978-0-494-49399-1
Our file Notre référence
ISBN: 978-0-494-49399-1

NOTICE:
The author has granted a non-exclusive license allowing Library and Archives Canada to reproduce, publish, archive, preserve, conserve, communicate to the public by telecommunication or on the Internet, loan, distribute and sell theses worldwide, for commercial or non-commercial purposes, in microform, paper, electronic and/or any other formats.

The author retains copyright ownership and moral rights in this thesis. Neither the thesis nor substantial extracts from it may be printed or otherwise reproduced without the author's permission.

AVIS:
L'auteur a accordé une licence non exclusive permettant à la Bibliothèque et Archives Canada de reproduire, publier, archiver, sauvegarder, conserver, transmettre au public par télécommunication ou par l'Internet, prêter, distribuer et vendre des thèses partout dans le monde, à des fins commerciales ou autres, sur support microforme, papier, électronique et/ou autres formats.

L'auteur conserve la propriété du droit d'auteur et des droits moraux qui protège cette thèse. Ni la thèse ni des extraits substantiels de celle-ci ne doivent être imprimés ou autrement reproduits sans son autorisation.

In compliance with the Canadian Privacy Act some supporting forms may have been removed from this thesis.

While these forms may be included in the document page count, their removal does not represent any loss of content from the thesis.

Conformément à la loi canadienne sur la protection de la vie privée, quelques formulaires secondaires ont été enlevés de cette thèse.

Bien que ces formulaires aient inclus dans la pagination, il n'y aura aucun contenu manquant.

Canada

uOttawa

L'Université canadienne
Canada's university

FACULTÉ DES ÉTUDES SUPÉRIEURES ET POSTOCTORALES

uOttawa

L'Université canadienne
Canada's university

FACULTY OF GRADUATE AND POSDOCTORAL STUDIES

Richard Surendrakumar

AUTEUR DE LA THÈSE / AUTHOR OF THESIS

Ph.D. (Electrical Engineering)

GRADE / DEGREE

School of Information Technology and Engineering

FACULTÉ, ÉCOLE, DÉPARTEMENT / FACULTY, SCHOOL, DEPARTMENT

Design Issues in the Next Generation Wavelength Division Multiplexed Optical Network

TITRE DE LA THÈSE / TITLE OF THESIS

Hussein Mouftah

DIRECTEUR (DIRECTRICE) DE LA THÈSE / THESIS SUPERVISOR

Hanan Anis

CO-DIRECTEUR (CO-DIRECTRICE) DE LA THÈSE / THESIS CO-SUPERVISOR

EXAMINATEURS (EXAMINATRICES) DE LA THÈSE / THESIS EXAMINERS

Trevor Hall

Vinod Vokkarane

Ashraf Matrawy

Tet Yeap

Gary W. Slater

Le Doyen de la Faculté des études supérieures et postdoctorales / Dean of the Faculty of Graduate and Postdoctoral Studies

Abstract

Resource fragmentation is one of the major problems affecting bandwidth provisioning in WDM networks. This causes longer lightpaths experience a higher blocking probability compared to shorter lightpaths. In this thesis we present a novel mechanism to mitigate this problem. We develop a Traffic Classification and Load Balancing (TCLB) algorithm that uses a cost function that incorporates waveband information in conjunction with criticality levels on a link to spread out the traffic homogenously throughout the network and mitigate the fairness problem. In addition, we show that using the TCLB algorithm with proper choice of criticality levels a lower net blocking probability can be achieved as compared to algorithms using only traffic classification.

We develop intelligent dynamic routing algorithms to route the signals considering the signal quality constraint (measured in terms of the Bit Error Rate (BER)) which is used as a measure of signal quality when routing a particular connection. By studying the network performance and signal quality we develop intelligent impairment aware algorithms to use the regenerators in an efficient manner and hence reduce the number of calls being blocked due to high BER, effectively reducing the net calls that are blocked due to poor signal quality. We also present dimensioning of the optical Cross-connect and develop policies to share the available resources (transceivers) and reduce cost at the node. To achieve optimal usage of transponders at nodes, we present three novel switching mechanisms to achieve steerability at Optical Cross-connect sites. By achieving steerability, the traffic that needs to be added/dropped at a node can be routed to any of the available transponders, thus improving the utilization of deployed transponders. We present nodal architectures that maximize system performance and deployment flexibility, while minimizing cost of sub-systems and components (like Wavelength Selective Switches, amplifiers etc.) which make up these nodes. In addition, the port dimensioning of such steerable architectures are analyzed and optimal port allocation based on the cost and loss compensation are calculated. Also the concept of Optical Reach for an optical network is explored and strategies to achieve the same are presented. We evaluate the network cost as a function of the WDM systems reach and

traffic volume (wavelength fill level). The impact of various technologies on the optimal reach is discussed and novel network architectures are presented. Finally the impact of these strategies on the normalized cost of the system is studied as a function of traffic volume.

Acknowledgement

I would like to express my deepest gratitude to my thesis supervisors Dr. Hussein T Mouftah and Dr. Hanan Anis for their valuable guidance and support, both scientifically and financially. Throughout the thesis their comments have guided me to come up with this piece of work.

I would like to thank the members of the Optical Networks Research Laboratory for the many long hours of constructive discussions and comments.

I would also like to thank my mother Philomina for her sacrifices and making me who I am.

Last but not the least, I would like to thank my love, Hanieh, for her endless support, patience and encouragement without which this work would never have seen its end.

Table of Contents

List of Abbreviations

ASE	Amplified Spontaneous Emission
BER	Bit Error Rate
CTMC	Continuous Time Markov Chains
CAC	Connection Admission Control
DWDM	Dense Wavelength Division Multiplexing
EDFA	Erbium Doped Fiber Amplifier
HDTV	High Definition TV
IPTV	Internet Protocol TV
IGP	Interior Gateway Protocol
ILP	Integer Linear Programming
FWM	Four-wave Mixing
MMOG	Massively Multiplayer Online Gaming
MEMS	Micro Electro Mechanical Switching
MZ	Mach-Zender
NRZ	Non-Return to Zero
OXC	Optical cross-connect
OSNR	Optical Signal to Noise Ratio
OADM	Optical Add-drop Multiplexer
O-VPN	Optical Virtual Private Network
OSPF-TE	Open Shortest Path First- Traffic Engineering
RWA	Routing and Wavelength Assignment
ROI	Return On Investment
PMD	Polarization Mode Dispersion
STR	Selective Trunk Reservation
SRS	Stochastic Recursive Sequence
SBS	Stimulated Brillouin Scattering
SRS	Stimulated Raman Scattering
TCLB	Traffic Classification and Load Balancing

TDC	Tunable Dispersion Compensation
TR	Transmitter-Receiver
VOD	Video-on-Demand
VOIP	Voice-over-IP
WCC	Wavelength Continuity Constraint
WDM	Wavelength Division Multiplexing
WSS	Wavelength Selective Switch
QoS	Quality of Service

List of Symbols

A	First Moment of Traffic Intensity
a	Offered Traffic intensity
Bw_o	Optical bandwidth
Bw_e	Electrical Bandwidth
B_c	Blocking probability for the c hop-count traffic
CP_i	Criticality parameter for the i^{th} waveband
$Cost_{Amp}$	Amplifier Cost
$Cost_{cir}$	Circuit Board Cost
$Cost_{Tm}$	Transponder Module Cost,
$Cost_{sh}$	Shelf Cost
$Cost_{OADM}$	OADM Cost
$Cost\_wb_i^j$	Cost of the i^{th} waveband on link j
D_t	Total Transmission Distance
D_p	Dispersion Parameter of a Fiber
D	The number of ports at a switching node
E	Total number of edges in the network under consideration
Fr	Normalized Frequency
G	Gain of the Optical Amplifier
G_n	Gain of the n^{th} amplifier in an n amplifier cascade
G_0	Small signal gain of an Optical Amplifier
G_{SCA}	Single Channel Amp Gain
h	Plancks constant
IL_{Sw}	1x4 Switch Insertion loss
IL_{TF}	Tunable Filter Insertion loss
IL_{TDC}	TDC Insertion loss
IL_{WSS}	Insertion Loss of WSS
K, K^*	Transition kernels for the corresponding embedded discrete time Markov chains as, X and Y respectively

L	Length of the Fiber
L_s	Span length
L_C	Connector Loss
L_{S4}	1:4 Splitter loss
L_{S16}	1:16 Splitter loss
M	Number of wavelengths on a Fiber
m	Mean
N_P	Number of multiplexers/demultiplexers at a switch
N	Numbers of ways an optical signal is split at a node
N_{ch}	Number of Channels
N_x	Number of drop outputs at switch X or number of outputs at the splitter X in a steerable Switch
N_y	Number of outputs at the splitter Y
N_{CP}	Number of cards per shelf
N_{TC}	Number of Transponders per card
Oc_p^l	Occupancy time of the p^{th} wavelength on the l^{th} link
P	Input Power into the Fiber
P_{ber}	Bit Error Rate
P_{3dB}	Output saturation power for an EDFA
P_{ase}	Spontaneous Noise of an Optical Amplifier
$P_{ASE,n}^{TOT}$	Total ASE noise power and signal power at the output of the n^{th} amplifier for an n amplifier cascade
$P_{sig,0}$	Transmitted signal power of an Optical Signal
P_{Tx}	Power level at Transmitter
P_{Rx}	Power level at Receiver
P_b	Probability that a wavelength will be available on a link
p_B^{cadd}	Blocking probabilities for the add-drop traffic under complete trunk reservation scheme

p_B^{creg}	Blocking probabilities for the regeneration traffic under complete trunk reservation scheme
p_B^{padd}	Blocking probabilities for the add-drop traffic under partial trunk reservation scheme
p_B^{preg}	Blocking Probability for regeneration traffic under partial trunk reservation scheme
p_B^{wadd}	Blocking Probability of add-drop traffic with reservation
p_B^{wreg}	Blocking Probability for regeneration traffic with reservation
p_B^{w}	Overall Blocking Probability without reservation
p_B^{c}	Overall blocking probability under the complete trunk reservation scheme
p_B^{p}	Overall blocking probability under the partial trunk reservation scheme
P_{Tx}	Power level at Transmitter
P_{Rx}	Power level at Receiver
$Q_t^{padd}, Q_t^{cadd}, Q_t^{wadd},$	Number of servers available after t transitions and the superscript indicates the regime and the category of servers
R	Set of the numbers of regenerators placed in the network
Rx_P	Power level at receiver
S	Set of regenerator selection strategies
T	Number of Transponders
V	Second moment of traffic intensity
V_n	Number of nodes in the network
W	Set of regenerator placement scheme
W_D	Number of wavelengths that are dropped at a node from each port
X	Indicator for an ergodic continuous time Markov chain with stationary (steady state) distribution π.
X_p	Number of receiver the signal from each output port of the splitter would reach

X_t^i	Number of occupied wavelengths in waveband i reserved for the j^{th} hop-count traffic where $j \geq i$ at time t
Y_t	Number of unavailable wavelengths at time t, for the link without the reservation scheme
y_i	Number of wavelengths in waveband i
Z	Peakedness
α	Attenuation Coefficient of Fiber
δ	Fraction of wavelengths dropped at each node per fiber at an add-drop node.
λ	Call arrival rate
β_2	Second order Group velocity dispersion
v	Variance
ψ	Set of different level of traffic loads
σ_0, σ_1	Standard deviations of the 0 and 1 levels of a detected bit received optical signal at a receiver
μ_i^a	The mean arrival rate for the i hop-count traffic
μ	Call departure rate
ρ	Average Link Utilization

List of Figures

List of Tables

Chapter 1. Introduction

1.1 Background

The Internet traffic in the past recent years has increased exponentially. Forecasts also indicate that this trend will continue for the years to come. Also with the increasing use of higher bandwidth services on the Internet a higher dynamics of traffic pattern changes have been observed. Quantum leaps in the way data is sent through optical fibers through optical networking technology have made the use of high bandwidth services on the Internet a tangible reality. As far as bandwidth is concerned optical fiber has no competition. Though in the recent years the cuts in capital expenditure have slowed down the progress in this field, new power-hungry applications and fundamental trends in telecommunications will bring optical networks and its technologies back into the spotlight. Bandwidth hungry applications like Video-on-Demand (VOD), Massively Multiplayer Online Gaming (MMOG), High Definition TV (HDTV), Internet Protocol TV (IPTV), Voice-over-IP (VOIP), have made it to the mainstream and are here to stay. Applications such as these are expected to generate in excess of 100 Mbps of bandwidth from/to each household in the coming decade, a 1000-fold increase from the days when voice accounted for the only bandwidth requirement. Additionally, personal and mobile communications will be an extension of the IP network, adding even more to the overall network load. In short, the emergence of these new applications requires a fundamentally new approach to networking. However, because optical infrastructure decisions are long-term and because many uncertainties still exist regarding future service mixes, traffic patterns, and bandwidth needs, many operators understandably are hesitant to commit to network changes. But in this fast-moving environment, a reactive wait-and-see approach simply will not work--and neither will the old standby method of simply adding more bandwidth as and when needed.

Over the last few years Dense Wavelength Division Multiplexing (DWDM) has emerged as one of the major transport technologies for the Internet infrastructure to support such bandwidth hungry applications. In a DWDM network, an Optical cross-connect (OXCs) inter-connects two fibers and switches data between them. In the next-generation optical

network the OXC will be switching terabits of data between optical fibers. At an OXC, wavelengths can be added or dropped through the add/drop part of the OXC. In a DWDM network data is carried over a lightpath. A lightpath is a set of contiguous links that provide an end-to-end connection using a same (or different) wavelength(s). Wavelength conversion technology in optical domain is still in its infancy and is not commercially available yet. Currently, wavelength conversion is done electronically which is not very efficient in terms of processing speed and cost. Therefore, wavelength conversion is generally avoided in optical networks or is used in a very limited way. Hence, in optical networks with no wavelength conversion; a lightpath is established using a single wavelength to meet the Wavelength Continuity Constraint (WCC). At the moment WDM networks are used for transporting high number of low bit-rate streams from one point to the other. The dynamic operation of a WDM network still suffers from technological challenges in the areas of the control plane and network management. Also the WDM networks were built on the assumption of predictable traffic where different locations were interconnected by predictable traffic streams. Therefore today's WDM networks usually provide "permanent" channels which are only manually reconfigurable or sometimes even completely static. However, it is seen from today's applications that predictability is a thing of the past and there is a need to build highly agile / reconfigurable networks. The network provider, in doing so should be able to utilize the available resources in an efficient manner to allow converged networks capable of scaling and adapting to user demands.

1.2 Motivation and Objectives

The dynamically reconfigurable mesh networking model is believed to be the answer to the demand for high bandwidth and emergence of differentiated-optical network services [GOL-00]. In such a network the control plane is responsible for dynamic assignment of resources (optical and electronic) to the different connections. This control plane would enable dynamic wavelength routing through multiple cross-connects with end-to-end signaling. Such agility in optical networks has started to arrive in practical deployments and we are now seeing them on the edge networks. In order to support such agility and reconfigurability a lot of research has been carried out in the area of dynamic

provisioning of lightpaths for traffic streams [BIR-96][BAR-96][KOV-96][SUB-00][ZHO-00]. The performance of such provisioning algorithms is generally measured in terms of the blocking probability i.e. the number of connections that cannot be set up due to the unavailability of resources such as wavelength, bandwidth etc. However, this does not fully capture all the effects and aspects of the network behavior (Fairness, load balancing etc), especially the ***Fairness.*** The fairness problem is caused because the longer (higher hop-count) lightpaths experience a higher blocking probability. This is because of the fact that, the longer the lightpath is, the less likely it is to find a path with available wavelength meeting the Wavelength Continuity Constraint. Though the fairness issue has been addressed in previous works [BIR-96] [OU-04] and mechanisms to mitigate the fairness problem have been proposed (namely wavelength reservation), it is seen that this results in a reduction of global efficiency. Hence there is a need to address this issue of Fairness and mitigate the unfairness in the network.

- The objective of this thesis is to first, quantify the unfairness experienced by the longer hop-count light paths. This can then be used as a measure to study the impact of strategies used to reduce the Unfairness in WDM routed networks. Also, this thesis aims at finding strategies and algorithms to reduce the unfairness and also to have a lower impact on the net blocking probability. We will develop a mathematical model of a link to prove that the wavelength reservation indeed does improve the fairness across connections of various hop-counts.

Another important aspect which can bring the next generation optical network into a reality is the highly-tolerant, ultra-long haul transmission systems which allow for transparent transmission through multiple cross-connects. In these ultra-long haul systems, light travels through multiple cross-connects and different types of fiber with different characteristics. These result in varying span losses, dispersion losses and crosstalk. Also the system is affected by fiber non-linearities which impose a restriction on how far the signal can be transmitted without using regeneration to compensate for the losses mentioned above. Thus, when provisioning lightpaths and bandwidth in such optical networks it is very important to consider the effects of the impairments in the networks.

- There is a need to study the effects of the transmission impairments on the transmission distance and routing of a lightpath. The objective is to develop intelligent impairment aware routing algorithms which will intelligently route the lightpaths in the next generation optical network, improving bandwidth efficiency while maintaining an acceptable transmission distance without regeneration. The aim is to develop algorithms that would use the available regeneration resources intelligently while provisioning a lightpath.

Optical techniques for such functionalities are not currently available or are too expensive to be implemented in the optical domain. So such functions are implemented in the electronic domain. The interfaces between the optical and electrical sections are provided with a limited number of transponders which are dynamically tunable to the required wavelength. These transponders being opto-electronic devices are very expensive and should be provisioned and used in such a way that maximizes the utilization of those devices.

- It is a part of our objective to investigate novel mechanisms for the architecture of the adjunct switch (used to switch added wavelengths from a transponder to the OXC and the dropped wavelengths to any available transponder) which will allow maximal sharing of the transceivers at an OXC and hence reduce the cost of the node. Also, we will evaluate the architectures based on the net cost, steerability, scalability and dependencies of the cost on the various elements in the sub-system.

1.3 Thesis Contributions

In order to address the above mentioned objectives, we have first investigated the problem of fairness and efficient resource utilization while provisioning a light-path. Particular emphasis has been placed on developing novel mechanisms to mitigate the fairness problem and also increase the efficiency (in terms of net blocking probability) on a global scale.

- We have presented strategies to reduce the unfairness and also improve the blocking probability of the network as a whole. We have quantified the unfairness by defining an unfairness factor which is used as a measure to study

the impact of the algorithms and strategies developed to mitigate the fairness problem. We have also presented link cost model for which we have implemented a cost function which will take into consideration the criticality levels when assigning a cost to a link. By allocating wavebands and assigning criticality levels to those wavebands we reduce the unfairness for higher hop count light paths. We also introduce a novel Traffic Classification and Load Balancing (TCLB) Algorithm that uses the above cost function to find the best path for a given connection. By assigning criticality levels to links, heavily used paths are avoided as much as possible. In this way the traffic can be spread evenly throughout the network. Also, two different wavelength assignment mechanisms, First Fit from the Top and First Fit from the Bottom, are explored to investigate the impact of these algorithms on the fairness and the net blocking probabilities. Our algorithms in conjunction with the cost function achieve an improvement in fairness and also an improvement in net blocking probability as compared to simple traffic classification mechanisms which only achieve an improvement in fairness.

In order to mitigate the impact of physical constraints on the routing of signals

- We have presented the impairment aware algorithms used to effectively reduce the impact of transmission impairments on the routing of an optical signal. Two novel impairment aware algorithms viz. On-Route Shortest Path regenerator selection and Off-Route Shortest Path regenerator algorithm are presented. The dynamic routing algorithms presented in this research route the signals by taking into account the degradations on the signal quality and hence guarantee an acceptable value of Bit Error Rate (BER). By studying the performance of the network and signal quality we have developed intelligent algorithms to use the regenerators in an efficient manner and hence reduce the number of calls being blocked due to high BER, effectively reducing the net blocking probability. Using available resources (regenerator cards in this case) allows for dynamic provisioning of lightpaths to meet the bandwidth requirements of the current day telecom applications. We have also presented mechanisms to achieve maximal utilization of available add/drop and regenerator cards to

affect a lower cost foot-print at a node. The impact of sharing mechanism to reduce the number of transceivers at an OXC hence reducing the cost is also discussed. A mathematical model for the sharing mechanism is also provided.

In order to achieve maximal utilization of available transponders at an OXC, we present novel switching mechanisms to achieve steerability at Optical Cross-connect. In this thesis we have investigated the concept of optimal optical reach and have provided mechanisms and strategies to achieve the same

- We have introduced 3 novel architectures for a steering switch. By achieving steerability we route the traffic that needs to be added/dropped at a node to any of the available transponders. We have developed these architectures taking into account cost and performance. We have also analyzed the cost of these sub-systems taking into account different price points of the components like wavelength switches, amplifiers etc. which make up these sub-systems. A comparative analysis of the cost of these architectures with varying fills is also provided. We have also analyzed the port dimensioning of such steerable architectures and calculated the best possible port allocation based on the cost and loss compensation.
- This research has also focussed on the means to achieve the best possible optical reach in Wavelength Division Multiplexed (WDM) transmission systems. We have evaluated the network cost as a function of the WDM systems reach and traffic volume (fill level). The impact of various technologies on the optical reach is discussed and novel network design architectures are also presented. This thesis has introduced different strategies like amplifier pump upgrades and spectral upgrades and transponder packing to achieve optimal optical reach scenarios. These modular design strategies offer a scalable pay-as-you-grow system to affect a lower startup footprint for the network provider. Also, the impact of these strategies on the normalized cost of the system has been studied as a function of traffic volume.

Until recently, the concept of optical reach has been treated as a distance that depends solely on the network topology and the impact of increasing the reach on the cost of the optical network has never been investigated.

- We have showed that the optical reach for a particular network varies depending on the total cost of ownership and can vary significantly depending on the technology used. The importance of this study is that it mimics practical deployments and examines the first-installed cost, along with the scalability in terms of wavelengths for different reach systems for various solutions to achieve optical reach. This approach allows fair comparison of the most suitable configurations for different architectures in real network situations.

1.4 Thesis Outline

The rest of the thesis is organized as follows. In the next chapter, a brief description of the various Routing and Wavelength Assignment (RWA) Algorithms is provided. Also this chapter briefly describes the various physical impairments that affect the optical signal as it traverses from the source to the destination. An overview of various research used to mitigate these impairments in an optical network are also discussed. Chapter 2 also presents models used in dimensioning of overflow systems. These models are used in dimensioning of sharable switch architecture. In Chapter 3 we investigate the fairness problem in detail and quantify the fairness by defining an unfairness factor. We also present strategies and algorithms (TCLB algorithms) to mitigate the impact of fairness, improve the net blocking probability and also distribute traffic homogenously throughout the network. Chapter 4 presents the impact of physical impairments on routing of an optical signal and ways to reduce this impact by using signal quality as a constraint while provisioning a light path. Also, in this chapter we present impairment aware algorithms that intelligently route the signal by using paths that have regenerators available to guarantee acceptable signal quality. In Chapter 5 we present 3 novel architectures for an adjunct switch to achieve full steerability in order to efficiently use all the transponders present at an OXC. Also a comparative cost analysis of these architectures is provided. In Chapter 6 we explore the concept of optical reach and provide architectures and strategies to achieve optical reach. Also, in this chapter the impact of the reach on the normalized cost of an optical network system is reported as a function of traffic volume. In Chapter 7

we discuss the conclusions drawn from this thesis and propose some future research work.

List of Publications

Journal papers

1) **S.R. Pramod**, H. Anis and H. T. Mouftah, "Novel Mechanisms for Achieving Steerability at an Optical Switching Node: Architectures and Cost-Models" OSA Journal of Optical Networking, Vol. 5, Issue 12, pp. 901-914, Dec 2006.

2) **S.R. Pramod**, S. Siddiqui, G. Lamothe, H. T. Mouftah, "A Novel Mechanism for Fairness and Load Balancing in Optical Networks", submitted to IEEE Journal on Selected Areas in Communications (JSAC).

3) **S. Richard Pramod**, Hanan Anis, H.T Mouftah, "Optimal reach for Optical Networks-How do we get there ?", submitted to IEEE Journal of Lightwave Technology

Conference Papers

1) B. Zhou, **S. R. Pramod**, and H. T. Mouftah, "Adaptive BER-Assured Routing in Translucent Optical Networks", Proceedings of High Performance Switching and Routing, Phoenix, Arizona, pp. 209- 213, April 2004 .

2) **S.R. Pramod** and H.T. Mouftah "Traffic Classification and Fairness in Wavelength Routed Optical Networks", Proceedings of 2004 International Workshop on Optical Networks Control and Management (ONCM'04) in conjunction with ,International Conference on High Performance Computing, Montreal, Canada, pp. 422- 426, August 2004 .

3) **S.R. Pramod** and H.T Mouftah, "A sharable architecture for efficient utilization of Transmitter-Receiver ports on a Optical Switch", Proceedings of Seventh International Conference on Optoelectronics, Fiber Optics, and Photonics (Photonics 2004), Cochin, India, Dec 2004.

4) **S.R. Pramod** and H.T. Mouftah, "Efficient Utilisation of Transceivers in Optical Crossconnects", Proceedings of IEEE International Conference on Communications (ICC 2005) Seol, Korea, pp. 1843 – 1847, May 2005.

5) **S.R.Pramod**, S. Siddiqui, H. T. Mouftah, "Novel Distributed Protocol for Dynamic Routing and Load Balancing for optical Networks", Proceedings of OFC/NFOEC 2005, Anahein California, March 2005.

6) **S. R. Pramod**, S. Siddiqui and H. T Mouftah, "A Novel Fairness Based Criticality Avoidance Routing Algorithm for Wavelength Routed Optical Networks", Proceedings of International Conference on High Speed Networks 2005, Montreal, Canada, pp. 281-285, August 2005.

7) **S.R Pramod**, B. Zhou and H.T. Mouftah,"Signal-quality Guaranteed Adaptive Routing in Translucent Networks" to appear in IEEE Communications Magazine.

Posters

"Dimensioning of Regenerators in Opaque Wavelength Routed WDM Networks" **S. Richard Pramod**, Bin Zhou, Hussein T Mouftah, CITO's Innovators Showcase Poster Presentation.

Chapter 2. State of the Art

2.1 Introduction

In recent years there has been an explosion in the amount of IP traffic with service and network providers moving away from voice centric networks to data centric networks. In this new millennium new real-time multimedia applications (streaming video, pay-per-view TV, bandwidth-on-demand applications) have emerged, which need a considerable amount of bandwidth. The only solution to satisfy these bandwidth hungry applications is the use of optical networks employing Dense Wavelength Division Multiplexing based wavelength routing. In the past 10 years we have witnessed a lot of growth in the studies [RAM-95] [BIR-96] [AGG-94] [RAM-97] [ELL-01] of deployment of cost-effective optical networks.

WDM partitions the available bandwidth into many orthogonal channels, where each channel is operated by an independent electronic device. Dense wavelength division multiplexing (DWDM) increases the capacity of embedded fiber by first assigning incoming optical signals to specific frequencies (wavelength, lambda) within a designated frequency band and then multiplexing the resulting signals out onto one fiber. Because incoming signals are never terminated in the optical layer, the interface can be bit-rate and format independent, allowing the service provider to integrate DWDM technology easily with existing equipment in the network while gaining access to the untapped capacity in the embedded fiber.

2.2 WDM Networks

The WDM network is characterized by the logical topology and the physical topology. The physical topology of a network consists of optical cross-connects (OXC's) connected by pairs of point-to-point fiber links in an arbitrary mesh topology as shown in Figure 2.1. The *logical topology* describes the lightpaths between the nodes and is determined by the configuration of the transmitters, receivers, and switches on each node. The physical topology of a network generally remains unchanged. However, the logical topology changes depending on the availability of wavelength transceivers etc. Each node shown in Figure 2.1 has a limited number of transmitters and receivers. Each of the links has a

limited number of wavelengths. Data is transferred from one point to another on a light path. A lightpath is a unique unicast session between a source and a destination carrying data [CHL-92]. More generally, it is a series of contiguous wavelengths (channels) between the source and the destination nodes. These wavelengths can be the same wavelength or different available wavelengths on different links.

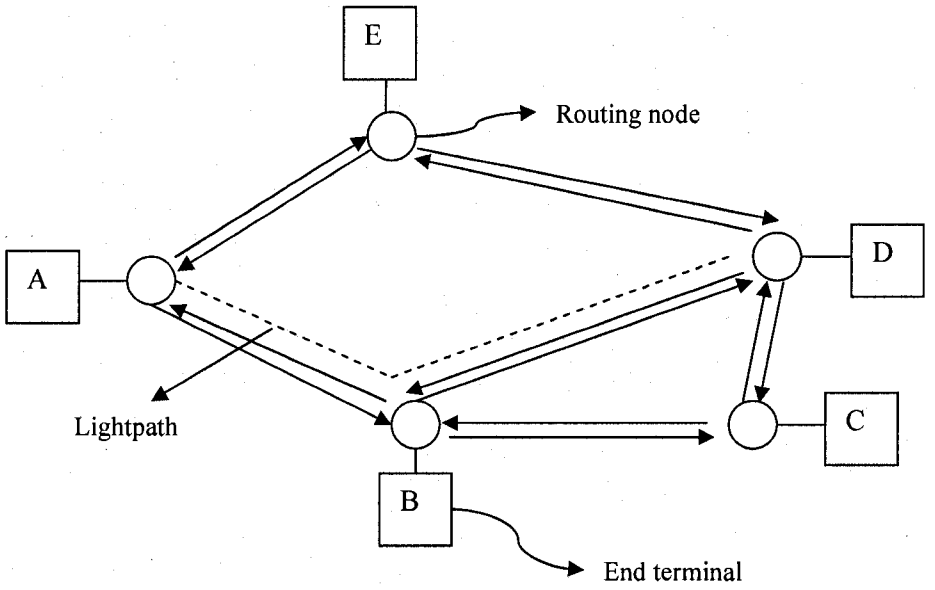

Figure 2.1 Physical Topology

2.3 Routing and Wavelength Assignment (RWA)

The mechanism of establishing a route from the source to the destination and assigning a wavelength to the lightpath for data communication is collectively called Routing and Wavelength Assignment (RWA) [RAM-95]. The routing and wavelength-assignment problem (RWA problem) for all-optical network has received intensive interest in the literature [GUR-01] [ZAN-00] [KAR-98] [FAN-03] [LU-05] [RAM-97] [ZAN-01][ZAN-99]. This involves selecting the best combination of the path from the source to the destination and the wavelength in that path such that the number of connections in the network is maximized.

Routing algorithms can be divided into two classes: static and adaptive. In static routing (fixed routing [GUR-01], fixed-alternative routing [GUR-01]) algorithms, one or several paths are pre-computed for each pair of source-destination nodes. Static routing can decrease the provisioning time, however, static approaches cannot respond to dynamic traffic changes in a network. Here the traffic between the source destination pairs is already known. In the case of using adaptive routing, the connection requests generally arrive into and depart from the network one-by-one in a random manner. Adaptive routing algorithms (such as, Shortest-Path [GUR-01], Shortest-Cost-Path [ZAN-00], Least-Congested-Path [ZAN-00]) usually use Dijkstra's algorithm to compute a minimal cost path from source to destination. The link cost function is critical for such algorithms. For the class of algorithms with static assumptions the objective is to minimize the number of wavelengths used in order to accommodate a given set of connections or to maximize the number of connections given a limited set of wavelengths. In the dynamic case the aim is to minimize the blocking probability. It is very important that these algorithms be simple and fast so that dynamically arriving connections can be setup without and delay. Two routing mechanisms can be used in an all-optical network: centralized and distributed. In a centralized architecture, a network control node monitors the network state and controls all resource allocations. Upon receiving a connection request, an edge node sends a message to the network control node. The controlling node executes the routing algorithm and the wavelength assignment algorithm. Upon deciding a path and free wavelength, the controlling node will reserve resources on all nodes along the path. This architecture poses problems such as performance bottlenecks, single point of failure and limited scalability. In distributed control architecture, information about network state is broadcast periodically using some link state protocol, and each edge node can compute the path upon receipt of a connection request. Various link-state update methods have been proposed for wavelength-routed networks to control the rate at which the link-state update messages are distributed [SHE-06][AL-F-04][SEN-02]. Distributed control is more scalable and robust. Upon receiving a connection request, an edge node first executes a routing algorithm to compute a path. It then starts a path and wavelength reservation protocol. The wavelength assignment algorithm can be executed by either the destination or source node to pick a free wavelength.

There are also several wavelength assignment algorithms in the literature. In the random algorithm, one free wavelength is randomly selected from among the unused wavelengths available on the source-destination path. A majority of the analysis presented in the literature assumed a random wavelength assignment scheme [KOV-95] [BIR-95][BIR-96][BAR-95][SUB-96][WAU-96][SUB-97] and fixed routing. Connections are established along a predefined route. The wavelength is then chosen randomly from the list of available wavelengths. Though many other wavelength assignment schemes provide better performance the assumption of a random wavelength assignment provides for a simpler means of performance analysis. In the first-fit algorithm, the free wavelength with the smallest index is selected. In the most-used algorithm [CHL-89], the free wavelength which is used most often in the network is selected. If several wavelengths share the same usage then the wavelength with the lowest index is chosen. In the Least-Used algorithm, the free wavelength which is used least in the network is selected. The Min-Product, Least-loaded, Max-Sum, Relative-Capacity-Loss algorithms have been proposed for multi-fiber networks. In the Min-Product Wavelength Assignment scheme [JEO-00] the algorithm calculates the number of fibers used for each wavelength. These values are multiplied together to determine the product of wavelength use per route. A connection is made available to the wavelength with the minimum product with ties broken, either by using the wavelength which is used on the most number of fibers in the network, or by allocating the lowest indexed wavelength. The Least-Loaded scheme is an alternative scheme for networks with multiple fibers on each link. This algorithm calculates for each wavelength the number of fibers on each link wherein the wavelength is available. The available capacity along the route is determined as the path with the minimum number of occupied wavelengths. A connection is assigned to the wavelength with the minimum capacity along the route. The Max-Sum wavelength assignment scheme attempts to minimize the network blocking by minimizing the effect of new connections. Using the Max-Sum algorithm, the effect of establishing a new connection is measured in terms of the number of routes whose capacities decrease by one.

A functional classification of wavelength assignment algorithms is provided in [CHO-00]. The performances of different wavelength assignment algorithms were compared in

[ZAN-00]. It was reported that when the network is lightly loaded, the Most-Used algorithm is the best and the Least-Used algorithm is the worst. When the network is heavily loaded, there are no major differences between the wavelength assignment algorithms in terms of link utilization. We notice that in the Most-Used algorithm, free wavelengths in the network are less segmented than with other algorithms. Hence connections with large hop count have a larger chance of being accepted. The performance of the RWA algorithms is generally measured in terms of the blocking probabilities. However this is not a very good measure of the performance. It is seen that most of the algorithms discussed in the literature try to decrease the blocking probability caused due to lack of available resources (wavelengths). These algorithms fail to take into consideration the efficient utilization of available wavelengths. Hence, it is seen that these RWA algorithms have a problem of fairness [BIR-95]. This is a problem caused in multi-hop networks with wavelength continuity constraints. It has been seen that the lightpaths with a higher number of hop-counts have a higher blocking probability. In [BAL-97] the authors showed that while the introduction of wavelength converters provides only marginal improvements in the average blocking in the ring topology, they can significantly improve the fairness. A detailed mathematical analysis is provided in the next chapter. In [WAN-03], a wavelength priority table is created in each node. Each time a connection is accepted using a free wavelength, the priority of this wavelength is increased resulting in connection requests from different nodes tending to use different wavelengths. Although the reservation conflict probability can be decreased, the blocking probability due to a lack of free wavelengths will increase, because it will be more difficult to find a free wavelength for a large hop-count connection. In order to mitigate the fairness problem a suggested solution is to divide the total number of wavelengths into bands [LI-03]. The bands are reserved for different classes of lightpaths. The association with any particular class would depend on the number of hops the lightpath has. In this way the higher hop-count lightpaths are guaranteed a minimum bandwidth to establish connections. This work, however, does not consider the impact of such a traffic classification on dynamic traffic demands. The RWA problem has been formulated as a multicommodity problem in [BAN-95]. As wavelength conversion is an expensive proposition, most of the research assumes that the same wavelength is used throughout

the whole lightpath (from source to destination). This is called the wavelength continuity constraint. The wavelength continuity constraint is also one of the causes of the fairness problem, as it forces a lightpath to find the same contiguous wavelength from the source to the destination. The wavelength conversion technology is still not mature enough to be cost-effective and economical to implement in optical networks. However, incorporating wavelength converters at the nodes reduce the blocking probability of the lightpaths as a higher number of wavelengths are available for the connection to be established. The impact of wavelength converters and their placement on RWA algorithms has been extensively studied in [CHU-02] [CHU-03] [KOV-96].

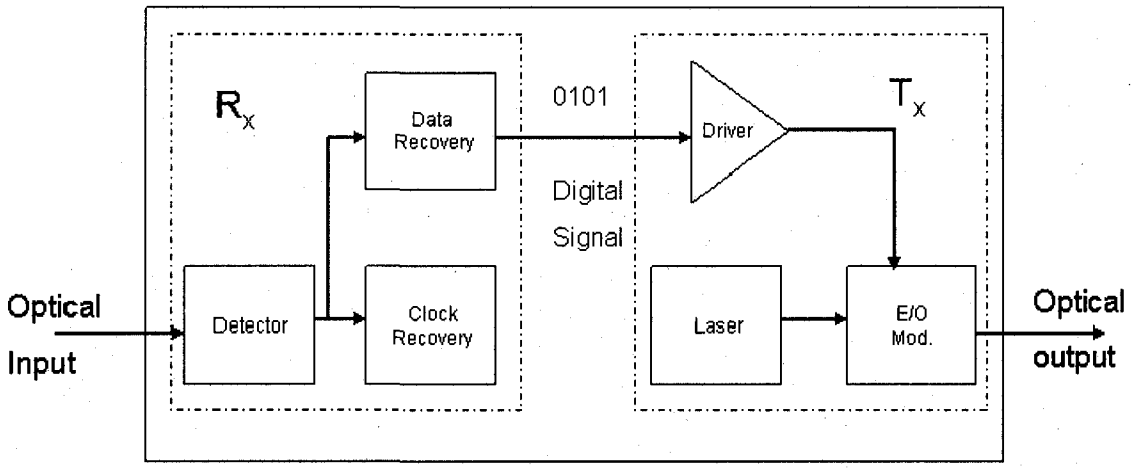

Figure 2.2 3-R Regenerator

2.4 Physical Impairments

In all the above studies, it is assumed that the underlying physical layer is perfect without any imperfections or any associated losses. Assuming an ideal physical layer leads to thinking that the optical signal that traverses a network has an infinite reach. This however, is not the case. There are impairments due to the physical characteristics of the underlying network infrastructure. These impairments reduce the signal quality which in turn leads to a failure in the proper detection of the transmitted signal. This leads to an increase in bit error rate (BER). A brief discussion of the various impairments in a fiber that affect the propagation of the signal and contribute to an increase in BER of the signal is provided in Appendix A.

The physical impairments in the underlying physical layer impose reachability constraints on an optical signal. The optical signal quality deteriorates because of these impairments and hence becomes very hard to detect at the receiver. Most of the provisioning mechanisms in literature do not consider the impact of physical layer impairments and constraints imposed by the physical layer. However, in order to effectively manage a large network, gaining access to the optical network inventory and the connectivity data at all nodes within the physical layer and the impact of these physical layer constraints on provisioning of lightpaths is very important. Currently many standards bodies are pursuing the establishment of a common control plane strategy to allow network operators to establish connections between any two types of elements and between different administrative domains. However, at the higher layers, an accurate picture of the equipment inventories and the established connections between the different layers is not available for the physical layer.

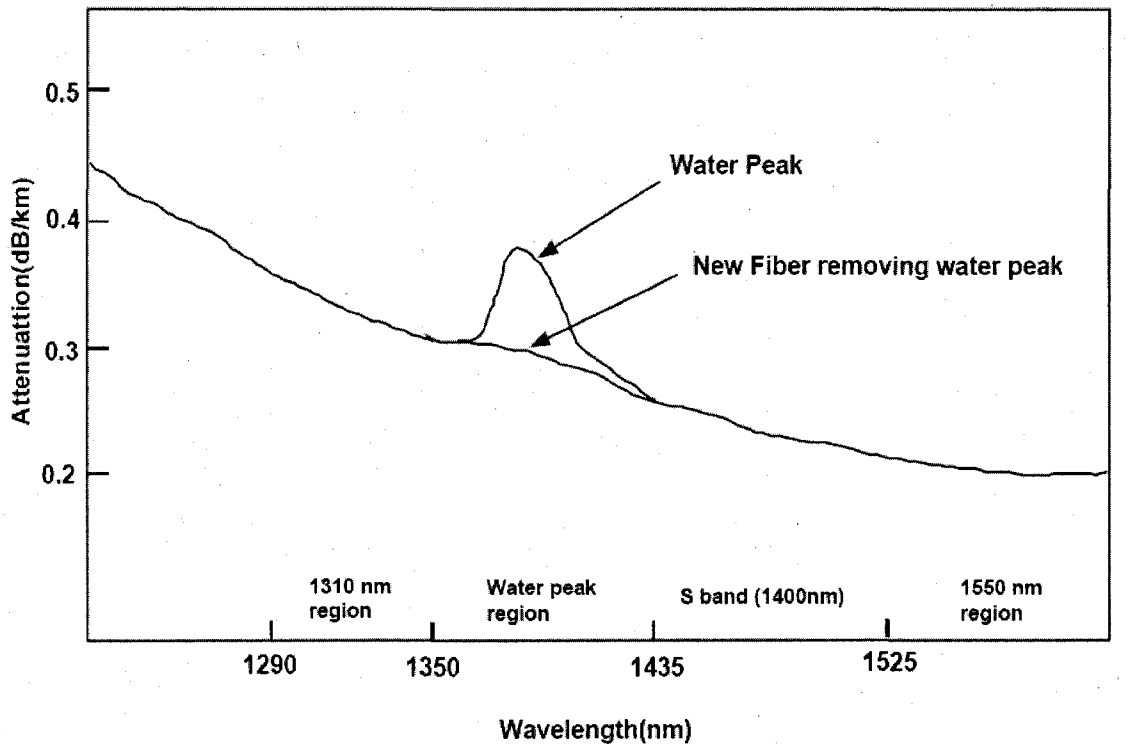

Figure 2.3 Optical Fiber Attenuation for Wavelength Bands

With most of the networks, the origin of the optical signals is unknown. In addition, the devices (like optical amplifiers, optical add/drop multiplexers) remain invisible to the

control plane, which makes it difficult for the network operator to locate faults and/or perform reliable traffic engineering or routing. The absence of the physical layer topology data results in the network operator operating in a sub-optimized world as he does not have a clear picture of the optical network resources which have been allocated to the network.

The knowledge of such a physical layer and the constraints imposed by it play a very important role as the network providers seek to expand the photonic core (OEO) boundaries by taking advantage of the long range optics. Some of the constraints are imposed by the optical fiber itself, the Optical Amplifiers, and insertion losses due to the different components and devices used.

Until recently, the WDM systems were limited to using the C-Band (1530 ~ 1560 *nm*) because of the gain of the EDFA and also because of the region of low attenuation. However, with the fiber manufacturers being able to manufacture new types of fiber which can eliminate the water peak the range of the available bandwidth is no longer limited by this water peak (Figure 2.3). The usable bandwidth is now the C and L band ,which encompasses (1530~1600 *n*m). However, with recent advances in manufacturing techniques, fibers like AllWave from Lucent and SMF-28 from Corning have managed to extend the range from 1250 to 1700nm, which results in higher capacity.

One of the first studies concerning the impact of transmission related issues on the routing strategies for transparent all-optical Dense Wavelength Division multiplexed (DWDM) transport networks has been reported in [RAM-99]. In [ALI-99][ROB-98], the authors incorporated the role of the physical layer in setting up lightpaths by employing appropriate models of multiwavelength optical devices (XCS's and EDFA's) such that the BER of a candidate lightpath can be computed, in advance, to determine if this lightpath should be used for the call. The impairments like crosstalk, Amplified Spontaneous Emission (ASE) noise and attenuation generated at every node co-propagate along with the signal thus degrading the Optical Signal to Noise Ratio (OSNR) and hence the BER. The BER is generally used to calculate the minimum optical power the receiver needs to operate reliably. Different manufacturers set different thresholds for the minimum BER. The operating thresholds generally vary from 10^{-9} to 10^{-12}. For instance SPRINT sets the threshold for a link to be 10^{-12} while ITU-T requires it to be 10^{-9}. In the

presence of these impairments it becomes imperative to regenerate the signal during its journey from the source node to the destination node. In order to mitigate the effects of transmission impairments the optical signal is regenerated at the intermediate nodes only if the signal falls below acceptable limits.

In order to mitigate the effects of these impairments, regenerators are placed at the nodes. These regenerators have three basic functions: regenerate, retime and reshape the optical signals. This is called 3-R regeneration. At a regeneration node as shown in Figure 2.2, the signal is dropped and reclocked, reshaped and regenerated to its appropriate levels locally. At a regenerator the optical signal is converted into an electrical signal and the signal is regenerated and converted back to an optical signal before it is sent into the network. Given the analog engineering constraints, and considering the current state-of-the-art in all-optical processing technology, the global or even national "all-optical" network is not attainable. In the absence of commercially available devices that perform signal regeneration to mitigate impairment accumulation and support wavelength conversion in the all-optical domain, some measure of opto-electronic conversion should be expected in practical optical-networking architectures. Because the use of opto-electronics is often associated with higher-cost solutions, the ensuing exercise in cost reduction involves establishing what constitutes the minimum required amount of opto-electronics necessary to ensure the presence of desired optical transport networking attributes enabled by their presence. Thus, in order to minimize the cost and reduce the effect of transmission impairments, the regenerators are placed strategically at a very few nodes in the network. In such a network the optical signal travels purely in the optical domain for a few hops, after which it is converted into the electronic domain and regenerated and converted into an optical signal and sent back into the network. This is called Opto-Electronic-Opto(O/E/O) conversion. Such networks are called translucent networks [RAM-01].

Studies [RAM-01] [ALI-99] [YAN-02] have been carried out which incorporate the effects of these transmission impairments on the routing algorithms. Though the effects of the routing impairments have been investigated, the effects of the number of transceivers at the regeneration node and the actual placement of regenerators have not been examined [DWI-00]. Also, the cost-benefit analysis of using fixed and tunable

transceivers at the regeneration node has not been investigated. These studies consider static traffic and do not examine the impact of physical impairments on dynamic traffic models. The studies are made under the consideration that the future traffic patterns are known. Also, the virtual topology designs are not considered for such translucent networks. The problem of virtual topology optimization is mathematically formulated by Integer Linear Programming (ILP) [RAM-96][BAN-96]. We can obtain an optimal solution by solving an ILP problem. However, this is very computationally intensive and it is possible that you may not find a solution for a very large network. Also, the BER consideration adds more complex nonlinear constraints, making the problem more difficult to solve. Therefore more work has been done using heuristics to find solutions to the problem [YOU-99].

An important characteristic of both single-hop and multi-hop WDM networks is the independence between the logical and physical topologies. Any logical topology may be implemented on a given connected physical topology if enough wavelengths are available. If each lightpath must be routed on a different wavelength, multiple wavelengths are required. Building networks with multiple wavelengths may not be feasible, since the number of wavelengths available is technology-limited. Furthermore, implementing one wavelength per connection may be an expensive and inefficient use of resources. Another important factor in the design in the optical networks is the number of transceivers and their tunabilities at the nodes. The number of transceivers also imposes a limitation on the number of lightpaths that can be established. The impact of the number of transceivers and their tunabilities has been studied in [SHE-00]. It has been shown that for given values of load with a limited number of transceivers and limited tunabilities, the performance achieved is equivalent to a network with a full number of transceivers and full transceiver tunability. This is an important result, as these transceivers, being opto-electronic devices, are very expensive and there is always an effort to minimize the number. This is one of the important constraints that can increase the routing cost.

2.5 Design Architecture of the Node

In all the research discussed above the layered OXC is an important device that is present at each node. The layered OXC is capable of switching the signals at the wavelength

level, waveband level or fiber level. Also such an OXC is capable of adding and dropping signals locally. It has opto-electronic transceivers to perform this function. It has also been shown that the regeneration function requires dropping the signal locally at the regeneration node, regenerating it and adding the signal back into the network. This process also makes use of the same add-drop ports at the OXC.

Traditionally, some ports are reserved for the add-drop function and some ports are reserved for the regeneration function as shown in Figure 2.4

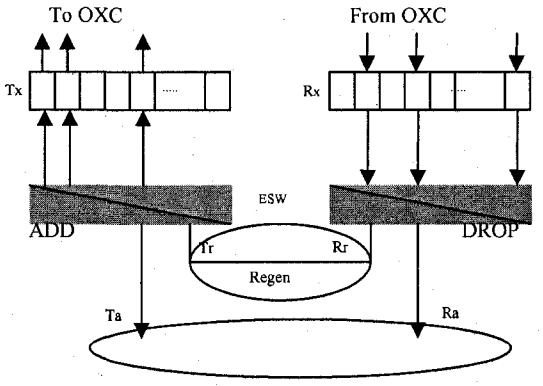

Figure 2.4 Add-drop Architecture of an OXC

The use of dedicated resources can sometimes result in underutilization of the available resources. Also, the lack of full tunability can also lead to underutilization of the transceivers (TR pairs).

2.5.1 Dimensioning of a Switch

An area which has been relatively unexplored in the context of provisioning sharable resources at an OXC is the classical overflow theory. Networks using fixed-alternate routing were modeled using this theory. However, this can also be applied to the dimensioning of switches especially in the area of sharing transponders at a switching node. An example is shown in Figure 2.5, where we consider a hierarchical network with traffic from A to B, and from A to C.

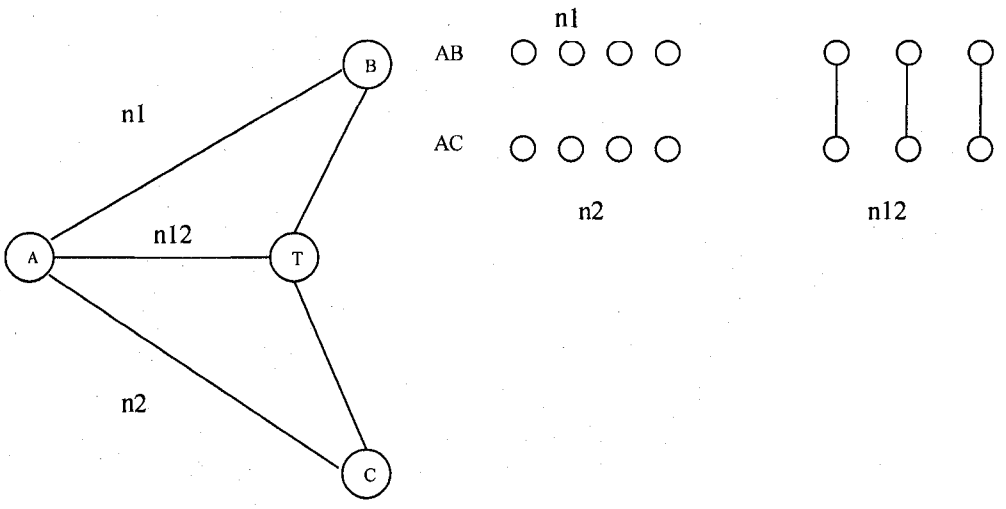

Figure 2.5 Overflow System

From A to B there is a direct (primary) route with n_1 channels. If they are all busy, then the call is directed to the alternative (secondary) route via T to B. In a similar way, the traffic from A to C has a first-choice route AC and an alternative route ATC. If we assume the routes TB and TC are without blocking, then we get the accessibility scheme shown to the right in Figure 2.7. From this we notice that the total number of channels is $(n_1 + n_2 + n_{12})$ and that the traffic AB only has access to (n_1+n_{12}) of these. In this case sequential hunting among the routes should be applied so that a call is only routed via the group n_{12}, when all n_1 primary channels are busy. It is typical for a hierarchical network that it possesses a certain service protection. Independent of how high the traffic load from A to C is, it will never get access to the n_1 channels. On the other hand, we may block calls even if there are idle channels, and therefore the utilization will always be lower than for systems with full accessibility. The utilization will, however, be bigger than for separate systems with the same total number of channels. The common channels allow for a certain traffic balancing between the two groups. This system has been used in hierarchical routing and alternate path routing. Studies relating to allocation of servers to two types of competing servers have been studied in [GOP-81]. This is also related to blocking experienced by different classes of traffic when they try to access a shared resource [KUF-81]. The model employed in these studies is a multidimensional generalization of the classical Erlang loss model. Different types of sharing policies are

discussed. They include a complete sharing policy in which the whole shared resource is completely shared by the difference classes of traffic; and complete partitioning, in which each class of traffic is allocated a specific amount of the shared resource. In this policy, each class has a reserved bandwidth for itself and then the rest of the bandwidth is shared with all the other classes. These policies can be analyzed by using a Markovian model using the Markov Decision Theory. A detailed discussion of these policies is presented in Chapter 5. The problem of fairness and resource sharing has been extensively researched in [FOS-81] [GOP-83] [KRA-84]. These have been used to study policies used in sharing link bandwidth by means of different classes of connections. In [GOP-83], the authors use the Markov decision theory to determine threshold policies that maximize link utilization. Reference [KARA-84] considers a class of restricted-policies, with the aim of reducing blocking probabilities. More recently in [MIT-99] the authors have reported a Virtual Partitioning scheme for sharing resources amongst different classes of traffic in a fair and robust manner. They use a reward penalty paradigm as a combined measure of efficiency and fairness. In this scheme a nominal capacity for each of the services is allocated such that they meet the required Quality of Service (QoS) conditions. For the shared resource, instead of each class of traffic having a fixed priority, the priorities are allocated depending on the state of the system. This state-dependant allocation of resources achieves a high throughput. This scheme can be used in conjunction with a Connection Admission Control (CAC) scheme that provisions differentiated allocations in a shared memory system. However, in [KRI-99] it has been proven that since the scheme uses a single value of nominal allocation per connection it is sometimes difficult to provide different loss levels. Also, it is difficult to protect against aggressive best-effort traffic and misbehaving sources without excessively restricting the number of best-effort sources admitted into the system.

2.5.2 Modeling of an Overflow System

The modeling of a general overflow system is described in this section. This method is similar to the Selective Trunk Reservation (STR) scheme described in [GIR-85]. Many studies have been made on the advantages of the STR scheme. In a recent study, [WAL-92] uses transform techniques to model such a system with infinite secondary servers.

The model is described keeping in mind the transceivers at an OXC. The regeneration and add-drop sub-system have two sets of TR pairs (servers). There are m_1 servers servicing add-drop traffic. The number of servers servicing connections requiring regeneration is m_2. Add-drop traffic that cannot find any available servers in the add-drop group of servers will overflow into the group reserved for regeneration. (traditionally the add-drop traffic that do not find any transponders would be blocked) This sharing architecture corresponds to an overflow system. The overflow is generated only when the TR pairs reserved for add-drop (primary group) connections is in the blocking state. The analysis of the overflow traffic cannot be done by a simple Erlang-B loss formula; because this will always underestimate the number of TR pairs (trunks) needed to achieve a desired blocking probability. This is because the overflow traffic does not conform to classical models of pure chance traffic (PCT). The overflow traffic is burstier than the ordinary Poisson process, and it is characterized by the Interrupted Poisson Process [KUZ-92]

The primary group (add-drop) of trunks has m_1 TR pairs. The secondary group (regeneration) has m_2 TR pairs. For our analysis we consider the traffic intensity (load) of the add-drop connections and regeneration connections to be the same. The regeneration traffic is offered only to the secondary group. Hence this can be considered to be overflow traffic from the primary group with no trunks in the primary group. The overflow traffic from the primary group, i.e. the regeneration traffic, is also added to the load for the secondary group. This traffic intensity is not Poisson. This overflow traffic is characterized by the peakedness *(Z)*. The peakedness can be defined as the variance (V, second moment of traffic intensity) to mean (A, first moment of traffic intensity) ratio of the traffic stream. The peakedness measures the degree of regularity in the arrival of the traffic. If Z is greater than 1 then the traffic is said to be peaked, while if Z is equal to or lower than 1 it is said to be smooth. Poisson traffic is smooth and has peakedness of 1 whereas the overflow traffic has peakedness greater than 1. The derivation of the variance to mean ratio is very involved. We will present only the results here

Consider that the traffic intensity to the primary group is *a*. The number of TR pairs in the primary group is *m1*. The traffic that is blocked, in other words overflow traffic from this group, is given by the Erlang-B formula:

$$E(m_2) = aE(m_2, a) = m \tag{2.1}$$

This traffic is the overflow from the add-drop group of TR pairs. In order to achieve the necessary blocking probability, this traffic is allowed to scan any free TR pairs from the regeneration group (secondary group) TR pairs. Such traffic is bursty in nature and is not smooth. The analysis cannot be done using the conventional Erlang-B formula. The peakedness is used as a measure to characterize this overflow traffic. The variance of the traffic from the primary group is given by

$$v = m(1 - m + \frac{A}{n + 1 - A + m}) \tag{2.2}$$

Thus peakedness is defined as the variance to mean ratio

$$Z = \frac{v}{m} \tag{2.3}$$

It has been observed that for pure chance traffic the peakedness is equal to 1 and for bursty traffic the peakedness is greater than 1. The overflow traffic has peakedness greater than 1 and hence is bursty. In order to analyze an overflow system, the effective traffic with an overflow mean is calculated as $m' = \sum_i m_i$ and variance $v' = \sum_i v_i$. From the given values of (m', v') it can be calculated using two equations with with unknowns. This requires an iterative procedure as $E_n(A)$ cannot be solved explicitly with respect to either n nor A. However, we can solve the equation with respect to n.

$$n = A.\frac{m + \frac{v}{n}}{m + \frac{v}{n} - 1} - m - 1 \tag{2.4}$$

Thus A is the only independent variable. We can use an iterative method to solve for A. However, in [RAP-65] the authors proposed a good approximate solution for A given by

$$A \approx v + 3.\frac{v}{m}.\left\{\frac{v}{m} - 1\right\} \qquad (2.5)$$

Substituting this value of A in the previous equation we can get n. The above traffic A can be applied to the total channels available $(n+n')$, where n' is the number of channels in the overflow group. We can find the net blocking probability using the Erlang-B formula $E_{n+n'}(A)$.

The challenge is now to find the blocking probabilities of the primary group and overflow traffic. It is observed that the primary traffic and secondary traffic have very different values of mean and variance and hence they do not experience the same blocking probabilities in the overflow group. It has been shown [KUZ-92] that the blocking probability experienced by a traffic stream is proportional to the peakedness.

One of the major challenges of the current market is to optimize the utilization of resources and reduce over-provisioning, and in turn reduce the overall cost of ownership. Also, there still is a need to address the issues of signal regeneration and cost-effective addition and dropping of channels. In order to reduce the processing granularity, service providers are moving to third-generation wavelength switches that replace the electrical core of today's OEO architecture with an optical matrix to improve network efficiency. The advantages of such systems in terms of the capital expenditure and operational expenditure are very well documented [AGG-97] [DOS-01] [RAM-02]. This optical switching matrix consists of a core optical switch (which performs the functions of switching and optical bypass) and an adjunct switching matrix to perform add-drop and signal regeneration. The signal regeneration and add-drop is done in the electrical domain. The interfaces between the optical and electrical sections are provided with a limited number of transponders which are dynamically tunable to the required wavelength. These transponders being opto-electronic devices are very expensive and should be provisioned and used in such a way that maximizes the utilization of those devices. For the current depressed Optical Market cost reduction and the return on investment are the keywords. This makes it very important to focus on the different methods of saving cost and to quantify the cost-savings. Many of the cost-reduction

opportunities are in the area of terminal equipment. The terminal equipment cost constitutes about 60% of the total network cost. In order to achieve this goal there is a need to minimize the number of transceivers at an OXC. In addition we would need to be able to utilize a fully agile Optical Crossconnect to fully share the available transceivers. Numerous solutions [SRI-03] [OKA-96] [KOG-96] [STA-99] [TES-98] have been provided in the literature. The general approach in these solutions is to split the signal and send the demultiplexed signals to the transponders. This approach leads to the signal power being weakened and an increase in the net bit error rate making the signal detection difficult. Thus there is a need to add more amplifiers into the system increasing the net cost per wavelength in the system. The other approach that has been provided is to use an electrical switching matrix to route the signals to the corresponding transponders. This, as we know is not scalable in terms of the cost. The third approach described in [SRI-03] is to use an adjunct switch, which is another OXC with a similar scale as the optical bypass section. This, however, is an expensive proposition and would result in the cost of the switching system almost doubling. The architectures of the adjunct switch provided in this research are smaller in dimension and easily scalable to a higher number of wavelengths. Also, in [SRI-03], no analysis of the losses involved and the means to compensate the losses and hence the increase in the cost of the node has been made. In [MOK-04] the authors present a dynamic sharing scheme to reduce the port count. However, these solutions do not consider the real issues of losses in such architectures, which makes them practically infeasible.

2.6 Summary

This chapter explored the various issues encountered in the provisioning and design of the next generation optical network. One of the issues not addressed in most of the literature on RWA algorithms is the fairness problem. This is caused by the longer lightpaths having a lower chance of getting established due to the Wavelength Continuity Constraint. Thus in a multi-hop network where the connections travel larger geographical distances through many links, the traffic carrying capacity for multi-hop connections is effectively reduced.

Another important aspect in the provisioning of lightpaths that travel large geographical distances and multiple hops is the signal degradation. Because of the many transmission impairments encountered by the signal during its path from the source to the destination, it becomes highly imperative for a routing algorithm to consider signal quality constraints while provisioning a lightpath. The devices like optical amplifiers, Optical add drop Multiplexers(OADM's), and dispersion management nodes tend to be invisible to the signaling and control layer. This makes it difficult for the network provider to perform reliable traffic engineering or impairment-aware routing assessments. Hence there is a need for impairment-aware algorithms and link state mechanisms, which will give the network an accurate picture of the equipment usage and link-budget requirements. This will allow a signal to travel large distances without significant signal impairment. Also, in order to move from static point-to-point systems to agile optical networks, there is a need to build flexibility and re-configurability into the network. This can also improve the resource utilization and increase the return on investment. These issues are addressed in the later chapters.

Chapter 3. Fairness in Wavelength Routed Optical Networks

3.1 Introduction

Establishing a lightpath in a DWDM network involves two steps: a) computing a route b) assigning a wavelength to the computed route, collectively referred to as the Routing and Wavelength Assignment (RWA) Problem. In the routing process, a shortest path is computed from the source to the destination using some metric such as minimum hop count, link congestion, etc. For wavelength assignment, a wavelength is sought that is available on each link of the computed route. The goal of the RWA is to maximize the number of connections. The RWA problem has been extensively studied in [BAR-966] [LI-03] [ELL-01].

The performance of an RWA algorithm is generally measured in terms of the blocking probability, i.e., the ratio of the number of connections that cannot be set up due to the unavailability of resources such as wavelength, bandwidth, etc., to the total number of connection requests arriving in the network. However, this does not fully capture all the effects and aspects of the network behavior, especially ***fairness.*** The fairness problem is caused by the longer lightpaths experiencing a higher blocking probability as compared to shorter lightpaths. This is because of the fact that, the longer the lightpath is, the less likely it is to find a path with available wavelength meeting the Wavelength Continuity Constraint. The fairness problem and strategies to mitigate the fairness problem have been investigated in [LI-03][BIR-95].

3.2 Analytical Model for Blocking Probability for a Lightpath

Consider a lightpath, which spans m links. Let $[\lambda 1, \lambda 2, \lambda 3, \ldots, \lambda w]$, be the set of free wavelengths available on a link $\underline{i}$. In order to establish a lightpath between a node pair (s,d), we must guarantee both enough capacity and wavelength continuity on the m links or use wavelength converters. Since wavelength conversion technology is not mature enough to be commercially viable, the use of wavelength converters is avoided.

Let q be the probability that a wavelength λ_j is used on the first link of the light path. The probability that the same wavelength is free on this link is *(1-q)*.The probability that this wavelength will be available on each of the m links of the lightpath is P_b

$$P_b = (1-q)^m \tag{3.1}$$

Thus the probability that this wavelength will not be available on any one of the links in the path is $(1-(1-q)^m)$.

The lightpath will be established only if any of the n wavelengths are available on all the m links. Thus the probability that at least one wavelength is not available on all the links of the lightpath is [BAR-96]

$$P'_b = (1-(1-q)^m)^n \tag{3.2}$$

These probabilities are calculated inder the assumptions that the links are independent and the probability of finding an available wavelength is the same for each link. It is seen that the blocking probability is proportional to the number of links a lightpath traverses. Thus, it can be concluded that the longer the lightpath is, the higher the probability that it will be blocked. This gives rise to the fairness problem. The shorter lightpaths have a higher probability of being established as compared to longer lightpaths. Also, the shorter lightpaths (1-hop, 2-hop) cause fragmentation of the available wavelengths on the links, resulting in higher blocking for longer hop lightpaths.

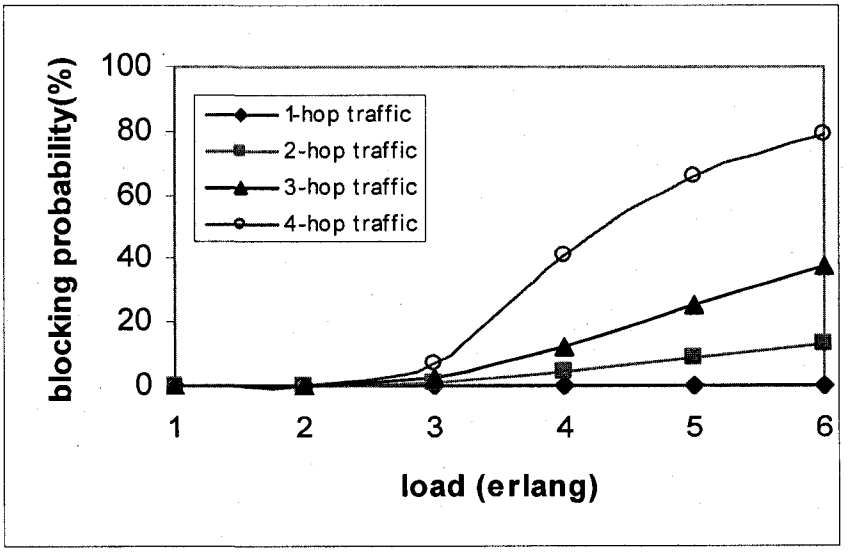

Figure 3.1 Blocking Probabilities of Lightpaths with Different Hop-count

This is a major problem in networks without wavelength converters as a lightpath must be established on a contiguous set of links having the same wavelength availability. This fairness problem is highlighted in Figure 3.1. The graph of load vs. blocking probability is plotted for the NSF network. It is assumed that the arrival of calls (requests) is Poisson, with exponentially distributed duration. Each source-destination pair has a call arrival process, and each process is independent.

It can be clearly seen that as the load increases, the blocking probability of the higher hop-count traffic increases at a much higher rate than lower hop-count traffic.

In order to address the fairness problem, the authors in [BIR-95] set a protection threshold in which single hop traffic connections are assigned a wavelength only if the number of available wavelengths is below a certain threshold. This is a mechanism to protect the multi-hop traffic from being blocked due to single-hop traffic fragmenting its resources. In this research, we use a traffic classification mechanism to achieve fairness among different classes of traffic. The traffic in the network is classified on the basis of the hop counts.

In order to limit the intrusion of shorter lightpaths into the wavelengths for longer lightpaths, we will use the traffic classification mechanism in [BAR-96] [LI-03]. As shown in Figure 3.2, the available bandwidth on each link is divided into a number of wavebands to be used by different traffic classes. Each class of traffic has the access only to the set of wavelengths in the waveband allocated to that class.

In his way we can ensure that the lightpaths having a higher hop-count have a higher chance of getting established. This is because the lightpaths having lower hop-counts can access only a small portion of the wavelength pool. The resource sharing is limited to a small number of wavelengths, resulting in less contention for the common resource (wavelength). Each waveband on a link has a cost associated with it. In order to achieve load balancing in the network we assign a criticality level to each of the wavebands. A waveband on a link is deemed critical if the number of occupied wavelengths in that waveband is greater than the criticality number. For a criticality number of, for example, 75%, a waveband on a link becomes critical when the wavelength occupancy is more than 75% of the total waveband capacity. Assigning a link to be critical during the computation of a light path will ensure that this critical link is not selected during the

provisioning process. The critical link will be selected only if there is no other path to the destination.

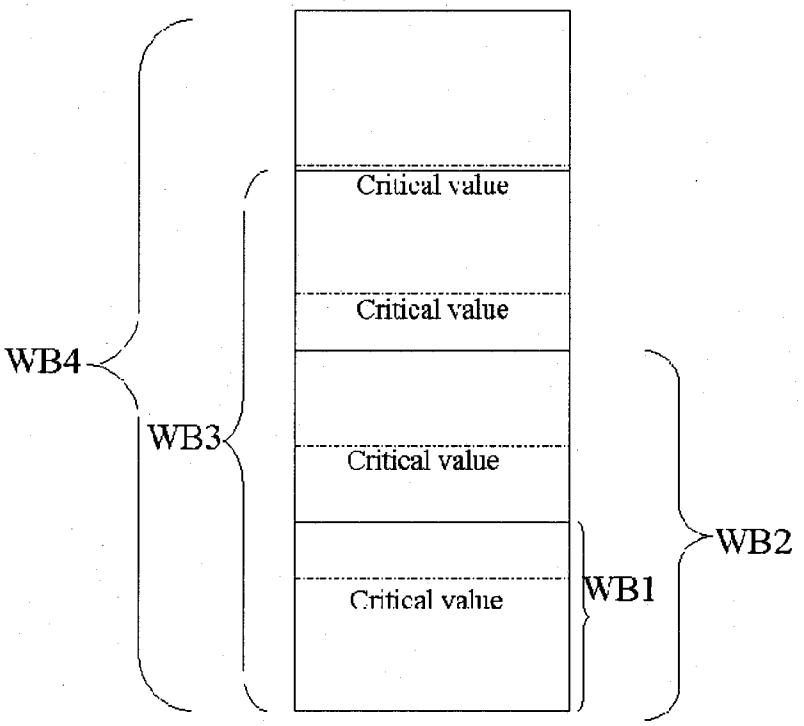

Figure 3.2 Traffic Classification and Criticality Levels

In the case of several critical links being present in the network, the path with the lowest criticality level is selected. These criticality levels decrease when wavelengths become free on that link and the number of occupied wavelengths drops to a number lower than the assigned criticality level. The utility of such a criticality mechanism is that an overly used link for provisioning is not used as often, and the traffic is distributed more homogenously throughout the network. By adding a criticality threshold to each waveband and routing traffic to avoid criticality we will ensure that traffic will be distributed on all the links in a balanced manner. With the criticality constraint in mind, we develop dynamic routing algorithms which provision connections in a fair manner. We will also quantify the unfairness by defining an unfairness factor which will be able to measure the relative unfairness experienced by lightpaths with different hop-counts. Using the criticality constraint we intend to develop routing algorithms that distribute the load more evenly on the links and improve load balancing.

3.3 Improving Blocking Probabilities under the Reservation Scheme

In this section, we will show that the use of the reservation scheme, as discussed in the previous section, will improve the blocking probabilities of the higher hop-count traffic as compared to a wavelength assignment mechanism without any reservation. In the assignment without reservation the first-fit or random wavelength assignment is used to assign the wavelength to any incoming traffic request irrespective of the path length (hop-count). In this example the highest hop-count traffic is 4-hop-count traffic. For simplicity, we only consider one link and model this link as a loss network. The wavelengths represent the trunks for this loss network. We will assume Poisson arrivals and exponential holding times with mean $1/\mu$. The arrivals are partitioned into four classes with respect to their hop-count. The mean arrival rate for the c hop-count traffic is denoted μ_c^a, for $c = 1,2,3,4$.

For the link without the reservation scheme we will only need to define Y_t as the number of unavailable wavelengths at time t. The total number of wavelengths is n. The process $Y = \{Y_t : t \geq 0\}$ is an ergodic Markov chain (Appendix B) with stationary (steady state) distribution π^*. Denote B_c^* the blocking probability for the c hop-count traffic under the no-reservation regime for $c = 1,2,3,4$. Since Poisson arrivals see time averages, then the blocking probabilities $\pi^*(n) = B_c$, for $c = 1,...,n$. It should be noted that in this case $\pi^*(n)$ is equal to the well-known Erlang-B formula.

$$B(k,a) = \frac{\frac{(a)^k}{k!}}{\left(\sum_{s=0}^{k} \frac{(a)^s}{s!}\right)} \tag{3.3}$$

Where a= offered Load and k= number of trunks in the system

To address the unfairness problem, we need a scheme that blocks the traffic with lower hop-counts with higher probability. We see that reservation does indeed achieve this end.

Consider the link under the reservation scheme as presented in Section 2. Denote X_t^i as the number of occupied wavelengths in waveband i reserved for the j^{th} hop-count traffic

where $j \geq i$ at time t. The total number of wavelengths in waveband i reserved for the j^{th} hop-count traffic where $j \geq i$ is denoted n_i and the total number of wavelengths is $n = n_1 + n_2 + n_3 + n_4$.

The process $X = \{X_t = (X_t^1, X_t^2, X_t^3, X_t^4) : t \geq 0\}$ is an ergodic continuous time Markov chain with stationary (steady state) distribution π. Denote B_i as the blocking probability for the i hop-count traffic. Since Poisson arrivals see time averages, then the blocking probabilities are, respectively,

$$B_1 = \sum_{i_2=0}^{n_2} \sum_{i_3=0}^{n_3} \sum_{i_4=0}^{n_4} \pi(n_1, i_2, i_3, i_4), \quad B_2 = \sum_{i_3=0}^{n_3} \sum_{i_4=0}^{n_4} \pi(n_1, n_2, i_3, i_4),$$

$$B_3 = \sum_{i_4=0}^{n_4} \pi(n_1, n_2, n_3, i_4) \quad \text{and} \quad B_4 = \pi(n_1, n_2, n_3, n_4).$$

It is evident that $B_4 < B_3 < B_2 < B_1$. Hence, reservation might be used as a solution to the unfairness problem.

We will end this section by showing that $B_4 \leq B_4^*$ that is, the 4 hop-count traffic experiences less blocking under the reservation scheme. We will consider the embedded discrete time Markov chains of the uniformized chains which have the same stationary regime as their original continuous time counterparts. Then, we will reconstruct the uniformized chains using a stochastic recursive sequence (SRS). The latter will enable us to use a sample path argument to show that the 4 hop-count will experience less blocking under reservation.

Both X and Y are continuous Markov chains (CTMC) on finite state spaces, denoted S_x and S_y, respectively. We denote the transition kernels for the corresponding embedded discrete time Markov chains as K and K^*, respectively, for X and Y. Since the state spaces are finite, then they both have a corresponding uniformized Markov chain. Let v_x and v_y^* be the rate out of state x and out of state y for the respective chains X and Y. Define $v = \mu_1^a + \mu_2^a + \mu_3^a + \mu_4^a + n\mu$. Note that v satisfies $v \geq \max\{v_x : x \in S_x\}$

and $v \geq \max\{v_y^* : y \in S_y\}$. The transition kernels for the embedded discrete time Markov chains (DTMC) of the uniformized chains are

$$K_u(x;x') := \begin{cases} 1 - v_x/v, & x = x' \\ (v_x/v)\, K(x;x'), & x \neq x' \end{cases}$$

and

$$K_u^*(y;y') := \begin{cases} 1 - v_y^*/v, & y = y' \\ (v_y^*/v)\, K^*(y;y'), & y \neq y' \end{cases}$$

It is well known that the (DTMC) uniformized chains have the same stationary distribution as the original continuous time counterparts, i.e. $\pi K_u = \pi$ and $\pi^* K_u^* = \pi^*$. We now present a SRS construction of these uniformized chains. Consider a sequence $U_0, U_1, \ldots$ of independent and identically distributed uniform $U[0,1]$ random variables. We construct the chains recursively using transitions rules $f : S_x \times [0,1] \to S_x$ and $f^* : S_y \times [0,1] \to S_y$. Let

$$X_0 = (0,0,0,0), \quad X_{n+1} = f(X_n, U_n) \quad \text{for} \quad n \geq 0$$

and

$$Y_0 = 0, \quad Y_{n+1} = f^*(Y_n, U_n) \quad \text{for} \quad n \geq 0.$$

Note that for both chains we are using the same sequence of uniform random numbers. Furthermore, if we choose transition rules that satisfy

$$P[X_{n+1} = x' \mid X_n = x] = K_u[x;x'] \quad \text{and} \quad P[Y_{n+1} = y' \mid Y_n = x] = K_u^*[y;y'],$$

then $\{X_n : n \geq 0\}$ and $\{Y_n : n \geq 0\}$ are Markov chains with stationary distributions π and π^*, respectively. Note that there is an infinite number of constructions of such transition rules. We will show that there is a construction of f and f^* for an arbitrary fixed sample path $u_0, \ldots, u_n$ then

$$X_{n+1}^1 + X_{n+1}^2 + X_{n+1}^3 + X_{n+1}^4 \leq Y_{n+1}.$$

In other words, the total number of occupied trunks under the reserved scheme is always less than or equal to the number of occupied trunks without reservation. If such a construction exists, then it should be evident that

$$B_4 = \pi(n_1, n_2, n_3, n_4) \leq \pi^*(n) = B_4^*.$$

We now construct the transition rules f and f^*. Without loss of generality, we can assume that $v = \mu_1^a + ... + \mu_4^a + n\mu = 1$. We will partition the interval [0,1] as a function of the current state of the Markov chains. Let x and y denote states for the respective Markov chains X and Y.

We start with the arrivals. The subinterval $[0, \mu_1^a + ..., \mu_4^a]$ is partitioned into four subintervals relative to the sizes of μ_i^a for $i = 1,...,4$. If the uniform random number falls within this interval, then this means an arrival wherein its type depends on where in the interval the value falls. The states x and y indicate if there are any available trunks, then the number of occupied trunks is incremented by one: otherwise we have a fictitious jump for the corresponding Markov chain.

We now consider services for the Markov chain X. Let $x = (x^1, x^2, x^3, x^4)$, i.e. the respective occupied number of trunks for each class of trunks. If the uniform number falls within $(\mu_1^a + ... + \mu_4^a, \mu_1^a + ... + \mu_4^a + x^1\mu]$, then it indicates a decrement in the number of occupied trunks for class 1. If the uniform number falls within $(\mu_1^a + ... + \mu_4^a + x^1\mu, \mu_1^a + ... + \mu_4^a + x^1\mu + x^2\mu]$ then this indicates a decrement in the number of occupied trunks for class 2 and so on. Finally, if the uniform number is larger than $\sum_{i=1}^4 \mu_i^a + x^i\mu$ then this will indicate a fictitious jump.

The services for the Markov chain Y will be similar. Let y be the number of occupied trunks. If the uniform number falls within $(\mu_1^a + ... + \mu_4^a, \mu_1^a + ... + \mu_4^a + y\mu]$ then there is a decrement in the number of occupied trunks. If the uniform number is larger than the upper bound of the last interval, then there is a fictitious jump.

All that remains to argue is that the total number of occupied trunks under the reserved scheme is always less than or equal to the number of occupied trunks without reservation. Recall that both chains are generated by the same stream of uniform random numbers. The following is a consequence of the construction of the transition rules and the fact that we are using the same uniform numbers for both chains. If the number of occupied trunks for the chain without reservation is larger than or equal to the number of occupied trunks under the reservation regime, then this inequality will be preserved for one-one transition.

The initial state for both chains is no occupied trunks: thus, both chains have an equal number of occupied trunks, and then the inequality will be preserved for all transitions. Therefore, for all $n \geq 0$,

$$X_n^1 + X_n^2 + X_n^3 + X_n^4 \leq Y_n.$$

3.4 Traffic Classification Mechanism Used in our Research

The traffic classification is similar to the method used in [LI-03]. As shown in Figure 3.2, higher hop-count traffic can also access the wavelengths reserved for lower hop-count lightpaths as the waveband for a traffic class overlaps with all the wavebands reserved for traffic that has a lower hop-count than itself. In his way we can ensure that the lightpaths with a higher hop-count have a higher chance of getting established which can reduce the unfairness. Each waveband on a link has a cost associated with it. In order to achieve load balancing in the network we assign a criticality level to each of the wavebands. A waveband on a link is deemed critical if the number of occupied wavelengths in that waveband is greater than the criticality number. For a criticality number of, for example 75%, a waveband on a link becomes critical when the wavelength occupancy is more than 75% of the total waveband capacity.

Let us consider a 19-node Network, as shown in Figure 3.3, to illustrate the idea. This is a network with a maximum hop-count of 4, assuming shortest path first criteria. Each link in the network is assumed to be bi-directional with a total number of wavelengths n =64. Wavelengths are grouped under different wavebands as follows: waveband 1 encompasses wavelengths from 0 to 15; waveband 2 is assigned wavelengths from 0 to 31, waveband 3 is assigned a range of wavelengths from 0 to 47 and waveband 4 is assigned a range of wavelengths from 0 to 63. The lower hop-count paths therefore do not have access to the wavebands reserved for paths having a higher hop-count. Let the cost of the i^{th} waveband on a link j be $Cost\_wb_i^j$. The number of wavelengths occupied in the waveband is y_i. The cost of the waveband is assigned as follows:

$$Cost\_wb_i^j = \begin{cases} y_i + 1, \text{ if } y_i \leq y_{i\,crit} \\ y_i + 1 + CP_i, \text{ otherwise} \end{cases} \quad (3.4)$$

where, $y_{i\,crit}$ is the minimum number of occupied wavelengths in the waveband for the waveband to be critical and CP_i is the criticality parameter for the i^{th} waveband.

The value chosen for the criticality parameter is very important as this parameter determines how well the algorithm performs in terms of load balancing. For the i^{th} waveband of a link j the value of CP_i is chosen as follows:

$$y_{i\,crit} + CP_i > y_{i\,crit} * \max hopCount \tag{3.5}$$

$$CP_i = y_{i\,crit} * \max hopCount - y_{i\,crit} \tag{3.6}$$

Where $\max hopCount$ is the longest path (measured in terms of the hop-count) in the network.

It is essential that the criticality parameter reflects the criticality level in the waveband. This will ensure that the critical link will not be chosen when there are non-critical links available when computing a route using the Minimum Sum Path (MSP) algorithm.

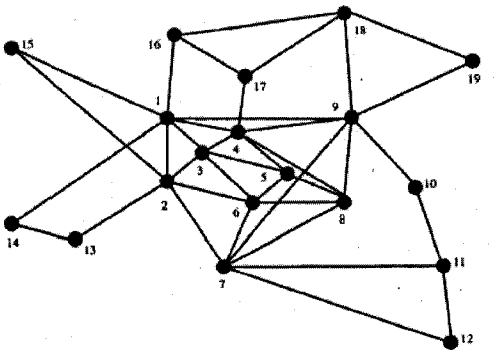

Figure 3.3 19-Node Network

Let us illustrate this with an example using the European Network. Here the maximum hop-count is 4. We assume two paths for an SD pair; a 4-hop-count path when using MSP algorithm and a 1-hop-count path when using shortest path first algorithm.

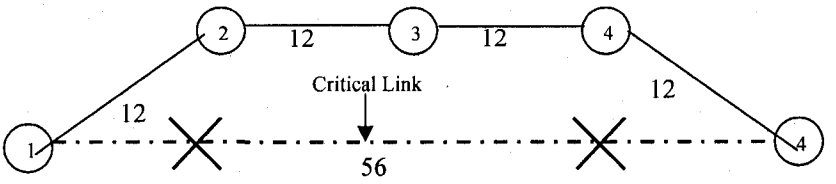

Figure 3.4 Critical Link Elimination

We choose a wavelength from the waveband reserved for 1-hop count traffic class to provision the connection between S and D (This is further explained in the next section). For a total capacity of waveband = 16 wavelengths, and a criticality level of 75 %, the waveband is marked critical if 13 or more wavelengths in the waveband are occupied. Assume that each of the links 1,2,3 and 4 of 4 hop-count path have 12 wavelengths in use. Since the number of wavelengths in use is lower than the criticality value, the cost of the links, computed according to the cost function described above in equation 1, is 13 and the total cost of the path is 56. For the 1-hop-count path, assume that the number of wavelengths occupied on the only link of 1-hop-count path is 13 and that the waveband is critical over this link. We determine the criticality parameter to be 42 from the equation 3.4 for the waveband, so that MSP selects the 4-hop-count path of cost equal to 52 and not the 1-hop-count path with a cost of 56. Thus the lightpath chooses a path that is less critical compared to other paths. Thus the load is more evenly distributed on the links in the network. The exact mechanism of how this is achieved in the algorithm is explained in the next section.

3.5 Traffic Classification and Load Balancing Algorithm

In the previous section we saw that using an appropriate cost-function to assign costs to heavily loaded links we could select a least critical path for a light path request. Also by partitioning the wavelength range into wavebands we can minimize the intrusion of lower hop-count lightpaths into the resources reserved for higher hop-count lightpaths. This achieves a higher degree of fairness among lightpaths with different hop-counts.

As shown in Figure 3.5, we see that the bandwidth is divided into wavebands. The dotted line represents the criticality level for each waveband. When the number of busy wavelengths in a given waveband exceeds the criticality threshold value, the waveband is deemed critical. In this research we use 25%, 50%, and 75% as the criticality threshold values and studied its impact on the net blocking probability, unfairness and load balancing. The results are compared with the static traffic classification using no criticality threshold and with no traffic classification at all.

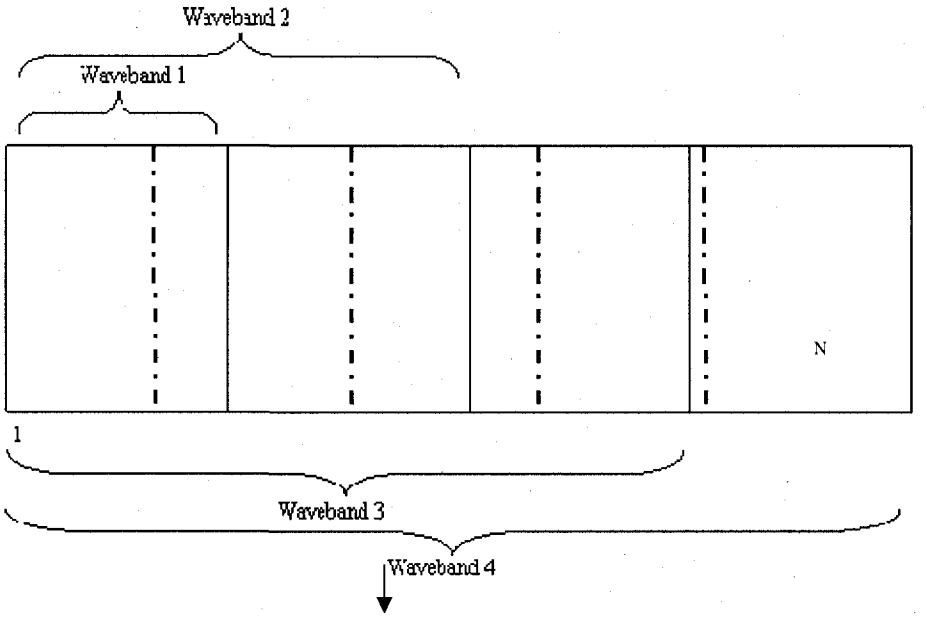

Figure 3.5 Traffic Classification with Criticality Threshold

In the static traffic classification with no criticality constraint a minimum hop-count path is chosen for a lightpath request. Depending on the number of hop-counts a lightpath traverses from the source to the destination, a waveband is selected to search for a free wavelength. A simple first-fit wavelength assignment mechanism is used to select the wavelengths for the lightpath. In the algorithm with no traffic classification, the MSP is used to find the shortest path from the source to the destination. Again, a first-fit wavelength assignment scheme is used to search a free wavelength.

The Traffic Classification and Load Balancing algorithm (TCLB) is a balance between static traffic classification and the scheme with no traffic classification. Also the addition of criticality constraints makes this algorithm perform better in terms of load balancing. The flowchart for the TCLB is shown in Figure 3.6.

As seen from the flow diagram the traffic is classified based on the number of hop-counts. The number of hop-counts is calculated using the Shortest Path First algorithm. This algorithm calculates the hop-count for a given connection finding the minimum hop-count from the source to the destination. For a given connection request, once the number of hop-count is found the virtual topology of the network is changed according to the waveband for the corresponding number of hop-count. In this way a lightpath will access only those wavelengths that have been reserved for it. Also, for the links whose

wavebands have reached criticality the cost is changed according to the cost function to reflect the criticality levels. To search a free wavelength we can use two schemes. In the first method which we call First-Fit from Bottom (FFB) we search for the first contiguous wavelength in all links from the bottom i.e. from wavelength 1. In this mechanism the higher hop-count lightpaths will always consume the wavelengths reserved for lower hop-count lightpaths. Thus the 1-hop lightpaths will be in disadvantage in finding free wavelengths as the other lightpaths will be contending for the wavelengths in waveband 1 even if there are free wavelengths in their own wavebands. We compare this mechanism with a second wavelength assignment mechanism which we call First-Fit from the Top (FFT). In this mechanism the wavelength assignment for any waveband starts from the last wavelength in the waveband. In this way the lightpaths with higher hop-counts intrude into the lower wavebands only if a free wavelength cannot be found in the higher wavebands. This ensures that the higher hop-count lightpaths do not overwhelm the wavelengths reserved for lower hop-count lightpaths.

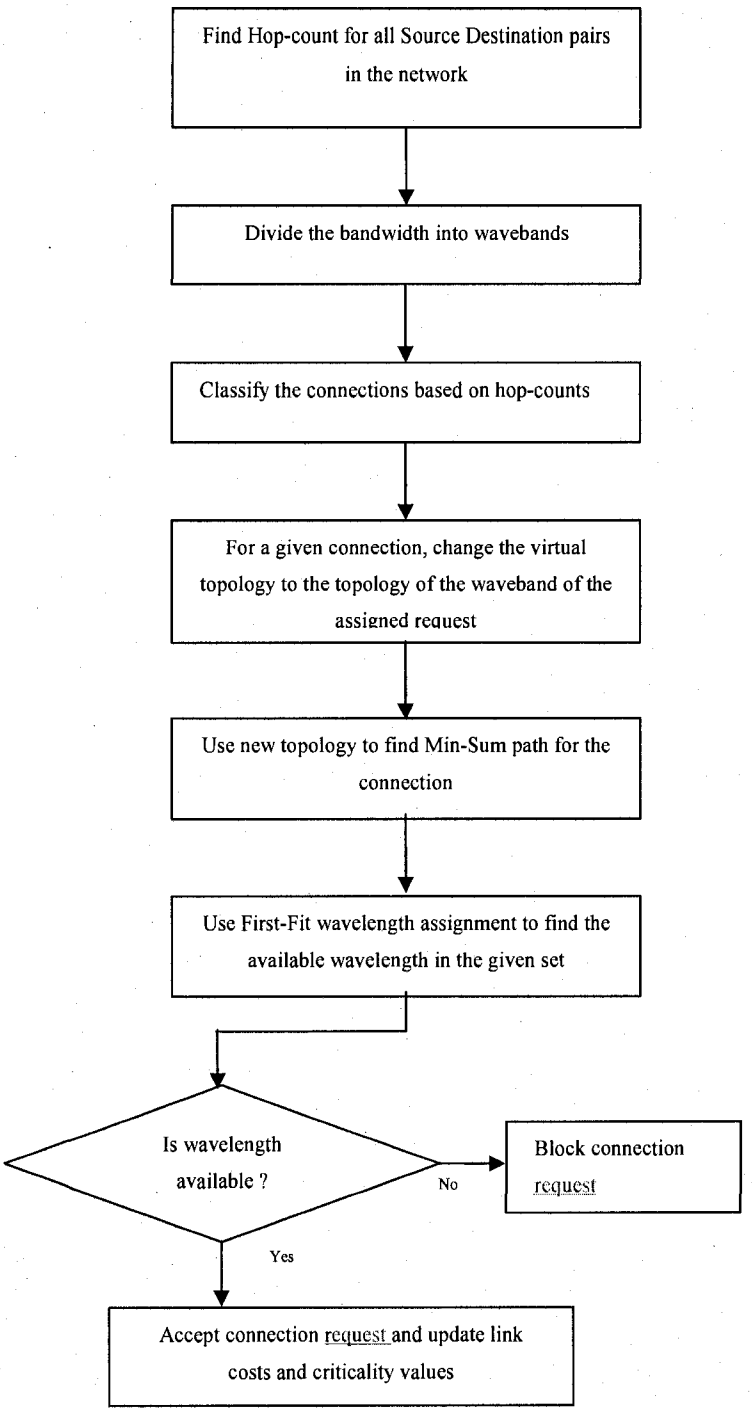

Figure 3.6 TCLB Algorithm Flow Chart

3.6 Simulation and Results

We use a 19 node topology (as shown in Figure 3.3) for our simulation. We use a discrete event simulation model developed in 'C' language. Calls arrive at each node in the network following a Poisson process with arrival rate of λ calls per unit of time. For the Poisson arrival process, the arrival rate is independent of the current number of established lightpaths or link state. The Figure 3.7 shows a Markov chain for Poisson arrival requests offered to a link with κ servers. The arrival rates for each state are $\lambda_i = \lambda$, $0 \le i \le \kappa$.

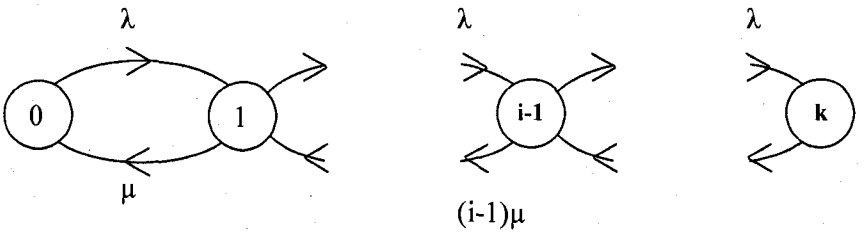

Figure 3.7: Poisson Process

The stationary probabilities for the Poisson distribution are

$$p(i) = \frac{\frac{\left(\frac{\lambda}{\mu}\right)^i}{i!}}{\left(\sum_{j=0}^{\kappa} \frac{\left(\frac{\lambda}{\mu}\right)^j}{j!}\right)} \qquad (3.7)$$

As the arrival rate is independent of the current link state, the arrival occupancy distribution is equal to the busy-circuit distribution.

The choice of the destination nodes are equally distributed. The connection holding time is exponentially distributed with a mean of 1/μ. Hence the load is given by $a = \lambda / \mu$. In our simulation we hold the call holding time to be constant. Hence the load is $a = \lambda$. Different values of load are obtained by varying the arrival rate. In this simulation we vary the criticality threshold from 25% to 50% to 75%. We investigate the impact of the

two wavelength selection schemes with varying criticalities on the following factors; Average Link Utilization, Fairness, Net Blocking probability.

3.6.1 Average Link Utilization

We define the average link utilization (avg_UTIL) to be the occupancy of the wavelengths normalized to the simulation time. It can be defined as:

$$\rho = \frac{\sum_{l=1}^{L}\sum_{\lambda=1}^{M} Oc_p^l}{SimTime * M * L} \tag{3.8}$$

where, L = total number of links in the network, M= total number of wavelengths in each link, Oc_p^l is the occupancy time of the λ^{th} wavelength on the l^{th} link, SimTime= total simulation time. The graphs of Average link Utilization vs. load for static traffic, no traffic classification, traffic classification with criticality, and traffic classification with no criticality are shown in Figure 3.8.

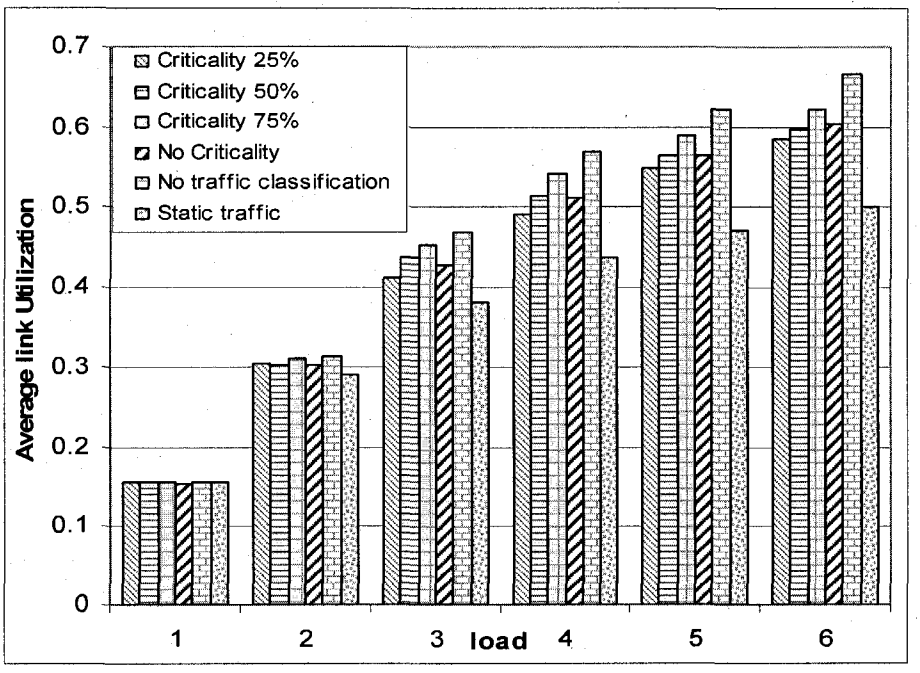

3.8 (a) First-Fit from Bottom

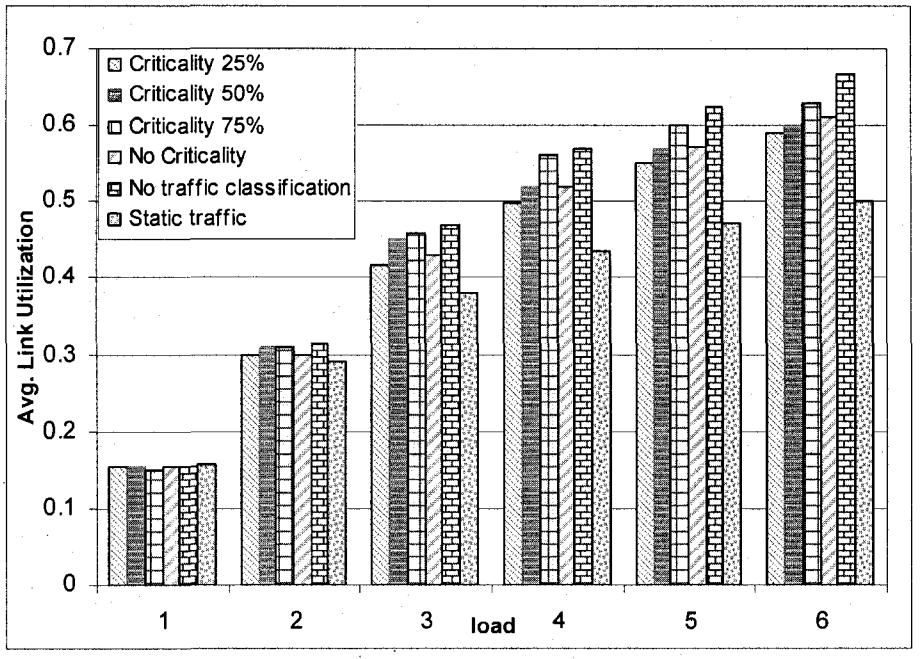

3.8 (b) First-Fit from Top

Figure 3.8 Graph of Load vs. Link Utilization

As shown in Figure 3.8, the link utilization using criticality information is similar to that obtained for the case with no traffic classification. Using a 75% criticality gives a slightly higher utilization at higher loads compared to 25% criticality and 50% criticality. The static traffic case gives the lowest link utilization. This is intuitive since in static routing the link state information is not considered in route calculation. This is because there is no link state information disseminated during the routing process. One of the key observations is that the average link utilization is not degraded when criticality value is increased to 75%.

Using the average link utilization values we plot the standard deviation of the link utilizations for each link. The higher the standard deviation is, the less uniformly the load is distributed in the network. This means that the traffic is concentrated on a few links even though there are more resources available in the network. A lower standard deviation indicates a better traffic spread in the network. The graphs of load vs. standard deviation for different levels of criticality and wavelength selection schemes are shown in Figure 3.9. Graphs with traffic classification with no criticality, no traffic classification

and static traffic classification are also plotted. From the figure we can see that the standard deviation is the lowest when criticality threshold is 75%. This further means that the load spread is more uniform when criticality threshold is 75%. From both graphs we see that static traffic classification gives us the worst results in terms of load balancing whereas, traffic classification combined with criticality avoidance achieves a better load balancing. Traffic classification with criticality avoidance distributes the load more homogenously throughout the network.

3.6.2 Net Blocking Probability

One of the key metrics for any routing and wavelength assignment algorithm is the Net Blocking Probability. The goal is to minimize the Net Blocking Probability. The Lower the Net Blocking Probability is, the higher is the number of connections that can be setup. We plot the graphs of load vs. Net Blocking probability for different criticality threshold levels and wavelength selection schemes as shown in Figure 3.10.

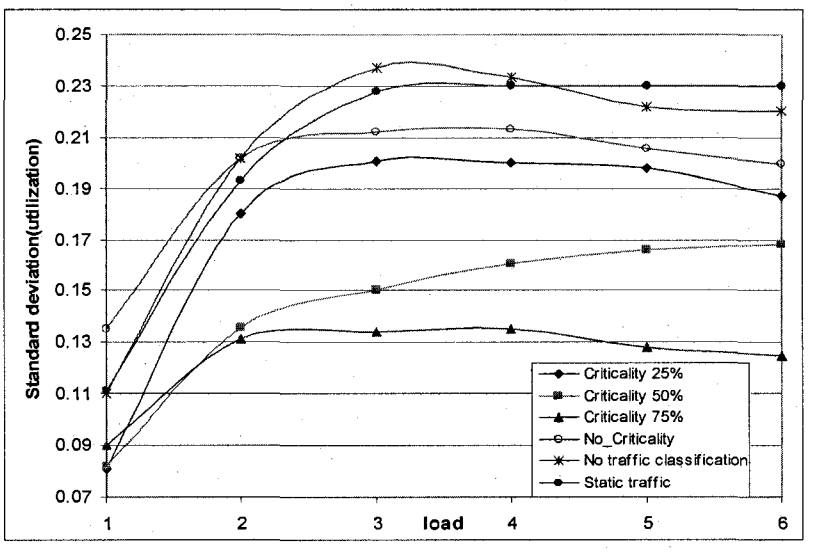

3.9 (a) First-Fit from Bottom

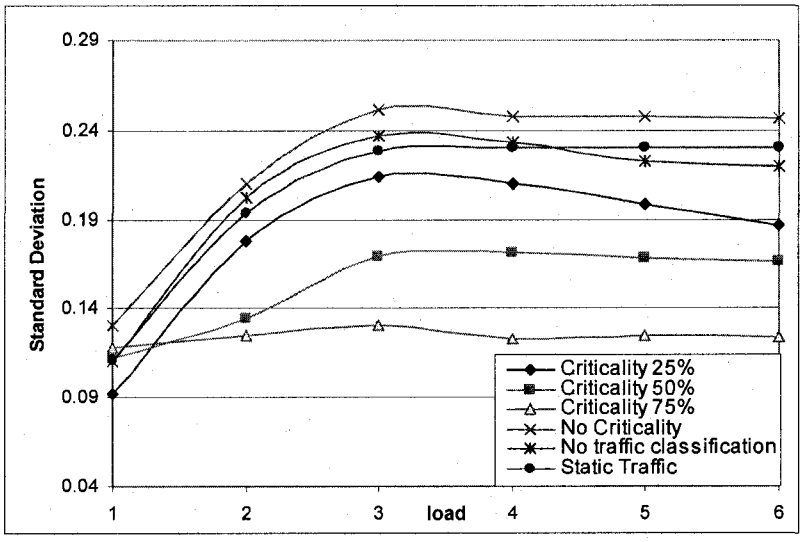

3.9 (b) First-Fit from Top

Figure 3.9 Graph of Standard Deviation vs. Link Utilization

For both wavelength assignment schemes we see that the performance of static routing with traffic classification is the worst. For the First-Fit from the bottom wavelength selection scheme we see that when criticality constraints are used, the net blocking probabilities are better than those obtained when static routing with traffic classification is used. It is however, slightly higher than those obtained in case of no traffic classification. However for the First-Fit from the top wavelength selection scheme, the blocking probability actually improves and for a criticality threshold of 75%, we achieve a blocking probability almost similar to what obtained in case of no traffic classification.

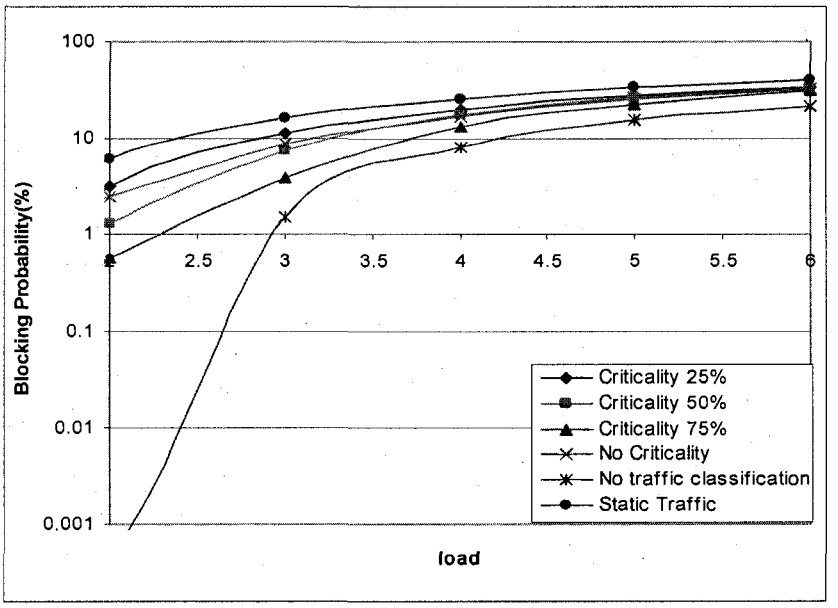

3.10 (a) First-Fit from Bottom

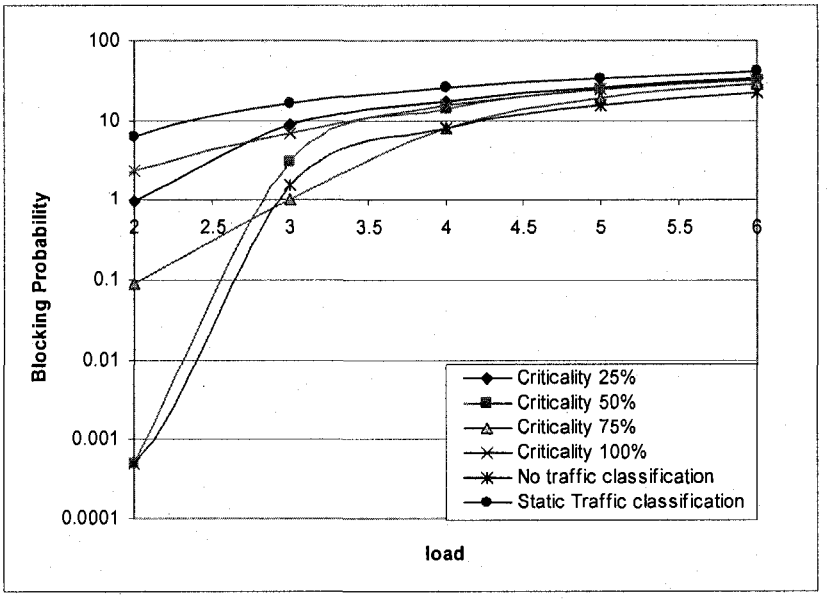

3.10 (b) First-Fit from Top

Figure 3.10 Graph of Blocking Probability vs. Load.

As we increase the criticality value, the blocking probability decreases. The First-Fit from top wavelength assignment scheme, gives a lower blocking probability as compared to First-Fit from bottom wavelength assignment scheme under different scenarios as shown in Figure 9. Graph of Net blocking probability vs. load under two wavelength assignment schemes and for different criticality values are shown in Figure 3.11 (a), 3.11 (b), and

3.11 (c). The net blocking probability is always lower when the First-Fit from top wavelength assignment scheme is used because the First-Fit from top wavelength assignment is less intrusive for shorter hop connections. In this scheme an i hop-count connection searches for available wavelengths in the i^{th} waveband before searching for available wavelengths in wavebands reserved for connections having hop-count lower than i.

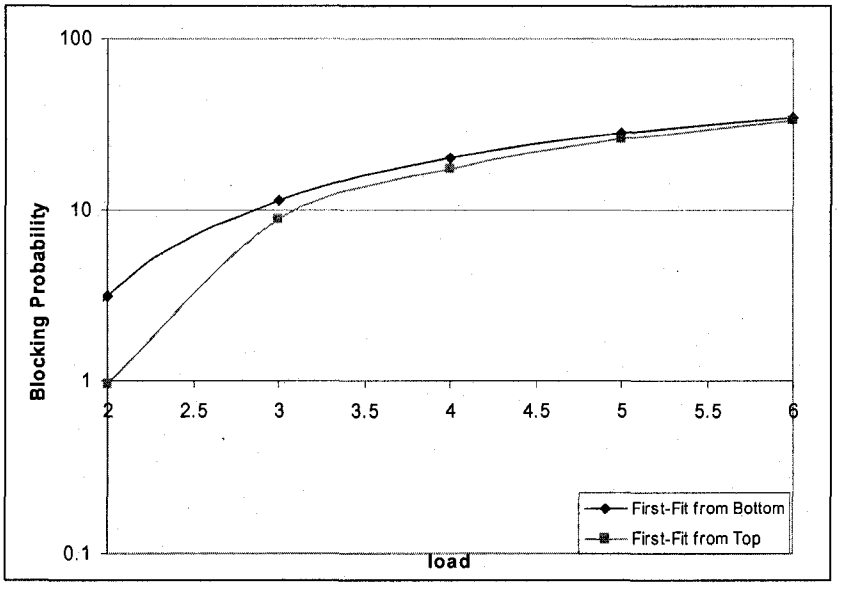

3.11 (a) Criticality 25%

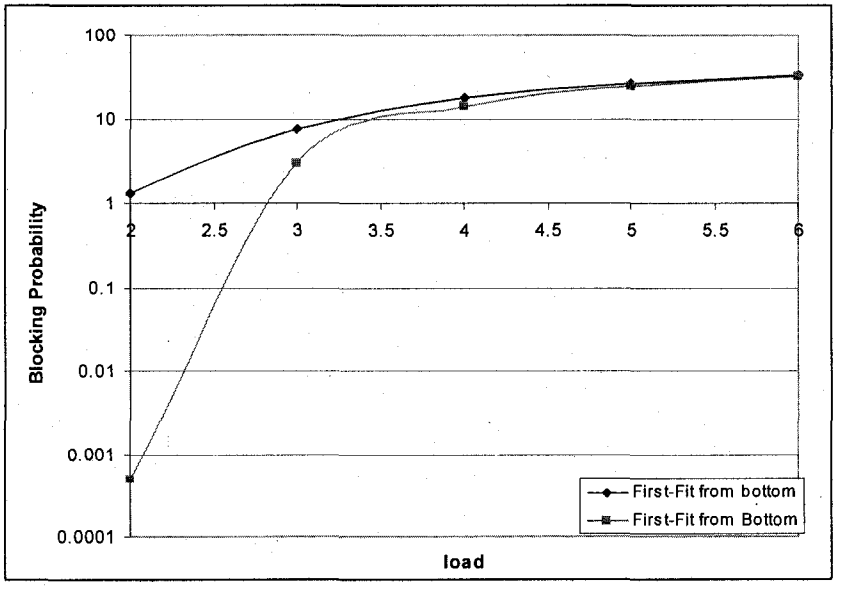

3.11 (b) Criticality 50%

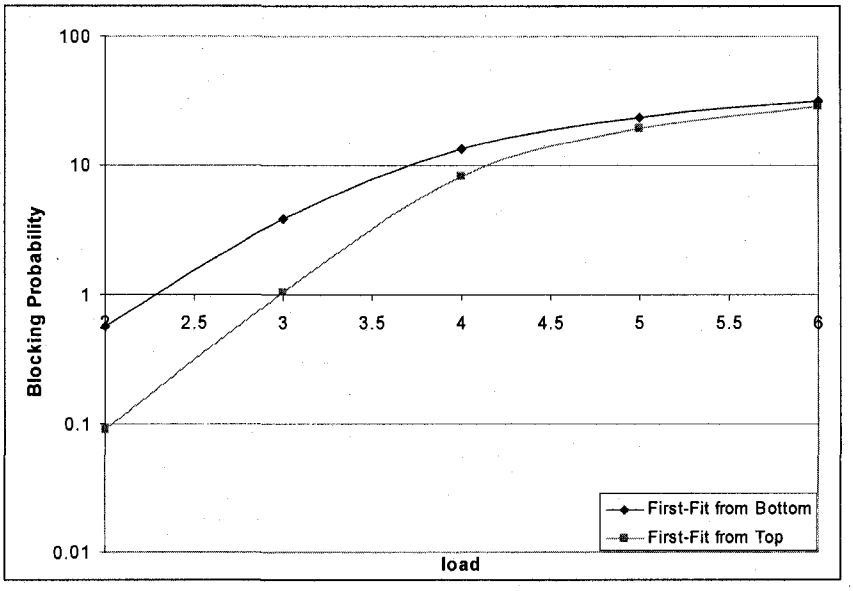

3.11 (c) Criticality 75%

Figure 3.11 Graph of Load vs. Blocking Probability for Different Wavelength Selection Schemes

3.6.3 Fairness

As discussed in Section 3.1 the blocking probability does not fully capture all the effects of the RWA algorithms especially the Fairness. Fairness is an issue because the shorter hop-count light paths have a higher probability of getting established as compared to the longer hop-count lightpaths. This is caused due to the fragmentation of the resources (in this case contiguous wavelengths) by shorter lightpaths. Using the traffic classification and criticality avoidance algorithm an effort is made to minimize the fragmentation of resources to reduce the blocking probability of higher hop-count lightpaths. In order to see the effects of traffic classification and criticality avoidance we quantify the Unfairness by defining an Unfairness Factor [RIC-03]. The Unfairness Factor is defined as the ratio of the average blocking probability of the longest hop-count lightpath to the average blocking probability of the shortest hop-count lightpath.

Ideally we want the Unfairness Factor to be equal to unity. From Table 1 we see that the Unfairness is very high for no traffic classification case. The longer hop-count lightpaths have a very high blocking probability as compared to the shorter hop-count lightpaths. When we use traffic classification the Unfairness is significantly reduced. In terms of fairness, the First-Fit from Bottom wavelength assignment scheme performs better than

First-Fit from Top wavelength assignment scheme and that use of traffic classification improves the overall fairness in the network.

Load	Criticality 25%	Criticality 50%	Criticality 75%	No Criticality	No traffic classification	Static traffic
3	0.44	0.11	0.016	0.25	15000	3.082218
4	0.92	0.69	0.41	0.77	4535	4.505222
5	1.19	1.03	0.768	1.12	1403	4.354146
6	1.39	1.17	0.97	1.26	410	4.333611

(a) First-Fit from bottom

Load	Criticality 25%	Criticality 50%	Criticality 75%	No Criticality	No traffic classification	Static traffic
3	1.890052	1.558824	12.2	1.347368	15000	3.082218
4	2.171171	1.987368	4.96	1.713675	4535	4.505222
5	2.274235	2.053593	2.600719	2.316147	1403	4.354146
6	2.446169	2.111111	2.321206	2.214085	410	4.333611

(a) First-Fit from top

Table 3-1Unfairness Factor for Different Criticality Levels Using Different Wavelength Selection Schemes

3.7 Summary

As seen from the above discussion longer lightpaths experience an unfairly high blocking probability. Conventional RWA algorithms fail to address this issue. It is shown in the above analysis that using conventional RWA algorithms the blocking probability of higher hop-count lightpaths is 10^2 to 10^3 orders of magnitude higher than lower hop-count traffic. By allowing the higher hop-count traffic to share the resources reserved for lower hop-count traffic we lower the Unfairness. One can see that there is a small tradeoff to achieve fairness in optical networks. There is a small degradation in the overall blocking probability to achieve fairness and load balancing in the network. A higher criticality threshold level results a better spread of traffic in the network. In this research we also use criticality threshold levels in combination with traffic classification to achieve a better load balancing in the network. We develop RWA algorithms that use the criticality levels of a link to include or exclude the link in the selected path for a lightpath. Thus by

being aware of the criticality threshold levels of the links the traffic is distributed more homogeneously in the network making the most use of the resources available in the network. The traffic classification mechanism used in combination with the criticality constraints ensures that higher hop-count traffic is always guaranteed a certain percentage of wavelengths in a link. By using the First-Fit from Top wavelength selection scheme and criticality level of 75% one can achieve optimum results i.e. a blocking probability is almost similar to that in case of no traffic classification. Also this achieves the highest traffic spread by achieving best load balancing and a lower unfairness value as compared to the algorithm using no traffic classification.

Chapter 4. Impairment Aware Routing Algorithms

4.1 Introduction

The routing of lightpaths over an all-optical network has received extensive attention [CHL-92][CHL-96][RAM-01]. When routing issues are discussed in all-optical networks it is generally assumed that all routes have adequate signal quality. This however is not the case. There are impairments caused due to the physical characteristics of the underlying network infrastructure. The effects of these impairments need to be considered when provisioning a lightpath to ensure signal-quality guaranteed connections.

4.2 Impairments Affecting the Transmission in Optical Networks

In a wavelength-routed optical network spanning large geographical area, an optical signal traverses through many intermediate nodes and long stretches of fiber segments. In order to enable the signal to propagate over a desired lightpath and also to enable wavelength routing, an OXC is deployed at each node. This OXC employs a passive and hence lossy switching through an electro-optic control mechanism. The cumulative losses incurred by the signal at all these nodes necessitates the use of optical amplifiers (generally, EDFA's) at strategic positions in the network to achieve loss compensation. However, the switches and EDFA's while offering transparent switching and loss compensation, respectively, may introduce significant transmission impairments such as amplifier noise (ASE), cross talk between different switching elements, dispersion, nonlinearities and polarization mode dispersion These impairments, which is discussed in appendix c, could severely affect the signal, and in turn, affect the routing strategies. Most of the provisioning algorithms existing in current literature assume an ideal physical layer which transmits the optical signal without any error. However, this is not the case. There are impairments caused by the physical characteristics of the underlying network infrastructure. These impairments reduce the signal quality by affecting the BER of the

detected signal at the receiver. Hence the effects of these impairments need to be considered when provisioning a lightpath to ensure signal-quality guaranteed connections.

The impairments like crosstalk, ASE noise and attenuation generated at every node co-propagate along with the signal thus degrading the optical signal to noise ratio (OSNR) and hence the BER. A specified BER is generally used to calculate the minimum optical power the receiver needs to operate reliably. Different manufacturers set different thresholds for the minimum BER. The operating thresholds generally vary from 10^{-9} to 10^{-15}. For instance SPRINT sets the threshold for a link to be at 10^{-12} while ITU-T requires it to be 10^{-9}. In the presence of these impairments it becomes imperative to regenerate the signal during its journey from the source node to the destination node. In order to mitigate the effects of transmission impairments the optical signal is regenerated at the intermediate nodes only if the signal quality falls below acceptable limits. The regenerators perform the function of reshaping, retiming and regeneration. This is called as 3-R regeneration. The existing technology is not mature enough to allow regeneration in the optical domain in a cost efficient manner. Hence, the only solution is to convert the optical signal into an electrical signal, regenerate it, and send it back into the optical network as an optical signal.

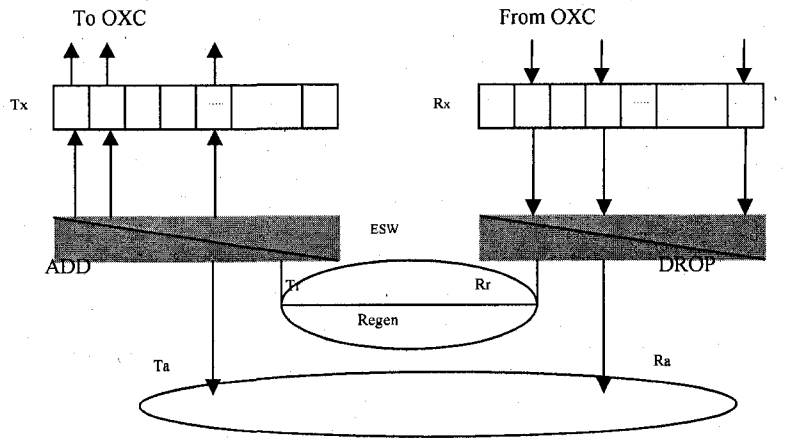

Figure 4.1 Add-drop Architecture of an OXC

This process is referred to henceforth as OEO (optical-electronic-optical) conversion. As shown in Figure 4.1, the signals that need to be regenerated are dropped locally at a node using the drop ports. They are then detected and their signal levels raised to the desired levels and added back to the network. Every time a signal is regenerated one transmitter-receiver (TR) pair is used.

The use of opto-electronics is often associated with a higher cost. Achieving a lower cost solution involves establishing what constitutes the minimum required amount of opto-electronics necessary to assure the presence of desired optical transport networking attributes enabled by their presence. In the short term, the result of this exercise is reflected in optical-networking architectures characterized by transparent (or all-optical) segments. The resulting optical networks are also referred to as "translucent" optical networks **[RAM-01].**

Routing strategies for translucent networks, which are aware of the current regeneration resources and link states and designed to smartly route the connection requests under quality constraints, are discussed in **[YAN-02].** The authors develop intuitive strategies for dynamic routing under signal degradation constraints. In [HUA-03] the authors develop routing algorithms, which are Impairment aware. With the signal-quality consideration, as compared to algorithms that are not impairment aware in a realistic optical network, the impairment-aware algorithms proposed in this thesis efficiently provide signal-quality-guaranteed connection while significantly reducing connection blocking probability. This results in better utilization of network resources and a reasonable computational requirement.

4.3 Network Model Used

The optical network consists of switching nodes interconnected by fiber links. Each node consists of an OXC and an access station as shown in Figure 4.2. The OXC consists of multiplexers, optical switches, and demultiplexers. The transmitters and receivers are in the access station. The incoming optical channels are at different wavelengths and can be switched to a different fiber or can be added or dropped at the node by configuring the optical switches.

We consider two types of transmitters and receivers in this thesis: tunable and fixed. The tunable transceivers can tune to the whole range of wavelengths available, while the fixed transceivers are tuned to a particular wavelength (frequency). We study the effects of tunability and the effects of the numbers of such transceivers in the network. The impact of tunability and the added value of such tunable transceivers in practical deployments are studied in [BUU-06].

When a signal needs to be added into the network, the transmitter is used for the holding time of the connection. The transmitter is made free as soon as the connection is torn down. Similarly when a signal needs to be dropped at the node, the receiver is used up for the time the lightpath is established. However, if the node serves as a transit node where the signal needs to be regenerated, then a transmitter-receiver (TR) pair is used for dropping the optical signal at the node and then regenerating it and adding the optical signal back into the network. The unavailability of transceivers at a node can cause blocking of the lightpath. Thus the routing algorithm should consider the number of TRs available at a node as an important constraint while setting up lightpaths. It is necessary to ensure that there are enough TRs available for the add-drop function. This is because regeneration is a distributed function (i.e., if no regenerators are available at a particular node, the signal can be regenerated at some other node), and if there are no transceivers available at a node the lightpath can be routed to another node with the necessary transceivers for the regeneration function. We consider two types of regenerator placement strategies in this research: Tunable-dense and Fixed-sparse. Due to high cost of T-Rs, regenerators using fixed T-Rs are placed in a few(less than 20%) nodes in the networks. This topology is not scalable for large number of wavelengths. This placement scheme is called **Fixed-Sparse** (FS) regenerator placement scheme in this thesis. In the **Tunable-Dense** (TD) architecture the T-R pairs are ***densely (more than 70% of the nodes)*** distributed through the network. Since the transceivers that are being used in the TD architecture are tunable a better utilization of the transceivers can be achieved with a lower number of transceivers. Since we do not need as many T-R pairs as compared to the fixed-sparse architecture this architecture is scalable and not prohibitive in cost.

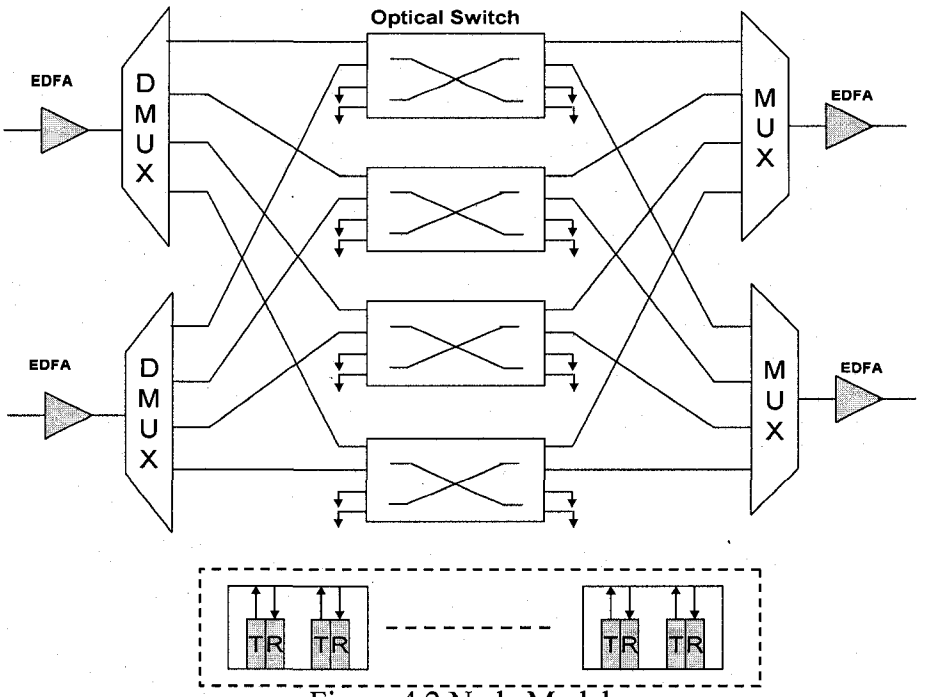

Figure 4.2 Node Model

These T-R pairs are tunable to all the N wavelengths available in the network. Also by placing the regenerators densely in the network we can get an optimal utilization of the available regenerators and a lower blocking probability is achieved for calls, which would otherwise be blocked due to high BER or low OSNR. In this application tunable lasers allow the resolution of blocking scenarios without the need for a full complement of transponders. More importantly it has been shown that about 80% of the traffic going through a node is pass-through traffic and only 20% of the traffic is add-drop traffic. Therefore an efficient design would be to use tunable transponders rather than having N transponders tuned to each of the wavelengths in use. Also, it has been shown using multi-cavity tunable thin film filter chip tunable filters can be made available at the cost of a fixed filter, however, they provide flexibility in the sense that they can tune to any of the wavelengths. Apart from reduced inventory advantages, transponders with broadly tunable lasers and receive-filters enable fully flexible remote selectivity and reconfigurability of up to 100 percent add/drop or pass-through wavelengths. Another benefit is efficient wavelength assignment to reduce wavelength blocking.

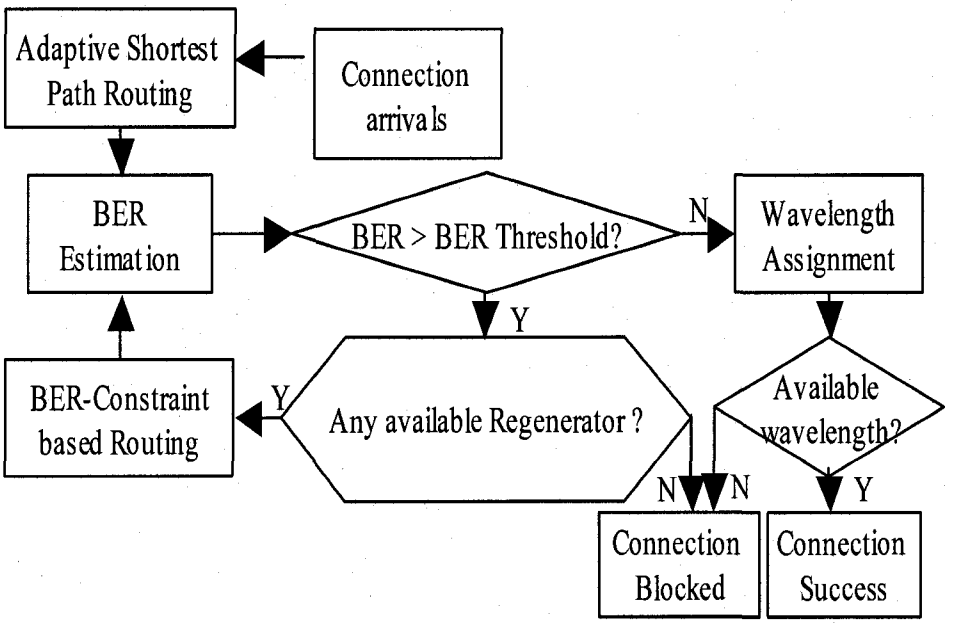

Figure 4.3 BER Aware Routing Algorithm

In addition, price and loss reduction are achieved by increasing the functionality and density of the optical components and active port count. Furthermore, tunability also applies to tunable regenerators or wavelength translators, when needed, to extend the reach and/or resolve the wavelength blocking.

Using these two regeneration architectures, we develop constraint-based modified shortest path algorithms to include the impairment constraints. These algorithms will ensure the necessary signal quality, measured in terms of the BER of the signal. A flowchart for the simulation of the heuristics is shown in Figure 4.3. Simulations of the BER-assured routing and wavelength assignment algorithms would be conducted using a WDM network modeling and simulation toolkits. The toolkits are developed using C++ and run in a Microsoft Windows environment. A few object-oriented class libraries have been developed, including the topology discovery algorithm, the flow traffic generator, the BER-evaluation module, various routing and wavelength assignment algorithms, protection planning, and so on. We simulate network topologies shown in Figure 4.5, where each node represents an optical wavelength switch node and an edge router connected directly to optical wavelength switch.

Obtaining the BER by error counting is impractical in optical system simulation, since the target BER values are typically of the order of 10^{-9} or less. Based on the assumption that the received signal tends to satisfy Gaussian distribution when the noise mainly comes from the electrical part of the receiver after photodetection,

$$P_{ber} = 0.25\left[erfc\left(\frac{I_{s1} - I_{th}}{\sqrt{2}\sigma_1}\right) + erfc\left(\frac{I_{th}}{\sqrt{2}\sigma_0}\right)\right] \quad \text{[AGG-97]} \qquad (4.1)$$

Where P_{ber} the BER, I_{th} is is the decision threshold, which is automatically optimized to minimize the BER. The decision threshold is used to compare the received bit and make a decision whether the received signal is a 1 or a 0. The functional form of the probability that a received signal is a 1 or a 0 depends on the noise sources responsible for current variations. The noise sources are thermal noise and shot noise, both of which are Gaussian in nature. Since the sum of 2 Gaussian random variables is also a random variable, the sampled value of the received signal has a Gaussian probability density function. Since the average and variance for the 1 and 0 bits are different, the standard deviations of the 1 and 0 bit are σ_0 and σ_1 respectively. I_{s1} is the signal level of the 1 bit. The BER estimator first samples the received signal for sufficient number of bits to gain accurate statistical mean and variance, then uses the above formula to derive the BER.

The transmitter consists of DFB lasers operating in CW (continuous wave) condition at wavelengths 1550 nm range. The wavelength spacing is equal to 100 GHz with the Bit rate of each channel at 2.5Gbit/s. The Bit type is NRZ with an ideal Extinction ratio.

Observed channel frequency: 193.4145 THz (1550nm). At the receiver the Optical bandwidth is10GHz while the electrical bandwidth $Bw_{e=}$ 2.5GHz. In particular we assumed that the network is cabled using Non-Zero Dispersion Shifted fibers. Fiber non-linearity, dispersion and crosstalk are neglected based on the assumptions stated above. An Attenuation factor of 0.2db/km is assumed for the fiber.

The summary system simulation parameters assumed are shown in Table 4.2:

The links connecting the nodes are bi-directional WDM optical links, and there is an implicit bi-directional control network link per WDM link. We assume the link distances are 100 km and that the pre-amplifiers at the nodes compensate for the losses in the

network. The crosstalk model for the switch is selected to be the same as that of [RAM-99]. It is also assumed that the tuning latency is very minimal and is therefore ignored.

Parameter	Value
Number of wavelengths	16
Mux/demux loss in db	4 dB
Insertion loss, tap loss	1 db
Fiber loss	.2 dB/km
Switch element insertion loss	1dB
Input EDFA gain	22 dB
Output EDFA gain	18 dB
Switch crosstalk ratio	30 dB
Bit rate(r)	1 Gbps
Electronic Bandwidth	0.7(r)
Optical Bandwidth	10 Ghz
BER threshold value	10^-12
Input EDFA Gain	22 dB
Output EDFA Gain	16 dB

Table 4-1 System Simulation Parameters

The traffic model used is a Poisson arrival of calls (requests) with exponentially distributed duration. Each source-destination pair has an independant call arrival process. We denote λ as the lightpath arrival rate for each source-destination node pair (in the following analysis, λ is set to 100 time units); $\mathbf{1/\mu}$ is the average call holding time for each source-destination node pair. We change the traffic load by setting $1/\mu$ with different values. The intelligent dynamic routing algorithms developed in this research are used to route the signals considering the above-mentioned aspect by measuring the BER. This is used as the signal quality constraint, which will be checked when routing a particular connection. By checking the BER during its whole path, it is ensured that the lightpath passes through enough regenerators to regenerate the signal to appropriate levels.

The value for BER is derived under the following assumptions:

a) The channel spacing is 50Ghz. Under this assumption, the heterodyne crosstalk can be ignored.

b) Standard fibers with in-line dispersion compensation are assumed. Thus, intersymbol interference due to linear dispersion is neglected.

c) Optical amplifiers are assumed to work in deep saturation and to have ideally flat bandwidth.

d) Each OXC's insertion loss is compensated by optical amplifiers, and OXC's coherent crosstalk penalty is assumed to be very low and hence is ignored.

e) The output per channel power from the amplifiers is relatively low and the nonlinear effects can be neglected.

Based on the above considerations, the degradation of the optical signal is assumed to be mainly caused by the ASE noise from the optical amplifiers, the crosstalk and the power penalty from the intermediate OXC's.

4.4 Link State Probe and Management

In translucent networks, regenerators are shared resources. The availability of the regenerators may change from time to time due to this sharing. Therefore, the availability of regenerators must be dynamically disseminated and updated at each routing node. Up-to-date link state and regenerator availability information can be disseminated using Interior Gateway Protocol (IGP) with a traffic engineering extension, for instance Open Shortest Path First –Traffic Engineering (OSPF_TE) or IS-IS_TE. Therefore, each node in the network has the wavelength utilization information and regenerator availability of the whole network. Ideally some regeneration-related information, such as bit rate, ONSR and BER can also be advertised using the IGP. However, some additional hardware and more control overhead are needed to probe and disseminate the information. Therefore a BER-evaluation module is developed to estimate the BER level of a connection according to the available dynamic link state information, such as the wavelength utilization, traversed nodes and hop-counts, as well as static physical layer parameters.

The flow chart of the BER-assured RWA algorithm is illustrated in Figure 4.3. Upon the arrival of the connection requests at a source node, an adaptive shortest path routing algorithm is carried out to compute the shortest path to the destination according to available bandwidth and hop counts. If the derived route cannot meet the requirement of BER constraint, one regenerator will be selected to regenerate the optical signal at an

intermediate node. It is assumed that all the node pairs can be connected via translucent lightpaths by regenerating the optical signal once at most. When a connection can be satisfied without regeneration, it needs only one transparent lightpath using a continuous wavelength. Otherwise, two transparent lightpaths are needed using regeneration.

One challenge of the design of dynamic routing algorithms is to select the available regenerators efficiently. Ideally, the regenerator selection scheme should be efficient, simple and scalable. We present two regenerator selection schemes in this thesis: on-route regenerator selection and off-route shortest-path regenerator selection, which is shown in Figure 4.4 (a) (b).

In the on-route regenerator selection algorithm, the shortest path from the source to the destination is calculated first, and then the signal quality is checked. Once it is seen that the signal quality is degraded by the time the signal reaches the destination node, the algorithm tries to find the available regenerators in its path. The selection of available regenerators is constrained to the path returned by the shortest path algorithm. Obviously, the on-route regenerator selection scheme can ensure that no over-long translucent lightpaths would be generated. However, even though there are regenerators available in the other nodes of network but not on the shortest path, the connection will be declined. Therefore, the blocking probability using an on-route regenerator selection scheme could be high.

In contrast, an off-route regenerator selection scheme can choose any available regenerators in the whole network. Therefore, the off-route method can make better use of the regenerators. However, this could result in long lightpaths. Moreover, the off-route method is more computationally intensive than the on-route method. The worst-case complexity of the off-route shortest-path algorithm is $O(N^2 log(V_n+E))$, whereas the time complexity of the on-route algorithm is $O(V_n\ log(V_n+E))$, where V_n is the total number of nodes in the network, and E is the total number of edges in the network .

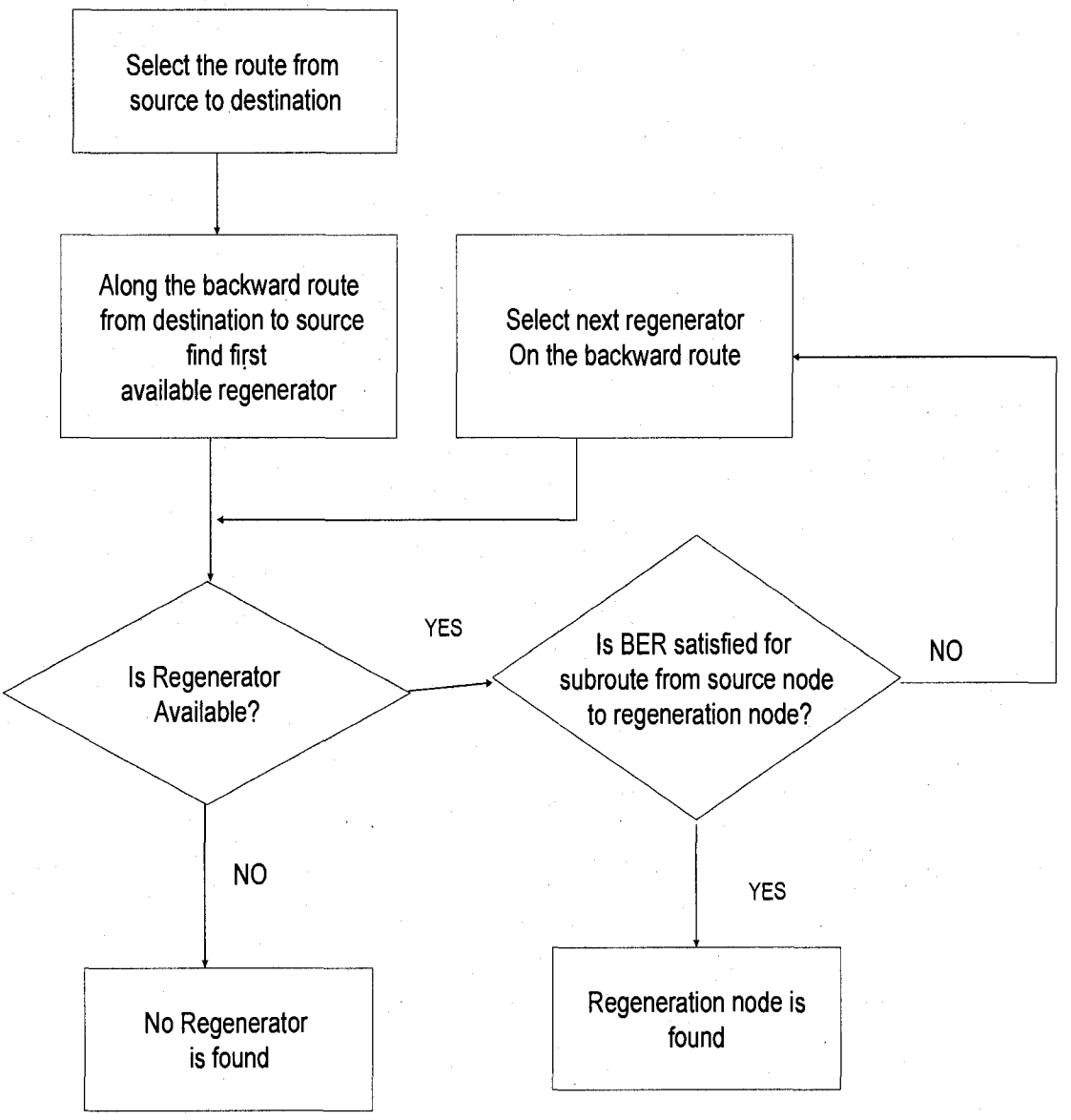

4.4 (a) On Route regenerator selection algorithm

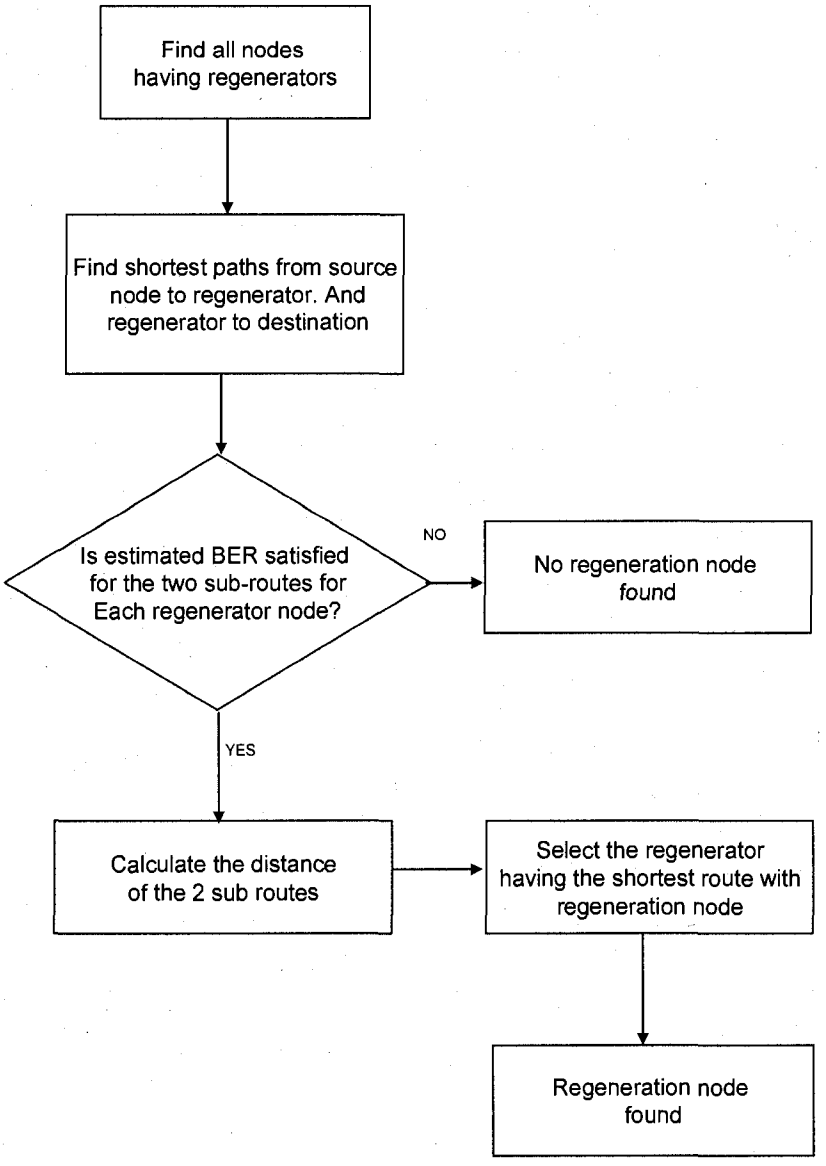

4.4 (b) Off Route regenerator Selection algorithm

Figure 4.4 Regenerator Selection Algorithms

The output of the BER-assured routing algorithm is passed to the wavelength assignment module. Without using regenerators at intermediate nodes, a lightpath have to use the same wavelength. Otherwise, the regenerators can perform wavelength conversion besides regenerating the optical signals. If no continuous wavelength is available for the transparent lightpath, the connection will be declined. Otherwise, the establishment of a

new lightpath will trigger an update of the available wavelengths and regenerators in the network.

We simulate the network topologies illustrated in Figure 4.5, where each node represents an optical channel switch node and an edge router connected directly to the optical channel switch. The links connecting the nodes are bi-directional WDM optical links, and there is an implicit bi-directional control network link per WDM link. We assume the node distances are about 500 km apart and optical amplifiers are placed at about 100 km spans .The characteristics of the networks are listed in Table 4.3. The pre-amplifiers at the nodes compensate for the losses in the network. The crosstalk model for the switch is selected to be the same as that of [RAM-99].

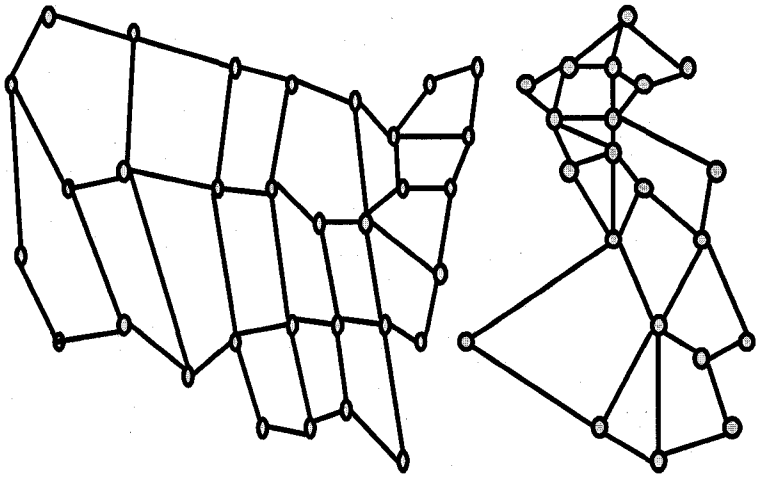

Network A Network B

Figure 4.5 Network Topologies Used in the Simulations

The performance measures considered in this study are:

- The blocking probability (BP), which is the probability that a connection request is blocked due to unavailability of a lightpath.
- The BER blocking probability (BER-BP), which is the probability that a connection request is blocked due to the lack of regenerators and low estimated BER at destination node.

In the following part of this section, we denote the set of simulation as $T = W \times R \times S \times \psi$. W is the set of regenerator placement scheme. W= {tunable-dense regenerator placement, fixed-sparse regenerator placement}. R is the set of the numbers of regenerators placed in

the network. S is the set of regenerator selection strategies. S= {on-route, off-route shortest path}. ψ is the set of different level of traffic loads. The possible values of R and ψ depend on the network scale. We present some numerical results obtained from subset of simulation set *T*.

In the following figures, "on-route" and "off-route" denote the two regenerator selection strategies and "dense" and "sparse" denote the two regenerator placement schemes: the tunable-dense placement scheme and the fixed-sparse placement scheme, respectively. With the sparse placement scheme, six fixed regenerator groups are placed optimally in network A, and three fixed regenerator groups are placed optimally in network B. The regenerators are placed at the nodes with the highest degrees. Each regenerator group consists of TR pairs, each of which operates at a different wavelength. Thus 18.75% of the nodes in the network A and 13.6% of the nodes in the network B have the capability of signal regeneration.

With the dense placement scheme, a total of 48 tunable regenerators (tunable T-Rs) are placed at 28 nodes in network A. 16 tunable regenerators are placed at 11 nodes in network B. Thus, in the dense placement scheme, 87.5% of the nodes in the network A and 65% of the nodes in network B are able to regenerate optical signals. Although more nodes have the capability of signal regeneration, much fewer TRs are installed in the networks.

# nodes	# links	Average Length	Average Node Degree
32	50	860 km	3.09
21	33	630 km	3.28

Table 4-2 Network Characteristics

The performance in terms of overall BP of the BER-assured RWA algorithms over network A and network B is demonstrated in Figure 4.6 (a) and (b), respectively. The overall BP represents both blocking probability for short distance calls and long distance calls. Short distance calls can be routed without regeneration of optical signals whereas, long distance calls need regeneration of optical signals at the intermediate nodes to meet

the BER requirement. The overall BP becomes higher with the increase of traffic load. At low traffic load, the RWA algorithms using an on-route regenerator selection strategy perform better than those using off-route regenerator selection strategy. Under a heavy traffic load, there is no significant difference in the performance of all the RWA algorithms.

In the evaluation of various regenerator selection strategies and regenerator placement schemes, BER-BP is a better performance indicator than overall BP, because only the long distance calls are evaluated. The BER-BP vs. traffic load over network A and network B is demonstrated in Figure 4.7(a) (b). Under the same regenerator placement, it is obvious that off-route regenerator selection schemes offer better performance than the on-route regenerator selection scheme, because it can search available regenerator throughout the whole network with a lower number of available transceivers. Although fewer total numbers of TRs are used in the dense placement scheme, the BER-assured RWA algorithms over a tunable-dense regenerator placement scheme can achieve better performance than those using a fixed-sparse scheme. We also compare the number of TR pairs needed to achieve a low blocking probability (< 10%). Obviously, the tunable-dense configuration requires a much smaller number of TR pairs to achieve a similar blocking probability when compared to the fixed-sparse configuration. This is because if the TR pairs are not tunable, it imposes an additional hop for which the wavelength continuity

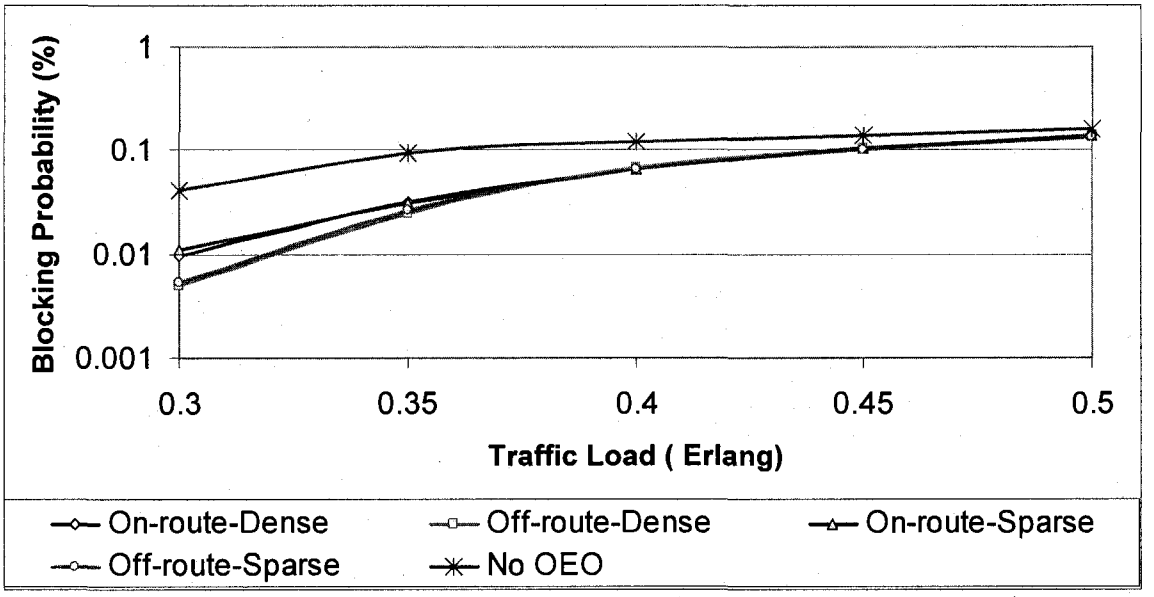

4.6 (a) Network A

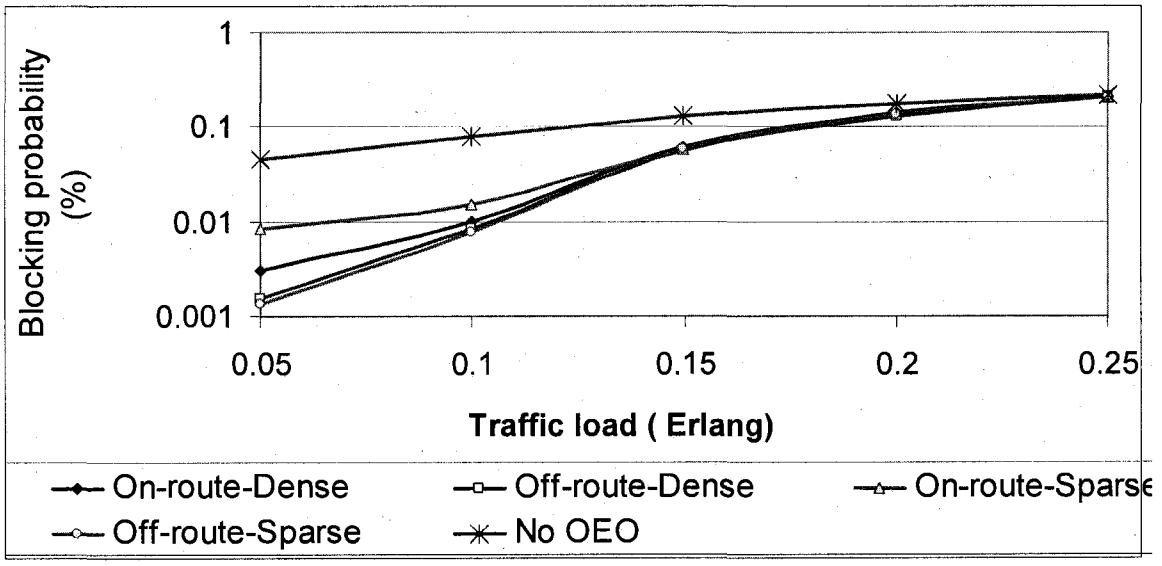

4.6 (b) Network B

Figure 4.6 Blocking Probability vs. Load for Different Regenerator Placement and Selection Schemes

constraint needs to be maintained. Hence we need only lower number of TR pairs in the tunable-dense configuration to achieve a blocking probability similar to that of the fixed-sparse configuration.

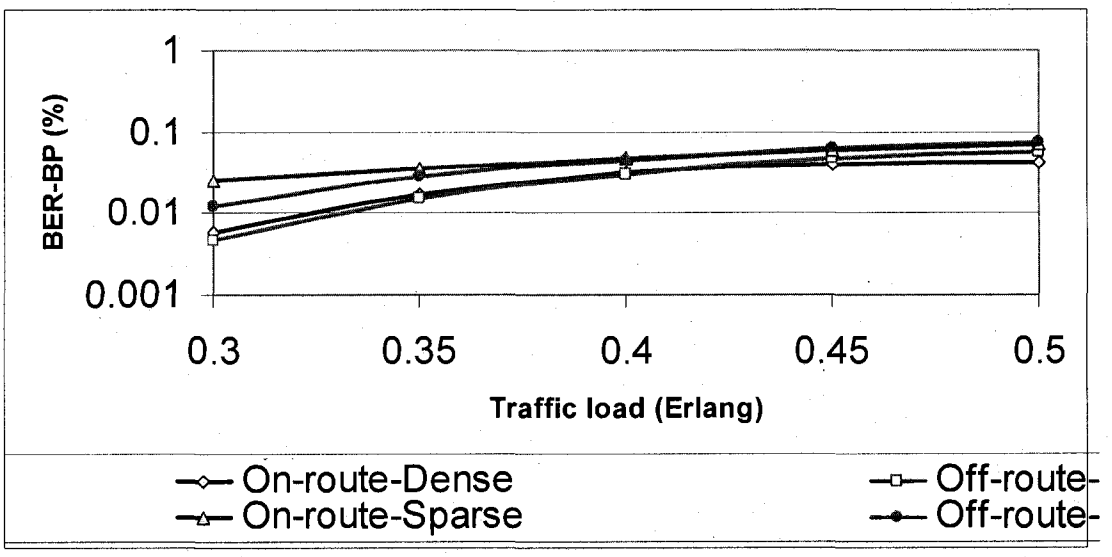

4.7 (a) Network A

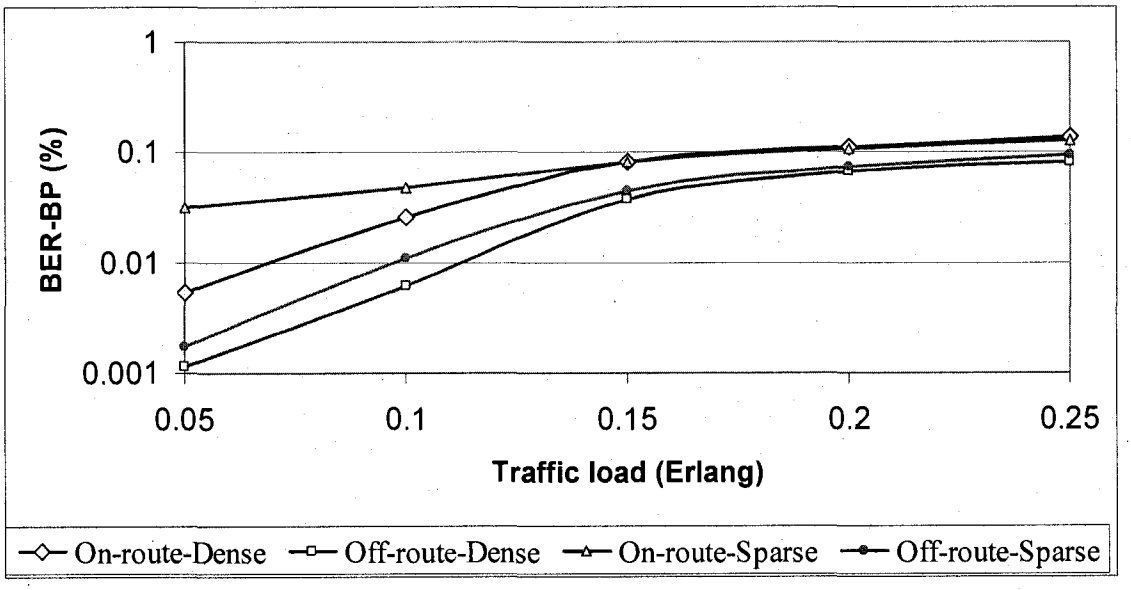

4.7 (b) Network B

Figure 4.7 BER-BP vs. Load for Different Regenerator Placement and Selection Schemes

4.5 Regeneration Mechanisms

In this current generation of optical networks, the service providers are looking to increase the capacity and reach without a substantial increase in cost. This can be achieved by the ability to build flexibility into the optical network, which would help the network devices to dynamically reconfigure it as needed to maintain a specific grade of service. The realization of reconfigurable and transparent WDM networks relies on several technologies. For point-to-point system technologies such as fiber, optical couplers, fiber amplifiers, receivers and lasers are required. Additional technologies needed to achieve reconfigurability are optical switches, optical filters and tunable devices like tunable lasers. The tunable lasers and filters can be used as building blocks in WDM networks with reconfigurability for improving protection and wavelength utilization. The add-drop multiplexers and the transmitter-receiver pairs in such networks are fully tunable to the whole range of wavelengths. The impact of the number of transceivers as well as the effects of the range to which they are tunable are studied in [SHE-03]. It is shown that increasing the tunability of the transceivers achieves a better utilization of the available TR pairs. In addition to tunability, the algorithms and strategies presented in the previous sections intelligently route the signals, optimizing the use of regenerators available in the network. This provides an added level of agility to the network. Another important constraint on the reconfigurability is the limitation on the number of available resources. With a limited number of resources and non-conforming traffic patterns it is possible that the QoS requirements might not be met. At any OXC the ability of the optical signal to be regenerated or add/dropped would depend on the number of available resources such as transceiver pairs available at that node. The blocking of a connection may be caused by the absence of TR pairs at either the source or the destination. This is because the transceiver cards for add-drop and regeneration function are very expensive (the cost of the regenerator cards is about 1/25 to 1/30 the cost of an OXC [SOL-02]). Hence, in a real optical network the number of regenerator cards and add-drop cards at a node is limited. Therefore, there is a need to efficiently utilize the sparsely available resources to increase the number of connections that can be established dynamically.

4.5.1 Add-drop and Regeneration Card Architectures

In this section a novel transponder card architecture is presented, however after reviewing some of the existing transponder card architectures. Figure 4.9 shows architectures used to regenerate optical signals. In the first mechanism, as shown in Figure 4.9 (a), two transponders are connected back to back. This type of regeneration is very inflexible in terms of reconfigurability. If any of the connections need to be torn down then it has to be done manually.

As shown in Figure 4.9 (b), the second mechanism consists of regeneration card that performs the regeneration function. This card is essentially both a transmitter and receiver on one card. In this mechanism the dropped signal is looped through the card and sent back into the optical network. Here again there is a loss of reconfigurability. Also, these regeneration cards can only be used for regeneration and cannot be used for add or drop.

The third approach, described in [SRI-03], is to use an adjunct switch which is another OXC having a scale similar to or slightly smaller than the optical bypass section.

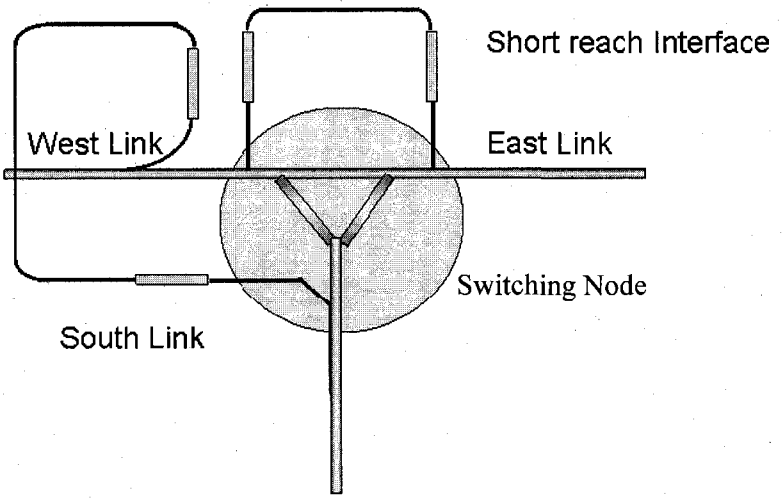

4.9 (a) Two Short reach interfaces connected back to back

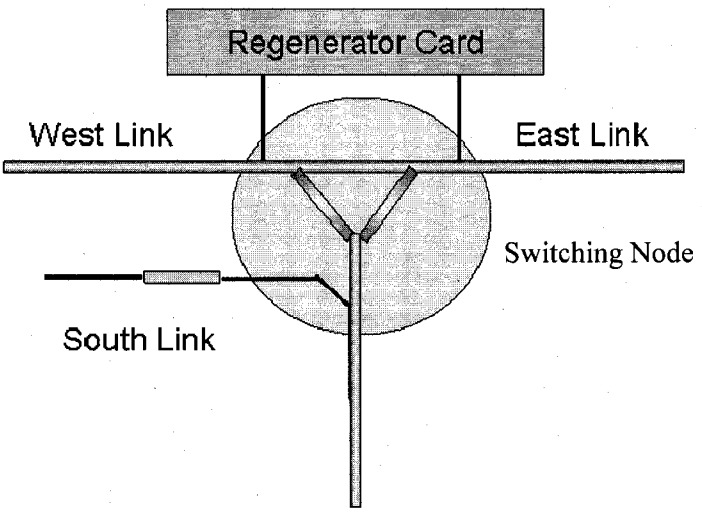

4.9 (b) Regenerator Card

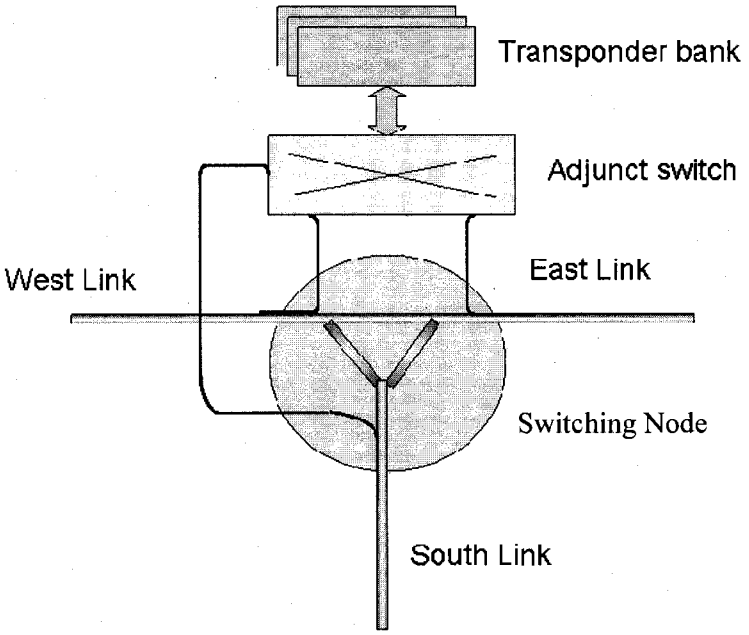

4.9 (c) Regeneration with adjunct switch

Figure 4.8. Regeneration Mechanisms

This is the general approach (Figure 4.9 (c)) that is followed to achieve steerability and maximal utilization of the available transponders in the system. Steerability is the ability to steer the traffic to any of the available transponders in order to fully utilize the available transponders. By proper design, it is possible for any wavelength in any direction to access any of the available transponders. The design of the adjunct switch is discussed in the next chapter.

The regeneration function and the add-drop function use the same TR pairs to add and drop the signals locally. A common approach is to reserve a specific number of transceiver pairs for regeneration traffic and for local add-drop traffic. Reservation of resources might have some problems associated with it, namely underutilization of resources caused due to unpredictable traffic patterns. At a particular moment, it might be possible that there are no transceivers in the add-drop section for transceivers to be added or dropped, whereas there might be free transceivers in the regeneration section that are not being used. Thus, this approach leads to under-utilization and/or sometimes over-provisioning of the common resource (transceivers). Over-provisioning of such transceivers would make the optical cross-connect used at that node less cost-effective, as the transceivers are very expensive sub-systems.

These transponders cards can be used for regeneration or for the add/drop function. Functionally the add/drop cards and regeneration cards perform the common function of signal regeneration. However, in an add/drop card, the signal is dropped locally via a client interface as shown in Figure 4.10 (a). This client interface is generally built into the card or is a plugin interface. In a regeneration card, the signal is dropped and regenerated and sent back into the network via two interfaces of the card. The functional block diagram of a regenerator card is shown in Figure 4.10(b). Since these two cards perform the common function of regeneration of the signal, the add/drop card can be modified to also accommodate the regeneration function as shown in Figure 4.10. This is achieved by placing a small switching element between the connections from the network side to the client side as shown in Figure 4.10(c).

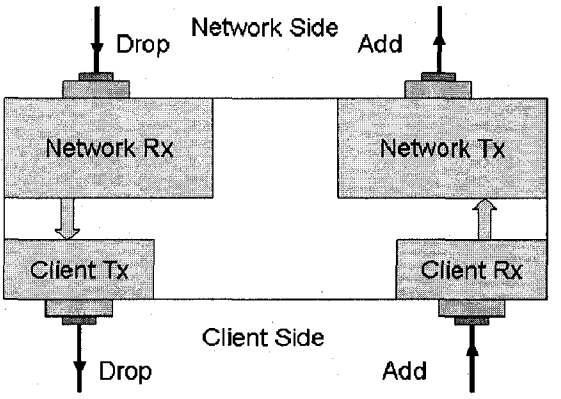

4.10(a) Simple Add/Drop Card

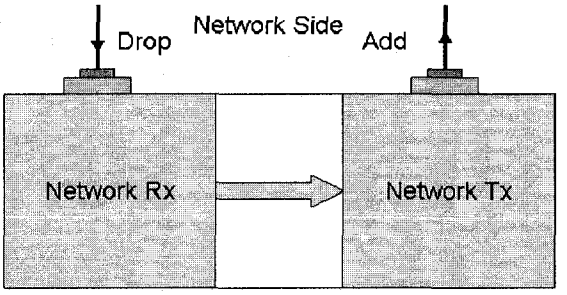

4.10(b) Regeneration Card

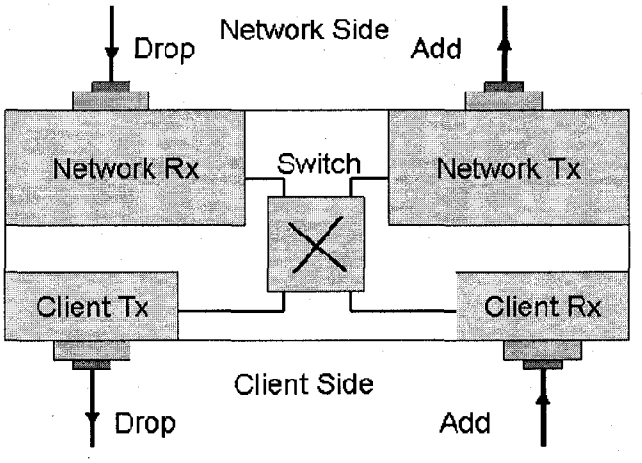

4.10(c) Add/Drop card with switching element to act as a regenerator

Figure 4.9 Add-drop Card Used for Regeneration

A switching node can have these two types of cards in the add/drop side of the switch. The add-drop connections can use the simple add/drop cards, whereas the regeneration connections can use the cards with the switching element in a loopback configuration, so

that the signal is sent back to the network. During a period of non-conformance of traffic, i.e., when there are more add/drop connections to be handled at a node, some of the connections can be routed to these cards dedicated for regeneration connections, and can be used in an add/drop configuration. Thus the need for over-provisioning can be avoided. Also, the blocking probabilities for the total number of add/drop connections are lower when using a sharing mechanism, as compared to a non-sharing mechanism with a fixed number of add/drop cards. In addition, the net cost of the system is reduced. In the next section we use an Erlang-B blocking model and overflow theory to show that sharing does indeed reduce the net blocking probability of the calls dropped at a node.

4.5.2 Loss Networks

We consider three optical switches modeled as loss network. The regimes under consideration are called "without-reservation," "with-partial-trunk-reservation" and "with-complete-trunk-reservation". Here, each available transponder card is referred to as a trunk (server). These terms are used interchangeably throughout the text. All three loss networks under consideration have n trunks.

We consider two types of arrival streams, add-drop traffic and regeneration traffic. The two arrival streams are modeled as independent Poisson processes with mean rate λ. So the pooled arrival stream is a Poisson process with mean rate 2λ. All three loss networks under consideration have n trunks (servers). We model all services as exponential with mean rate μ.

Under the without-reservation regime, a call is blocked if all n trunks are busy at arrival. This is an Erlang loss network, and the blocking probability for this network is given by Erlang's well-known B-formula

$$p_B^w = E[n,a] = \left(\frac{a^n}{n!}\right) \Big/ \left[1 + a + \frac{a^2}{2!} + \ldots + \frac{a^n}{n!}\right],$$

where $a = 2\lambda/\mu$ is the offered traffic intensity. Note that for this network, both types of traffic experience the same blocking probabilities that we denote as p_B^{wadd} and p_B^{wreg} for add-drop and regeneration, respectively. Hence, $p_B^{wadd} = p_B^{wreg} = p_B^w$. Note that the w stands for without reservation.

Under the partial-trunk-reservation regime, s of the n servers represent the add-drop section. Upon the arrival of an add-drop call it will check if there is an available server in the add-drop section. If there are no available servers, then it will try to find an available server in the regeneration section, that is the other $n-s$ servers. If there are no servers available in this section either, then the call is blocked. Upon the arrival of a regeneration call, it will check if there are available servers in the regeneration section. If not, then it is blocked. We denote the overall blocking probability as p_B^p and the respective blocking probabilities for the add-drop traffic and the regeneration traffic are p_B^{padd} and p_B^{preg}.

Under the complete-trunk-reservation regime, s of the n servers represent the add-drop section and the remainder will be the regeneration section. An add-drop call is blocked if there are no available servers in the add-drop section, and a regeneration call is blocked if there are no available servers in the regeneration section. This is the no sharing scheme. Using a c superscript notation for this regime, the blocking probabilities are

$$p_B^{cadd} = E[a', s] \quad \text{and} \quad p_B^{creg} = E[a', n-s],$$

where $a' = \lambda/\mu$ is the offered traffic intensity for each section. The overall blocking probability is $p_B^c = (E[a', s] + E[a', n-s])/2$.

Each loss network can be represented as a two-dimensional continuous time Markov chain (CTMC). The respective stationary distributions for these CTMC are denoted π_w, π_p and π_c. For convenience and for comparison, we also model the loss network without reservation as a two dimensional CTMC. The stationary measures are probability mass functions defined on $\{0,1,...,s\} \times \{0,1,...,n-s\}$, where for example (i, j) means that i add-drop servers are occupied while j regeneration servers are occupied.

Since Poisson arrivals see time averages, then the blocking probabilities are:

$$p_B^w = p_B^{wadd} = p_B^{wreg} = \pi_w(s, n-s), \tag{4.2}$$

$$p_B^{padd} = \pi_p(s, n-s), \; p_B^{preg} = \pi_p(\cdot, n-s) = \sum_{i=0}^{s} \pi_p(i, n-s) \tag{4.3}$$

and

$$p_B^{cadd} = \pi_c(s,\cdot) = \sum_{j=0}^{n-s} \pi_p(s,j),\ \ p_B^{creg} = \pi_c(\cdot, n-s) = \sum_{i=0}^{s} \pi_c(i,n-s). \qquad (4.4)$$

In the next section we order the per class blocking probabilities.

4.5.3 Ordering the Class Blocking Probabilities

In this section we show the following inequalities:

$$p_B^{padd} \le p_B^{cadd} \quad \text{and} \quad p_B^{padd} \le p_B^{wadd} \qquad (4.5)$$

and

$$p_B^{creg} \le p_B^{preg}. \qquad (4.6)$$

We obtain our result by considering the *uniformized* discrete time Markov chains associated with the continuous time Markov chains presented in the prequel. It is well known that these two chains have the same stationary distributions.

We construct the uniformized discrete Markov chains as stochastic recurrence sequences, which leads to a sample path argument to prove the inequalities. Without loss of generality, we assume that $2\lambda + n\mu = 1$ and partition the interval [0,1] as follows $C_1 = [0, 2\lambda]$, $C_2 = (2\lambda, 2\lambda + s\mu]$ and $(2\lambda + s\mu, 1]$.

We prove that the number of busy servers for the add-drop traffic satisfies the following inequality almost surely:

$$Q_t^{padd} = Q_t^{cadd} \le Q_t^{wadd}, \qquad (4.7)$$

where Q_t represents the number of servers available after t transitions and the superscript indicates the regime and the category of servers. The following inequality

$$Q_t^{creg} \le Q_t^{preg} \le Q_t^{wreg}. \qquad (4.8)$$

for the regenerative traffic is also be proven.

We assume initially that all servers are available. Hence, the preceding 2 equations are satisfied at time $t = 0$. We generate a sequence of independent uniform [0,1] random variables. We construct the uniformized Markov chains recursively with these uniform variables.

If the uniform variable falls in the lower half of C_1, then this will mean an add-drop arrival. The upper half of C_1 is for regeneration arrivals. If the uniform variable falls in C_2 either an add-drop server becomes available or it is a fictitious jump of the uniformized chain. We always dedicate the lower part of the interval to the service completions. For example, if at time t there are 5 busy add-drop servers, then if the uniform variable falls in $(2\lambda, 2\lambda + 5\mu]$, at time $t+1$ there are 4 busy add-drop servers. It is similar for the interval C_3, the lower part of the interval represents a regeneration service completion.

We assume that all servers are initially available so the inequalities $Q_t^{padd} = Q_t^{cadd} \le Q_t^{wadd}$, and $Q_t^{creg} \le Q_t^{preg} \le Q_t^{wreg}$ are satisfied for time $t = 0$.

For the partial-reservation and the complete-reservation regime, only the add-drop traffic has access to the s add-drop servers, and hence Q_t^{padd} and Q_t^{cadd} will coincide for all t, while due to overflow of the regenerative traffic into the add-drop servers for the without reservation regime, Q_t^{wadd} will always be larger or equal to the latter two quantities. Therefore, we obtain inequality $Q_t^{padd} = Q_t^{cadd} \le Q_t^{wadd}$, for all t.

There are no overflows of the add-drop traffic into the regenerative servers for the complete reservation scheme. But for the other two regimes the add-drop traffic overflows into the regenerative servers. Furthermore, we know that $Q_t^{padd} \le Q_t^{wadd}$, and thus they are more overflows for the without-reservation regime. Therefore, we obtain inequality $Q_t^{creg} \le Q_t^{preg} \le Q_t^{wreg}$, for all t.

From $Q_t^{padd} = Q_t^{cadd} \le Q_t^{wadd}$, we know that the Markov chains under complete-reservation and under partial-reservation will occupy states where the s add-drop servers are busy with the same long-run relative frequency. These states are the blocking states for the add-drop traffic under the complete-reservation regime but not for the partial- reservation regime. To block the add-drop traffic we require that all the servers be occupied. Therefore, $p_B^{padd} \le p_B^{cadd}$.

We also know that $Q_t^{padd} + Q_t^{preg} \le Q_t^{creg} + Q_t^{creg}$. Since for both the partial and complete reservation, we require that all servers are occupied to block the add-drop traffic, then by

the latter inequality we have $p_B^{padd} \leq p_B^{wadd}$. Thus, we have proven the inequalities $p_B^{padd} \leq p_B^{cadd}$ and $p_B^{padd} \leq p_B^{wadd}$.

From $Q_t^{creg} \leq Q_t^{preg} \leq Q_t^{wreg}$, it should be clear that $p_B^{creg} \leq p_B^{preg}$, since under the complete and partial reservation regimes the regenerative traffic is blocked if all $n-s$ regenerative servers are busy.

These sample path arguments do not allow us to compare p_B^{preg} and p_B^{wreg}.

It should be noted that if the add-drop traffic is of higher priority then the partial reservation regime should be considered the best regime, since it does improve the blocking probabilities for this higher class of traffic.

The effect on the overall blocking probability is investigated numerically in the next section.

4.5.4 Loss Networks Numerical Evaluation of the System

In order to evaluate the effects of sharing of transponders on the add-drop section we set up 2 systems defined in the above section. A numerical analysis is done for the system using a sharing (partial-reservation) scheme and is compared to a system that does not use a sharing (complete-reservation) scheme. The advantages of using the sharing scheme in terms of cost and blocking probabilities are explored in this section.

The number of available transponders for add/drop and regeneration traffic greatly impacts the blocking probabilities at an optical node. In the complete-reservation case, the traffic in the add/drop section and the regeneration section are mutually exclusive and do not impact the occupancies of the transponders in each section. On the other hand, in a sharing mechanism, the occupancies of the transponders' regeneration section is a function of the traffic load in the regeneration section and the add/drop section. A higher load in the add/drop section can overwhelm the regeneration traffic and can eventually lead to a decrease in the net blocking probability of the node. In order to study the impact of the variations in traffic load on the net blocking probability, an optical add/drop node with sharing and no sharing is considered. Here the number of transponders for add/drop and regeneration $M_1 = M_2 = 6$. For the complete-reservation scheme the blocking probabilities are evaluated using a simple Erlang-B blocking formula.

However, the sharing architecture corresponds to an overflow system. The overflow is generated only when the TR pairs reserved for add-drop (primary group) connections are in the blocking state. The analysis of the overflow traffic cannot be done by a simple Erlang-B loss formula, because this will always underestimate the number of TR pairs (trunks) needed to achieve a desired blocking probability. This is because the overflow traffic does not conform to classical models of pure chance traffic (PCT). The overflow traffic is more bursty than the ordinary Poisson process and is characterized by the Interrupted Poisson Process [KUZ-92].

The primary group (add-drop) of trunks has m_1 TR pairs. The secondary group (regeneration) has m_2 TR pairs. The arrival rate of add-drop connections is λ_1.The regeneration traffic arrives with an intensity of λ_2. The add-drop and regeneration traffic leaves the system with rates μ_1 and μ_2 respectively. The regeneration traffic is offered only to the secondary group. Hence this can be considered overflow traffic from the primary group, with no trunks in the primary group. The overflow traffic from the primary group, i.e., is the add-drop traffic is also added as to the load for the secondary group. This traffic intensity is not Poisson. Hence, the blocking probabilities for this system are evaluated numerically by solving the system of equations for the boundary conditions.

We assume all transition rates and the joint probabilities exist and are finite since we have a finite number of servers. The system described above is represented by a 2-D markov chain as shown in Figure 4.11. The equilibrium condition equations for this boundary condition are given by the following equations

Region 1: This region occurs when there are only add-drop calls in the system

$$y[i,0](\lambda_1+\lambda_2+i\mu_1)=\mu_2 y[i,1]+(i+1)\mu_1 y[i+1,0]+\lambda_1 y[i-1,0]$$

for $0< i< m1-1$ (4.9)

Region 2: This is the part of the system when there are only regeneration calls arriving in the system and no add-drop calls

$$y[0,j](\lambda_1+\lambda_2+j\mu_2)=\mu_1 y[1,j]+\mu_2 y[0,j+1]+(j+1)\lambda_2 y[0,j-1] \quad (4.10)$$

for $0< j < m_2-1$

Region3: This region represents those states when all the regeneration transponders are occupied and add-drop calls start arriving in the system

$$y[i,m_2](\lambda_1+i\mu_1+m_2\mu_2)=\lambda_1 y[i-1,m_2] +(i+1)\mu_1 y[i+1,m_2]+ \lambda_2 y[i,m_2-1] \quad (4.11)$$

for $0< i< m_1-1$

Region 4 : This region represents the states when the add-drop transponders are all used and more calls (add-drop or regeneration) arrive and use the transponders in the regeneration section.

$$y[m_1,j](\lambda_1+\lambda_2+j\mu_2+m_1\mu_1)=(j+1)\mu_2 y[m_1,j+1]+\lambda_1 y[m_1-1,j]+\lambda_1 y[m_1,j-1,k]+\lambda_2 y[m_1,j-1] \quad (4.12)$$

for $0<j< m_2-1$

Region 5: This region represents all the states enclosed within the boundaries

$$y[i,j](\lambda_1+\lambda_2+i\mu_1+j\mu_2)=\lambda_1 y[i-1,j]+ \lambda_2 y[i,j-1]+(i+1)\mu_1 y[i+1,j]+(j+1)\mu_2 y[i,j+1]$$

for $0< i < m_1-1$ *and* $0< j < m_2-1$ (4.13)

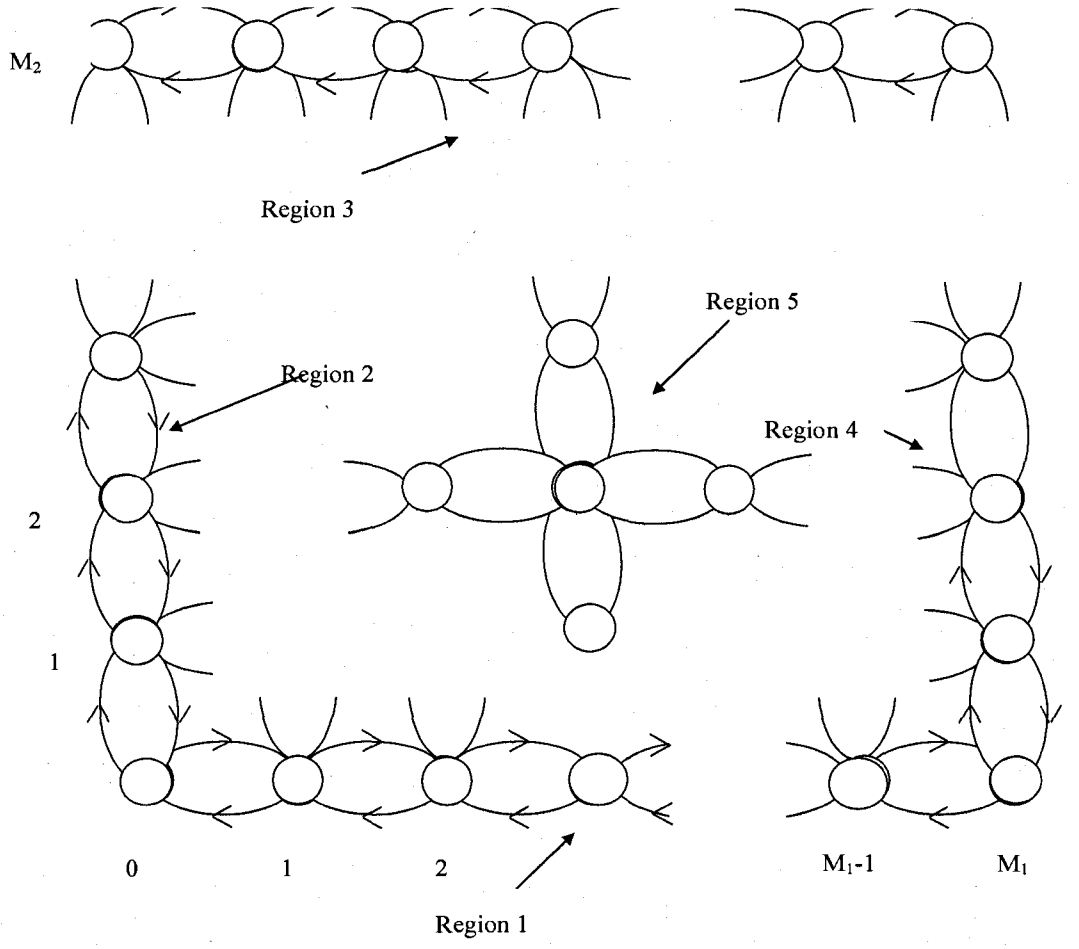

Figure 4.10 State Diagram for Overflow Model

The following 4 equations represent the 4 corners of the 2-D markov chain

$y[m_1,0](\lambda_1+\lambda_2+m_1\mu_1)=\mu_2 y[m_1,1]+\lambda_1 y[m_1-1,0]$ (4.14)

$y[0,0](\lambda_1+\lambda_2)=\mu_1 y[1,0]+\mu_2 y[0,1]$ (4.15)

$y[0,m_2](m_2\mu_2+\lambda_1)=\lambda_2 y[0,m_2-1]+\mu_1 y[1,m_2]$ (4.16)

$y[m_1,m_2](m_1\mu_1+m_2\mu_1)=(\lambda_1+\lambda_2)y[m_1,m_2-1]+\lambda_1 y[m_1-1,m_2];$ (4.17)

Solving these boundary conditions, we can determine the steady state blocking probabilities. The normalization equation is given by

$$\sum_{i=0}^{m1}\sum_{j=0}^{m2} p_{ij} = 1 \qquad (4.18)$$

The add-drop calls will be blocked only when there are no transponders in both the add-drop and regeneration section. The blocking probability for add-drop calls can be then given by

$$P_b^{add-drop} = y(m_1, m_2) \tag{4.19}$$

The blocking of the regeneration calls will however depend on the add-drop calls and the regeneration traffic load. Hence we sum across all the states

$$P_b^{regen} = \sum_{i=0}^{m_1} y(i, m_2) \tag{4.20}$$

The blocking probabilities of the regeneration sub-system and the add-drop subsystem system with and without sharing are plotted. From Figure 4.12(a) it is clearly evident that for the regeneration section, the sharing results in an increase in the blocking probability of the regeneration calls. For a low load of add-drop traffic and low load of regeneration traffic, there is not a significant difference in the blocking probabilities between sharing and no sharing mechanisms. However, for the add-drop calls, the sharing results in a net decrease in blocking. This is because the add-drop calls that do not find enough resources in the add-drop section are allowed to find free resources in the regeneration section.

It is clear that for the no sharing mechanism, the regeneration blocking probability is only dependant on the load of the regeneration traffic. This is intuitive, as there is mutual exclusion in the usage of the transponders for the different types of traffic. However, in the sharing mechanism, the net blocking probability is dependant on both the add/drop and regeneration loads as seen in Figure 4.13. By using the sharing mechanism it is visible that the net number of calls that are dropped at a node (add-drop calls or regeneration calls) are higher as compared to the no-sharing mechanism. This can be clearly seen in Figure 4.13. The surface plot for the sharing mechanism is lower than that for the no-sharing mechanism. The impact on the blocking probability on the sharing on the regeneration calls can be reduced by using a resource aware algorithm, which results in using regenerators at nodes with a higher availability.

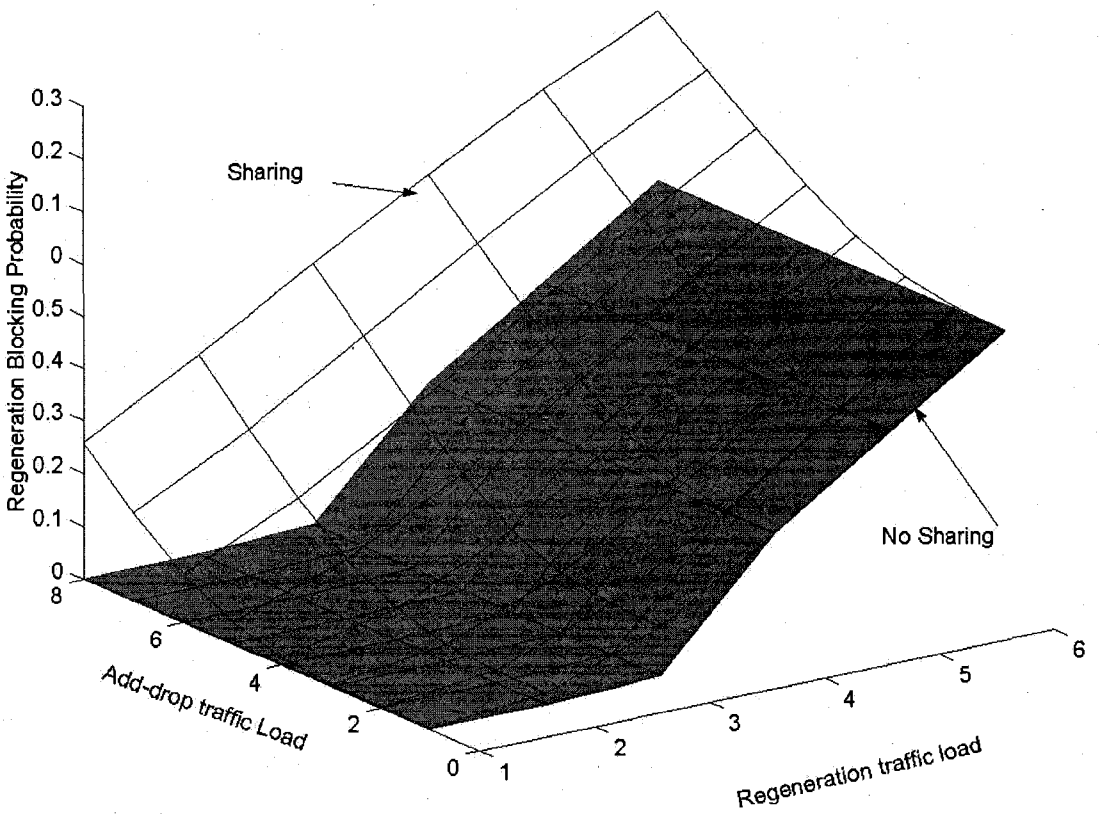

4.12 (a) Regeneration Traffic

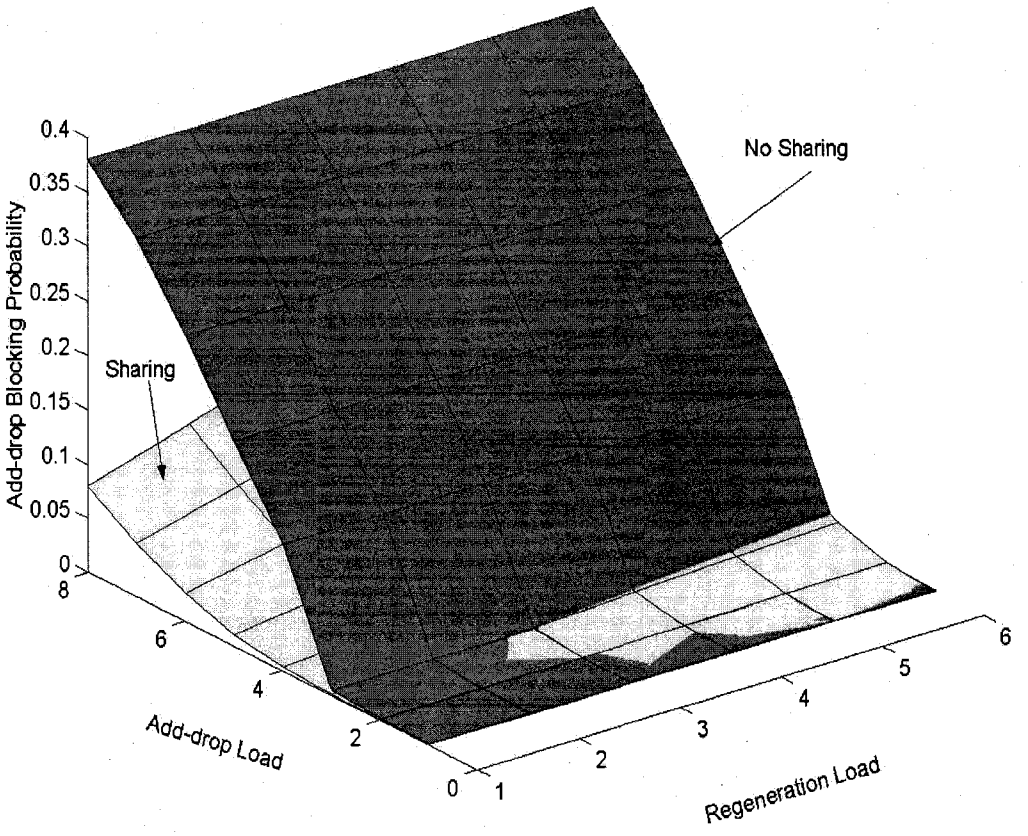

4.12 (b) Add-drop Traffic

Figure 4.11 Blocking Probability for Various Load Levels of Add/drop and Regeneration Traffic M1=M2=6 for Add-drop and Regeneration Traffic

It can be seen that though the blocking of regeneration calls increases due to sharing the net blocking of the total number of calls and is lower at low and medium loads, the sharing mechanism is actually better in terms of the blocking probability. This is because a higher number of add-drop calls get accepted due to the sharing of transponders from the regeneration side.

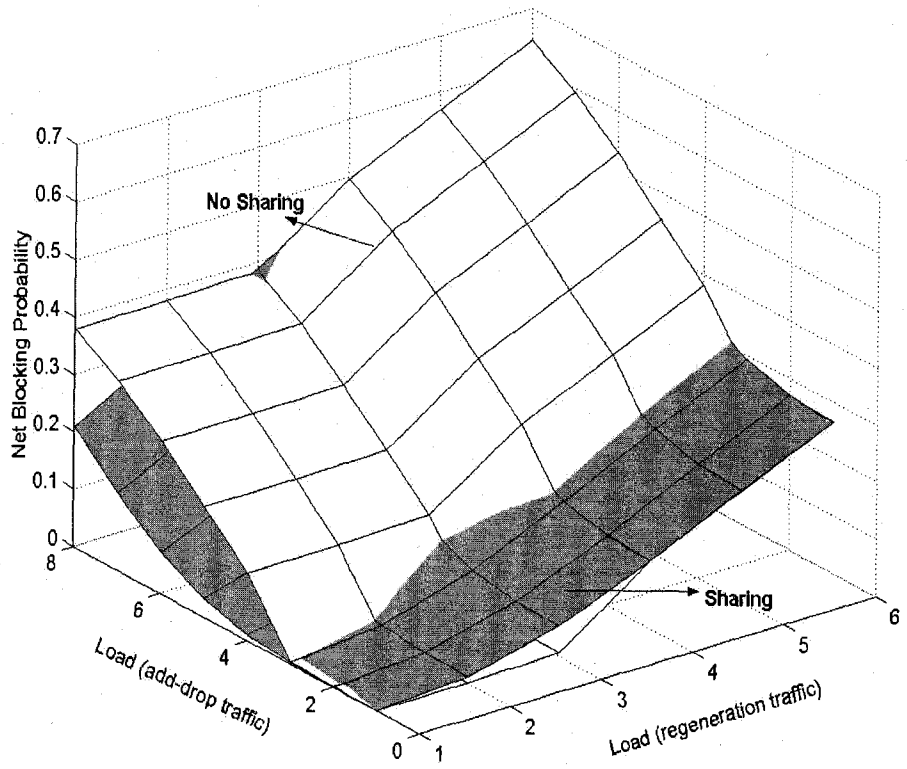

Figure 4.12 Net Blocking Probability for Various Load Levels of Add/drop and Regeneration Traffic M1=M2=6

4.6 Summary

The transmission impairments in optical networks due to the underlying physical layer cause a severe degradation of the optical signal. This is more pronounced in signals that travel long distances and many hops. The way to limit or minimize the impact of these impairments is by having 3-R regeneration at all or a few nodes in the network. By proper placement of the regeneration nodes and using impairment aware routing algorithms the impact of these effects can be minimized. In this research, we developed intelligent routing algorithms which are aware of the placement of regenerators and the number of regenerators in the network. These algorithms provide signal quality guaranteed connections, which reduces the impact of the physical impairments.

We investigated different regenerator placement schemes and the design of a novel BER-assured routing and wavelength assignment algorithm. We first provided a

qualitative analysis of fixed-sparse and tunable-dense regenerator-placement schemes. Then, by using the BER-assured RWA algorithms, we provided a quantitative comparison of the two regenerator-placement schemes. From the simulation results, we observed that the tunable-dense regenerator-placement scheme can achieve similar or equivalent performance to the fixed-sparse scheme, with, however, a much smaller total number of transponders in the network. Therefore, the tunable-dense regenerator-placement scheme is more cost-effective than the prevailing fixed-dense regenerator-placement scheme. We also examined the performance of several regenerator selection strategies. The numerical results demonstrated that the off-route shortest-path regenerator selection strategy can achieve consistent high performance by using the regenerators efficiently. However, due to the high computational complexity associated with the off-route shortest-path regenerator selection strategy, other simple regenerator selection strategies, i.e. on-route regenerator selection strategy, could be a favorable alternative, especially when sufficient regenerators are available in the network.

In this chapter, we also developed a novel architecture to achieve maximal sharing amongst transponder cards. By adding a small switch between the transmit and receive interfaces of a transponder card, we were able to make it function as an add-drop and regenerator card. Thus, when traffic was bursty for certain time periods, the additional transponders needed to handle the bursty load could be borrowed from the regeneration section. This allowed maximal sharing of transponder cards during periods of non-conformance of traffic.

Chapter 5. Steerability at an Optical Switching Node: Architectures and Cost models

5.1 Introduction

The advent of an agile optical networks and revenue generating services like Optical Virtual Private Networks (O-VPNs) and Optical Ethernet (OE) have pushed the need for a dynamically reconfigurable optical network. The numbers of Transmitter-Receiver (TR) pairs present at a node play an important part in the agility of the network. At present this evolution is largely technology driven with vendors pushing the technology envelope to provide solutions, which have higher capacity, can go further all-optically and are more reconfigurable and cost effective. This can be easily represented by a Cost-Reach-capacity graph as shown in Figure 5.1:

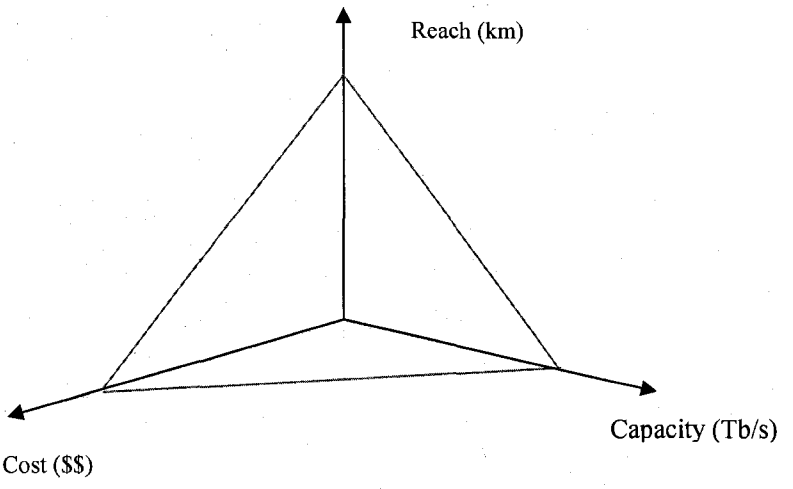

Figure 5.1Cost-Capacity-Reach Curves

As the vendors pursue their diverse visions it is possible that the underlying optical layer is made up of a varied range of technologies, which have varying implications on the routing strategies. Hence, there is a need to push for standards in the Optical control plane. Standards like Generalized Multi-protocol Label switching (GMPLS), Private-Network to Network Interface (PNNI), Optical-User to network interface (O-UNI) and Automatic Switched Transport Network (ASTN) have been proposed.

Currently several standards bodies are pursuing the definition of a common control plane strategy at the signaling layer, to allow the network operator to establish service connections between any two types of network elements, and between any 2 types of administrative domains. An example of such a network is illustrated in the Figure 5.2. In order to increase the size of the Cost-capacity-Reach envelope in a cost effective manner an accurate equipment inventory and established connections needs to be available.

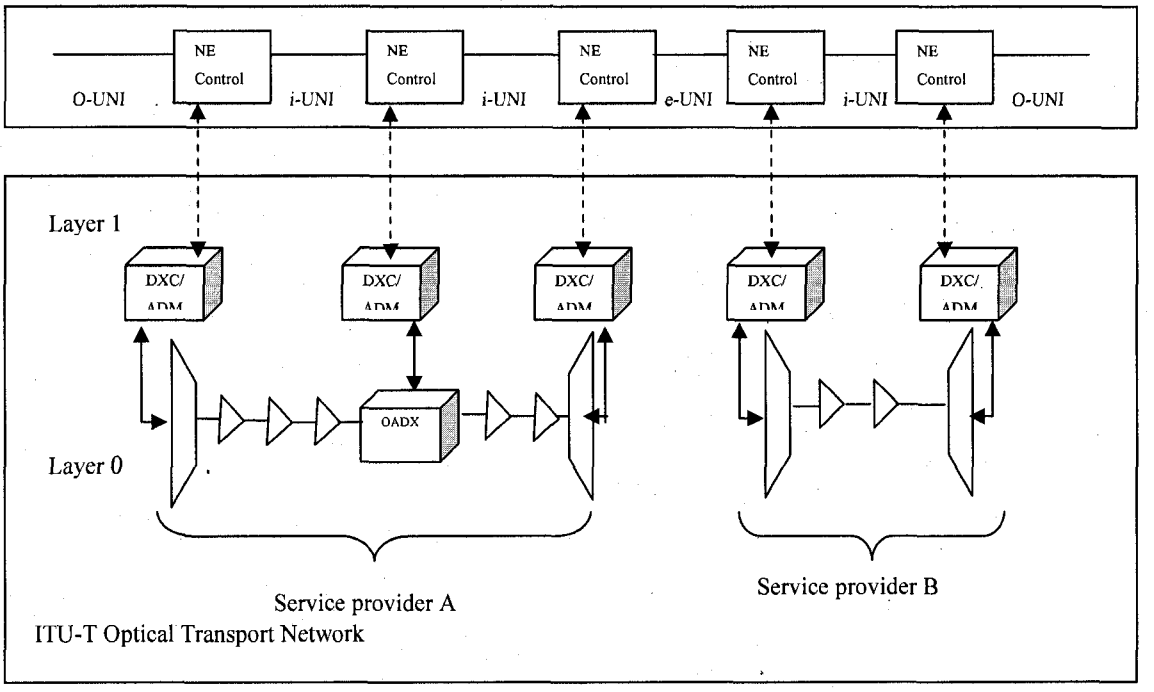

Figure 5.2 Optical Transport Network Layers

However, in order for this to become a reality, the architecture and cost structure of the equipment infrastructure has to evolve dramatically from the static point-to-point systems that are currently prevalent in order to support unique service delivery models. The dynamically reconfigurable mesh networking model is believed to be the answer to meet highly variable bandwidth demand and support for the emergence of differentiated optical networking services [GOL-99]. In such a network, the control plane is responsible for dynamic assignment of resources (optical and electronic) to the different connections. This control plane would enable dynamic wavelength routing through multiple cross-connects with end-to-end signaling. Optical techniques for such functionalities are not currently available, or are too expensive to be implemented in the optical domain. Great

strides in optical technologies (in signal transmission and regeneration) have been made, bringing the vision of all-optical networking closer to reality. One of the major challenges of the current market is to reduce the infrastructure cost of deploying bandwidth. This creates an imperative to reduce over-provisioning of bandwidth and maximize utilization of bandwidth that is deployed. In order to reduce the processing granularity, service providers are moving to third-generation wavelength switches that replace the electrical core of today's OEO architecture with an Optical Cross-Connect (OXC) matrix to improve network efficiency. The advantages of OXCs in terms of the capital expenditure and operational expenditure are very well documented [DOS-01][AGR-97][RAM-02]. This optical switching matrix consists of a core optical switch (which performs the functions of switching and optical bypass) and an adjunct switching matrix to perform add-drop and signal regeneration. The signal regeneration and add-drop is done in the electrical domain. For each signal wavelength, the interface between the optical and electrical sections is provided by a transponder which is dynamically tunable to the required wavelength. These transponders are very expensive opto-electronic devices and should be deployed on an as-needed basis and fully leveraged once in service. Transponders and associated hardware constitute the terminal equipment, which originates and terminates signal wavelengths for transmission. In today's DWDM transmission system architectures, terminal equipment typically constitutes about 70% of the total cost of deploying a transport network. In tomorrow's agile optical network, in the absence of steerability and sharing of transponder resources, terminal equipment cost could represent an even higher percentage of the overall cost. Maximizing network bandwidth efficiently and flexibly, while simultaneously maximizing return on invested capital (ROIC), requires that the number of transponders at an OXC be minimized. This chapter presents three novel architectures for the adjunct switch which allows maximal sharing of deployed transponders and thus reduce the cost of the node. The switching architectures presented in this thesis are made up of a combination of splitters and combiners or a combination of Wavelength Selective Switches (WSS) and splitters and combiners. WSSs are ordinarily used in a *1xK* (or equivalently a *Kx1*) configuration, in which any wavelength channel or channels on the input line can be independently routed to any of the K output lines. A number of solutions for the adjunct switch architecture

have been provided in the literature [SRI-04][OKA-96][KOG-96][STA-99][MIT-98]. One of the approaches discussed in literature is to split the incoming signal, de-multiplex it and send the demultiplexed signals to the transponders. This approach leads to the signal power being weakened, making signal detection difficult and increasing the net BER. To counter this, more amplifiers are added to the system, increasing the net cost per wavelength in the system. A second approach that has been suggested is to use an electrical switching matrix to route the signals to the corresponding transponders. This is not scalable in terms of the cost [DOS-01][AGR-97][RAM-02]. The third approach, described in [SRI-04], is to use an adjunct switch which is another OXC with a similar scale as the optical bypass section. This is, however, an expensive proposition and would result in the cost of the switching system to almost doubling. Moreover, the implications of optical loss and the nodal cost impact of compensating for such losses have not been addressed [SRI-04]. In [MOK-04], the authors present a dynamic sharing scheme to reduce the port count. However, these solutions do not consider the transmission impairments in such architectures, which make them practically infeasible. The architectures of the adjunct switch provided in this thesis are smaller in dimension and easily scalable to a higher number of wavelengths. To our knowledge, the research presented herein is the first of its kind to study steerable architectures that are based on wavelength selective switching and account for transmission impairments. In addition, this part of the thesis analyzes the cost of the switch as a function of the WSS and the number of add/drop ports. This work also examines different architectures used in the add-drop sub-section for a 4-degree node as shown in Figure 5.3. The OXC shown in Figure 5.3 is a layered OXC, with a transparent switching matrix followed by an add-drop sub-section. The transparent optical core can be made up of various technologies, such as a MEMS-based switching fabric arranged in a Clos structure [WOS-01] or a non-blocking optical cross connect (OXC) using multimode imaging (MMI)-based generalized Mach–Zehnder (MZ) interferometers [EAR-03]. In this thesis, we focus on the add-drop sub-section, and present three different architectures for the use in the steerable switch. The main objective of this thesis is to propose architectures that support 100% steerability of wavelength traffic in a scalable and cost-effective manner. Steerability is the ability to steer the traffic to any of the available transponders in order

to fully utilize the available transponders. The architectures presented in this work are fully steerable, which allows a wavelength on any fiber to reach any transponder, and can fully share interface shelves across directions and wavelengths. We evaluate the architecture based on the net cost, steerability, scalability and dependencies of the cost on the various elements in the sub-system.

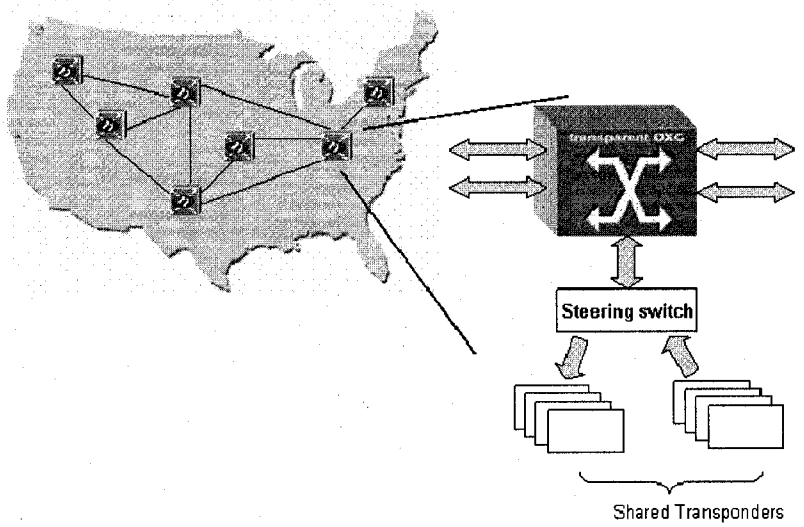

Figure 5.3 Functional Diagram of a 4 Degree OXC

5.2 Add-drop Architectures

We investigate three types of fully steerable add-drop architectures on a 4-degree node. The steerable switch architectures are broadly classified into A) Splitting and combining method, B) Parallel WSS Design, C) Cascaded WSS design. The Parallel WSS design can be implemented using a 1x5 WSS or a 1x9 WSS. These are representative of a 4-degree node with 4 fiber pairs as shown in Figure 5.3. We assume that the transparent core of the steerable switch is made up of a low loss compact integrated optics based WSS [DOE-02]. Such an element can direct any DWDM signal on the input fiber to any one of multiple output fibers. In this study, we assumed that a low-cost, non-blocking WSS with low insertion loss in the express path is used in the transparent core switching fabric. The WSSs devices are reciprocal and can be used to both separate and combine DWDM signals. All the steerable switching architectures presented in this thesis can be functionally divided into three sections: a splitting/combining section, a switch fabric

(switching) section and a transponder section. In the splitting/combining section the signal is split into (or combined from) the number of ports (D) from which the optical signal arrives at (and departs from) the node. The signal that comes out of the splitting/combining section is passed to the switching section, where the signal is routed to the transponder section. Depending on the architecture in question, the switching section is made up of a combination of splitters or combiners, or a combination of WSS and splitters/combiners. Compensating amplifiers are provided in order to compensate for the losses encountered by the signal due to the different elements in the steerable switch. The insertion losses of the different elements used in the steerable switch are listed in Table 5.1. Each transponder in the transponder section receives the signal from each direction. The transponders are provided with a Dx1 (or a 1xD) switch, which allows the transponder to select (send) the signal from (to) one of the D ports. Thus an optical signal from any port can reach any available transponder. Also, it should be noted that loss and power levels at the transmitters and receivers for all architectures are the same. Though we present steerable switch architectures for a 4 degree node, these results can be scaled up or down for higher or lower degree nodes. It has been assumed that we are able to add-drop 65% of the connections in a fiber. This assumption has been made in order to have multiples of 8 in the design. Also, when the signals are dropped at a node, they can terminate at the client equipment or can be regenerated and sent back into the network. An add signal can be generated from a client equipment or can be a regenerated signal. The different architectures for the regeneration side are presented in [SIM-05]. The total number of wavelengths that are available for signal transmission is assumed to be 98. These architectures can be scaled from 0 to 100% fill. The wavelength fill level indicates the number of wavelengths that are lit. Thus, a wavelength fill of 50% indicates that about .5*98= 48 wavelengths are lit, and a fill level of 100% indicates that all the 98 wavelengths are lit.

Table 5-1 Optical Components Specification

Symbol	Description	Value	Unit
L_{S4}	1:4 Splitter loss	-6.8	dB
L_{S16}	1:16 Splitter loss	-13.5	dB
L_C	Connector Loss	-0.4	dB
IL_{Sw}	1x4 Switch Insertion loss	-1.5	dB
IL_{TF}	Tunable Filter Insertion loss	-3.5	dB
IL_{TDC}	TDC Insertion loss	-4.5	dB
P_{Tx}	Power level at Transmitter	-5	dBm
P_{Rx}	Power level at receiver	-6	dBm
G_{SCA}	Single Channel Amp Gain	18 to 20.4	dB
IL_{WSS}	Insertion Loss of WSS	-7	dB

5.2.1 Splitting and Combining Architecture

In this architecture, the add/drop optical signal is routed through combining/splitting into identical copies equal to the number of transponder ports as illustrated in Figure 5.4. As seen in Figure 5.4, the sub-system can be functionally divided into 3 sections: a splitting section, a switch fabric section and a transponder section. Initially, after the splitting section, the signal is amplified and then split without any other intervening amplification. At the switch fabric Section, 1:4 splitters/combiners and 1:16 splitters/combiners are used in tandem for wavelength steerable with full non-blocking property. This non-blocking switching functionality can be explained as follows: Let us consider the drop side. Here, at the splitting section the signal is divided into identical copies by the 1:4 splitter. Each copy of the signal is then passed to the switching section. At each switching section the signal is further split 4 ways by a splitter and a 1:16 splitter further splits each output. The outputs of each of these splitters are connected to tunable transponders. Thus each transponder receives a copy of the dropped signal with the full wavelength spectrum. The transponder can now tune to the corresponding wavelength and the signal can be dropped at that transponder. The add functionality is the reverse of the drop function. Thus any transponder can reach any wavelength on any fiber, irrespective of the direction of propagation, and can reside in any shelf which provides the interface between the optical

layer and the client layer. As seen in Figure 5.4, each transponder section uses a single channel Erbium Doped Fiber Amplifier (EDFA) and a tunable filter on both the transmit and receive sides. The tunable filter removes amplified spontaneous emission (ASE) outside of the signal wavelength. For the drop (receive) side, a tunable filter must precede the receiver to pick up the wavelength of interest from the full spectrum of 98 wavelengths. A single channel EDFA is required to compensate for the losses of coupler array. This architecture supports 65% add-drop (265 transponders out of a total possible 392, based on 98 per fiber pair). This can, however be scaled up to support 100% drop. One of the drawbacks of this architecture is its inefficient utilization of the optical power budget. High-gain, high-power EDFAs are required to boost the signal prior to and following the multitude of splitters and combiners, resulting in a significant portion of the optical power budget being utilized for loss compensation of the branching tree. The various losses encountered and signal levels at the transponders are indicated in Table 5.1. The EDFA gain required can be calculated by adding the various losses. Since loss and power levels at the transmitters and receivers for all architectures are the same, the power budget for add side can be given as

$$PowerBudget = L_{Tx} + G_{SCA} + IL_{TF} + IL_{sw} + L_{S16} + G_{EDFA} + 2 * L_{S4} + 13 * L_C = -10.2dBm$$

From the above equation, the EDFA gain for the add side can be calculated as 9.1dB. Similarly the amplifier gain for the drop side can be calculated by the following equation

$$-5.2 + 2 * L_{S4} + G_{EDFA} + L_{S16} + IL_{SW} + IL_{TF} + G_{SCA} + IL_{TDC} = -6dBm$$

From the above equation, the gain on the drop side can be calculated to be 18 dB. In addition, the first wavelength cost is high as the splitters & amplifiers supports 64 transponders. Moreover, as there is no tunability inherent in the architecture, the additional cost of tunable filters is incurred on both add and the drop sides.

5.2.2 Parallel WSS Architecture

In the second architecture, we use a 1X5 port Wavelength Selective Switch (WSS) to perform the switching function. This design can also be functionally divided into the 3 sections described in the above paragraph. Here, the switching matrix comprises a set of

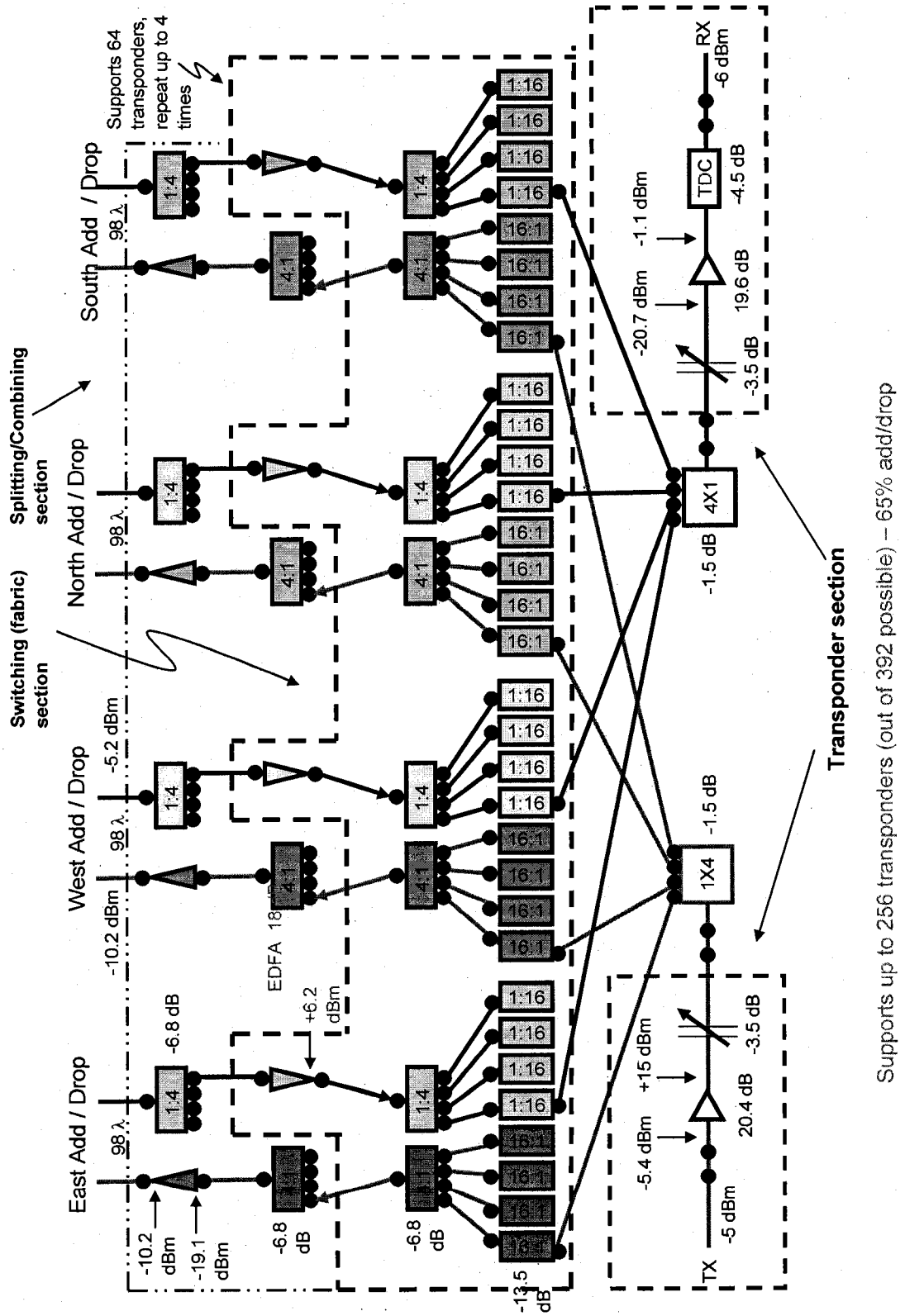

Figure 5.4 Steerable switch architecture using only Splitters and Combiners

WSS used in parallel, which provides per port wavelength selectivity, unlike the passive splitter/combiner architecture. The WSS has numerous integrated functions like de-multiplexing, flexible wavelength switching, multiplexing, power attenuation, and wavelength blocking. A particular strength of the WSS is its ability to switch a wavelength or a group of wavelengths at its input port to any of its output ports. The WSS is commercially available, with an insertion loss of about 7 dB. In the Parallel WSS architecture, we use a 1: N splitter to split the incoming signal initially. The value of N is dependent on the number of ports on the WSS and the number of wavelengths that need to be dropped. This is discussed in detail in section 5.4. For a fair comparison across the different architectures, the percentage of add/drop wavelengths supported was assumed to be identical at 65%, which necessitates the use of 1:4 splitters to split the signal. The split signal is then passed onto the 1x5 WSS, which has circulators at the inputs/outputs. The optical circulator is a 3-port device, which allows the light to travel in one direction. This isolates the add channels from the drop channels that are traveling in opposite directions. This is merely a design choice. We can use the 1x5 coupled with circulators or two 1x5 WSS by replacing the circulators. The pricing of these elements would be of paramount importance when choosing either design. Since wavelength selectivity is provided by the WSS, the wavelength that must be dropped is simply selected and switched to the port where it will be dropped. Following the WSS, the signal is amplified in order to compensate for the insertion loss of the WSS, and to compensate for the loss in power due to the 1:16 splitter. Each splitter output is connected to a transponder and thus the signal can be routed to an available transponder. With this configuration, any wavelength can be switched to any output port, and can fully share interface shelves across ports and wavelengths.

The addition of wavelengths involves largely the same functions mentioned above, but in reverse. This architecture is a highly integrated solution, reducing the overall system complexity and cost by reducing the number of discrete components and interconnections. On the drop path, the integrated demultiplexing capability of the WSS ensures that only the selected wavelengths are amplified by the subsequent EDFA. This eliminates the need to amplify the full spectrum of wavelengths unnecessarily, thus

utilizing the optical power budget optimally. The EDFA gain can be calculated in a way similar to the previous section. The amplifier gain on the add side is calculated to be 25.7 dB, and the amplifier gain at the drop side is calculated to be 21.6 dB. On the add path, the built-in attenuation capability of the WSS eliminates the need for tunable filters on each transmitter to suppress ASE. Again, the use of the 1X5 steerable switches maintains the full non-blocking property. One of the disadvantages of this architecture is its inability to support pay-as-you-grow economics through modular addition of building blocks. The deployment of the first transponder triggers the deployment of 4 wave switches and some EDFA's. Also, the presence of circulators increases the component count and cost.

An alternative solution is to use a 1x9 WSS as shown in Figure 5.6. This architecture eliminates the use of the circulators while preserving all of the advantages of the Parallel WSS architecture proposed above. The elimination of circulators results from the added number of input/output ports in the 1x9 WSS. The use of the 1x9 WSS instead of the 1x5 WSS is a design choice, which is dependent on the cost of the 1x9 WSS. A quantitative analysis is provided in the next section.

5.2.3 Cascaded Add-drop Architecture

In the architectures discussed above, the initial investment for a network operator is large; as the switch fabric infrastructure to support the full anticipated add/drop capacity needs to be deployed upfront. A useful and commonly used metric is the "first wavelength cost" which computes the total infrastructure cost incurred by the network operator before the first wavelength can be provisioned in service and starts generating revenue for the operator. In the previous architectures, the requirement for splitters, combiners, and EDFAs is primarily driven by the need to support add/drop scalability for the future. Although it could be several years before these splitters, combiners and EDFAs are actually put to use in adding/dropping wavelengths, the expense involved in deploying these components is incurred initially, well before they are able to generate revenue for the network operator. The cascaded add-drop architecture (Figure 5.7) seeks to alleviate the cost of deploying the first wavelength. In this design as well, the incoming signal is split N times depending on the number of add/drop ports and wavelengths. We can see

that half of the ports on the WSS are used for adding and the other half is used for dropping. Since the

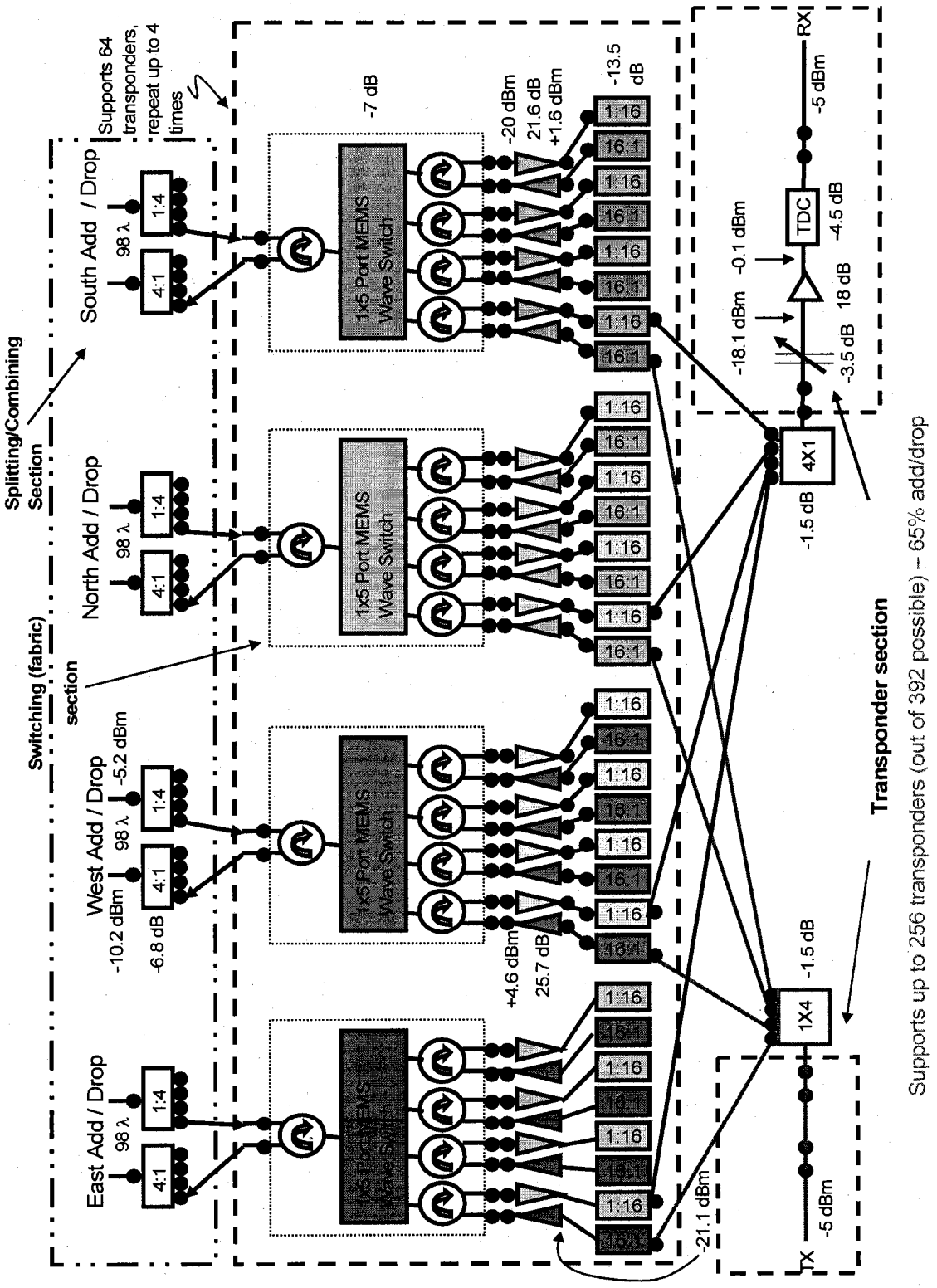

Figure 5.5 Steerable Architecture using 1x4 Wave Switches(Parallel Design)

WSS provides multiplexing and de multiplexing this function is possible. The wavelengths are switched to the lower levels till they reach the corresponding transponder. In this design, additional stages are added serially to the wave switch. Thus, in this architecture, additional stages are not needed unless the switch needs to scale to a higher number of transponders. Thus, if the system has only four wavelengths in use, only one 1x9 wave switch would be required to support the given number of wavelengths. As the number of wavelengths increases, this architecture can be scaled up by adding more 1x9 wave switches. This architecture is beneficial for the network provider as it gives them the flexibility to incrementally increase the size of the switch over time, commensurate with demand.

5.3 Price sensitivity of Steerable Architectures

In this section, we investigate the price sensitivity of the Steerable Switch against the different architectures. The pricing and the different designs would make certain architecture more feasible at a given cost. There are, however, other considerations like initial startup cost, pay-as-you-go property, etc., that would also play a role in making the choice for the right design.

The analysis looks at the fractional contribution of each component towards the net cost of the node, as a function of the number of transponders. The fractional contribution to the system cost of each component per transponder is listed in Table 5.2 for all three architectures. This table quantifies the cost per additional transponder in the system. The numbers are explained by considering the Splitting/Combining architecture. In this architecture, each transmitter and receiver is connected to a 1x4 steerable switch. Thus, the addition of every transponder requires 2 1x4 Steerable switches. Similarly, every 64 transponders require an additional add EDFA and every 32 transponders require an additional drop EDFA. These amplifiers have been strategically placed to meet the link budget and compensate for losses due to splitting of the signal. Similarly, the addition of each transponder would lead to the addition of 2 single amplifiers, 2 tunable filters and a tunable band laser. The breakdown for the other architectures is calculated in a similar way.

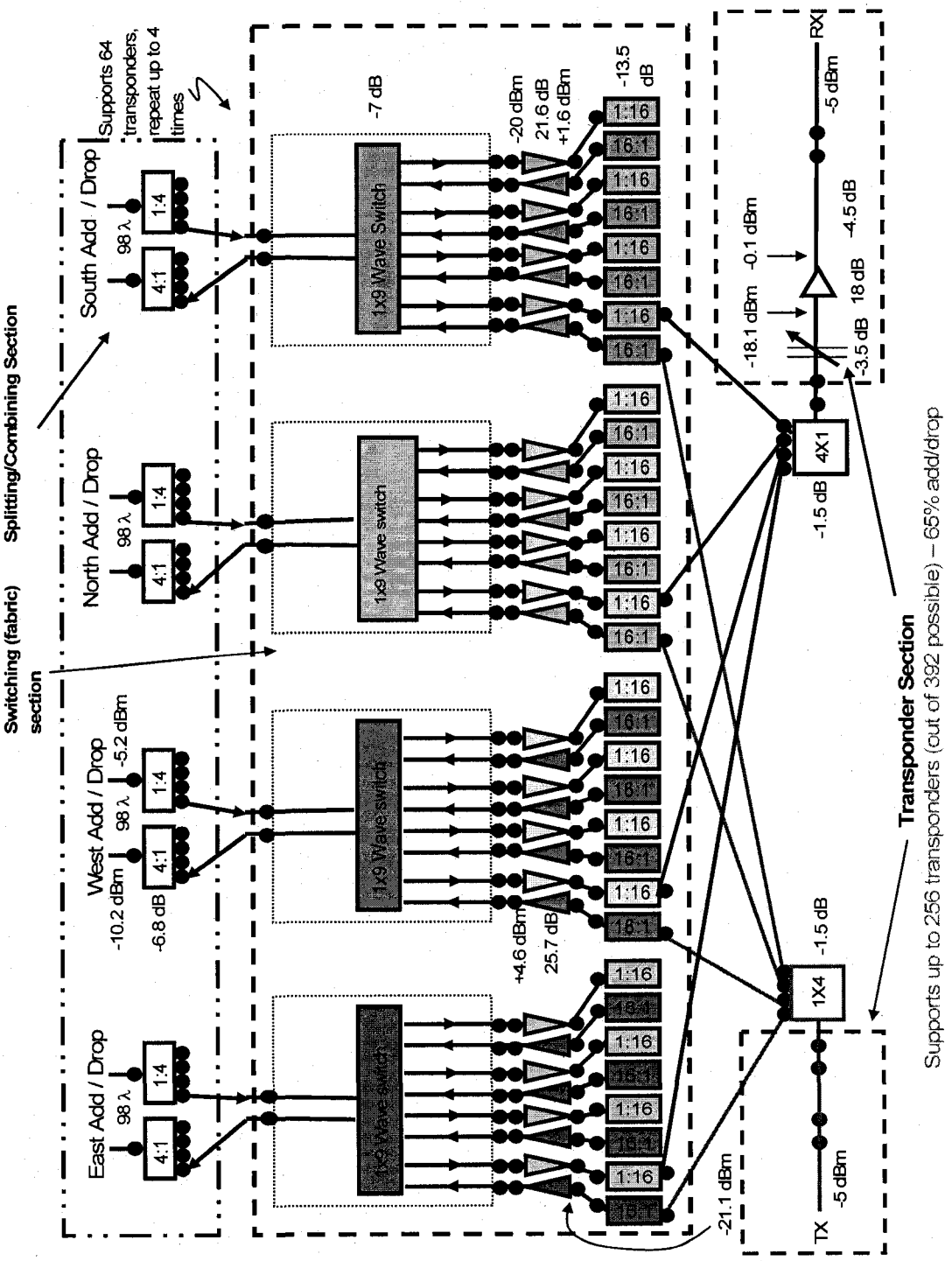

Figure 5.6 Steerable Architecture using 1x9 Wave Switches

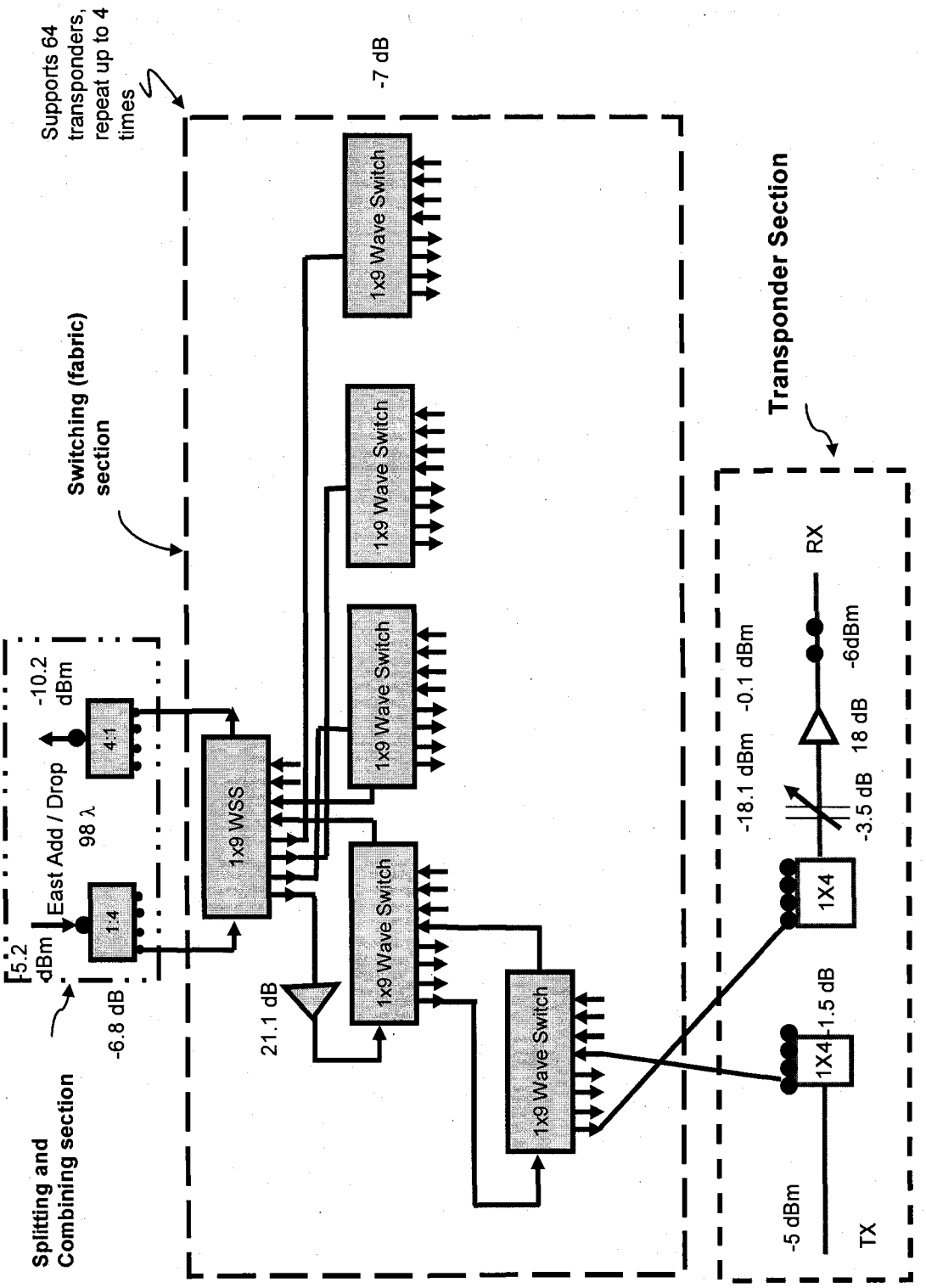

Figure 5.7 Steerable Architecture using 1x9 Switches(cascaded design)

This analysis is a conservative estimate and does not include other fixed costs such as the switching fabric, or any one-time add/drop EDFAs needed coming into/out of the switching fabric. This table allows us to calculate the increase in system cost per add/drop port, as a function of a particular component cost. Such an analysis provides insight into the cost sensitivities of different architectures on a specific component, and in particular the WSS. As well, such an analysis is useful in estimating the day 1 infrastructure cost of deploying the first wavelength, and the total cost after deploying all of the wavelengths. The graph of the cost per additional add/drop port (transponder) vs. the cost of the Wavelength Selective Switch (WSS) is plotted in Figure 5.8. Here the cost of the WSS is varied from $2000 to $30,000. From the graph of Figure 5.8 it can be seen that if the cost of the WSS is low, the 1x5 and the 1x9 parallel architectures have a higher cost per add/drop port than the cascaded architecture. However, if the cost of the WSS is high, the cascaded architecture becomes cost inefficient due to the large number of devices required. The crossover point for the cascaded architecture occurs at a cost level of $10,000 for the WSS. Below this value, the 1x9 Cascaded design is a cheaper option per add/drop transponder port. The slope for this curve is much steeper than the two parallel architectures because the cost of the 1x9 WSS is a much higher fraction of the net cost in the cascaded instance, as confirmed by Table 5.2.

A graph such as this can help a network operator determine the optimum architecture based on the cost of the underlying technology to support the architecture. Such a graph also helps a device manufacturer with pricing strategies to create market demand.

Another useful metric to plot is the overall node cost as a function of increasing wavelength fill (from 0% to 100 %) and as a function of the cost of the WSS. The graphs in Figure 5.9 show the overall cost of the node at two different wavelength fill levels (20% fill and 100% fill) as a function of the cost of the WSS. From Figure 5.9 it can be seen that at low WSS cost of $5000, the 1x9 cascaded designs is a much better choice than the other 2 designs using the WSS. It is observed that as the price of the WSS increases there is a tendency for the 1x9 Cascaded Design to become less advantageous.

Splitting and Combining method	
Item	# Per transponder
1X4 Steering Switch	2
Add EDFA	0.015625
Drop EDFA (26.2 dBm)	0.0625
1:4 couplers for add & drop	0.625
1:16 coupler for add & drop	0.5
Single Channel Amp	2
Tunable Filter	2
Extra for band tunable laser	1
TDC	1

1x4 Parallel Design	
Item	# Per transponder
1x5 Port Switch	0.0625
5 Circulators for 1x9 WSS	0.0625
1X4 Steerable Switch	2
Add EDFA	0.25
Drop EDFA	0.25
1:16 coupler for add & drop	0.5
Single Channel Amp	1
Tunable Filter	1
Extra for band tunable laser	1
TDC	1

1x9 Parallel Design		1x9cascaded Design	
Item	# Per transponder	Item	# Per transponder
1x9 WSS	0.125	1x9 WSS	0.4375
0 Circulators	0.0625	0 Circulators	0.0625
1X4 Steering Switch	2	1X4 Steering Switch	2
Add EDFA	0.25	Add EDFA	0.0625
Drop EDFA	0.25	Drop EDFA	0.0625
1:16 coupler for add & drop	0.5	1:16 coupler for add & drop	0
Single Channel Amp	1	Single Channel Amp	1
Tunable Filter	1	Tunable Filter	1
Extra for band tunable laser	1	Extra for band tunable laser	1
TDC	1	TDC	1

Table 5-2 Fractional Cost of Elements for Different Steering Switch Configurations

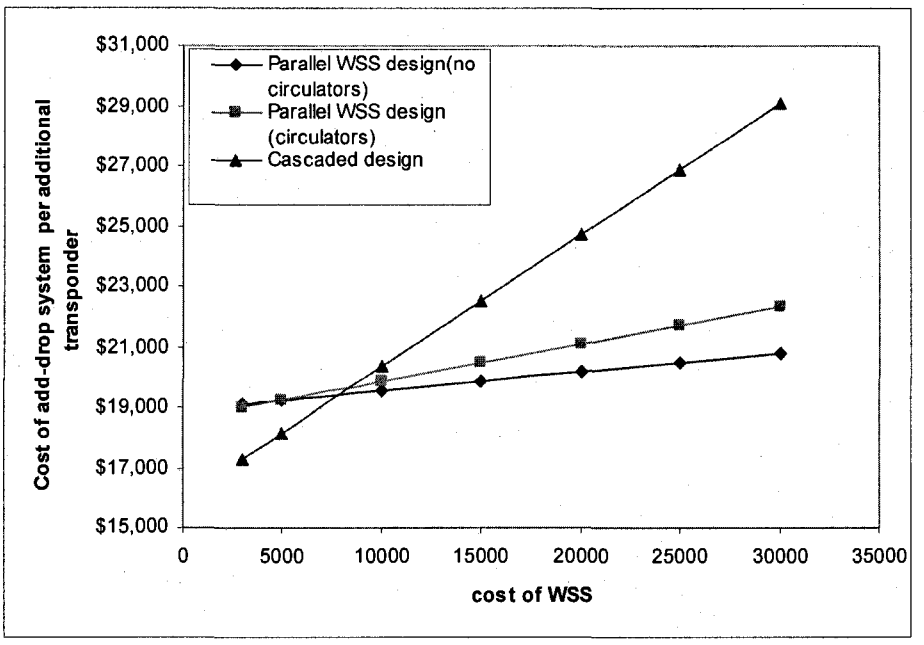

Figure 5.8 Cost of WSS vs. Cost per Additional Transponder

It can be seen from the graphs that at a low cost (WSS cost < 12,000) the cascaded design is clearly the winner. The cost advantage is neutralized at WSS cost = 12,000 and at WSS cost >12k the Cascaded Design is more expensive than the other designs. Here it is more advantageous to use either the Splitting and Combining method or the Parallel design without circulators. The decision to use any particular technology would depend on the price points of such a technology.

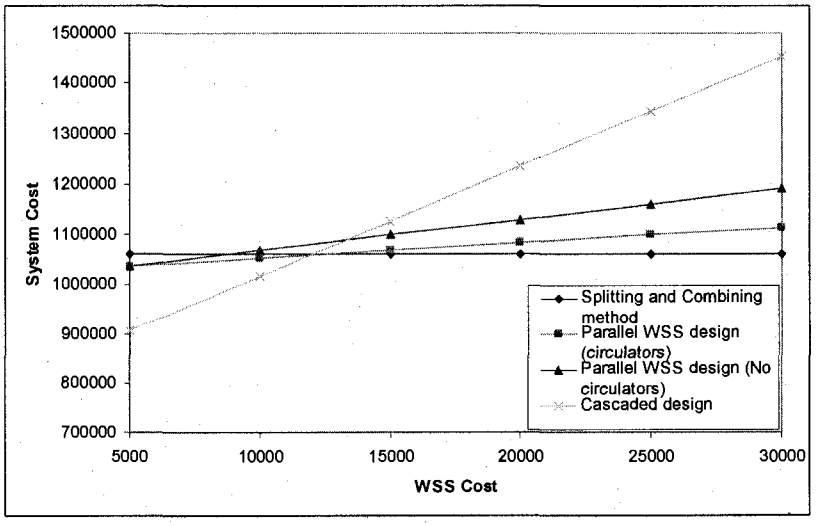

(a) 20 % Fill

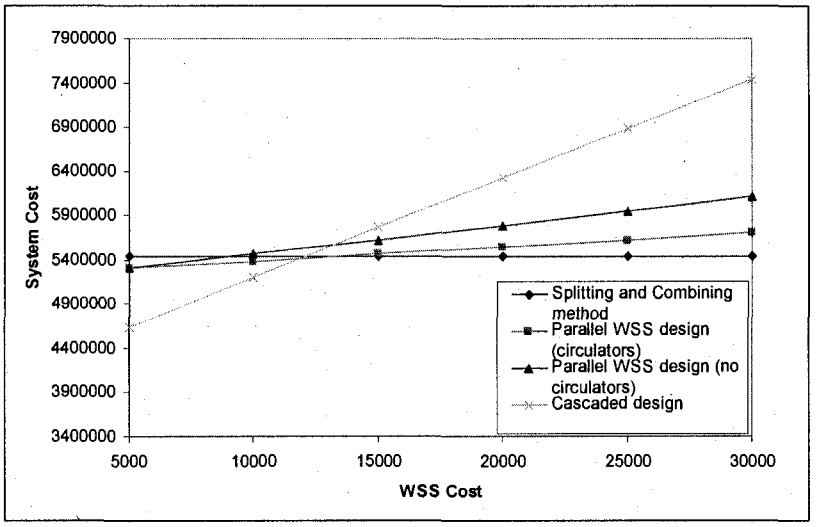

(b) 100% Fill

Figure 5.9 System Cost for Different Steering Mechanisms

5.4 Physical Impairments and the Impact of Cost in the Steerable Switch

In the previous section, we presented different architectures for achieving steerability and compared the cost foot print for each of these architectures. An additional consideration in the design of the switching fabric is the size of components (splitters, switches etc) used. In this section, we analyze the impact of using different splitter/combiner devices in the switching fabric and its impact on the insertion loss and cost.

The path of the signal through the switching portion is shown in Figure 5.10. In Figures 5.4-5.7 it can be noted that every transponder would require two single channel amplifiers, a tunable filter, a tunable laser and a TDC. The intermediate switches and splitters are represented as fractions per transponder. The number of ports on these devices can be varied, which would change the insertion losses and splitting losses accordingly. The signal path through these components can be represented graphically as shown.

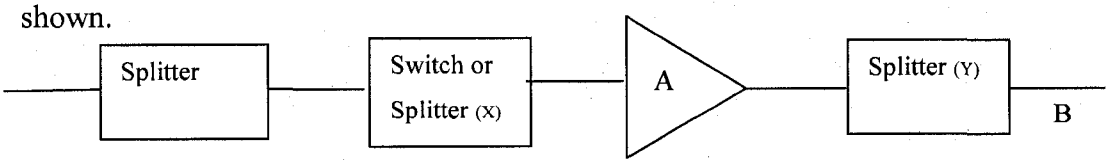

Figure 5.10 Path of the Signal Through the Switching Portion of the Steerable Switch

The dimensioning of the drop side is presented. Let us assume that we have T transponders, i.e., T transmitters and T receivers. Let the number of wavelengths that are dropped from each port be W_D. Let δ $(0<\delta\leq 1)$ be the fraction of wavelengths dropped at each node per fiber.

The number of transponders

$$T = D * W_D * \delta \tag{5.1}$$

The number of ports is D

Let us consider the drop side. The signal transmitted needs to reach T receivers.

Let us also assume a 1:N drop splitter which is connected to the drop fiber.

Thus signal from each output port of the splitter would reach

$$X_P = \left\lceil \frac{T}{N} \right\rceil \text{ receivers} \tag{5.2}$$

We have to ensure that the following equality is valid

$$N * X_P = D * W_D * \delta \tag{5.3}$$

The size of the next splitter would depend on the number of ports at that node.

Thus the splitter would be a 1:D splitter which would serve each port

The output of each splitter would go to another

$$1:\left\lceil \frac{X_P}{D} \right\rceil \text{splitter.}$$

Each output of this splitter from each port will be the input to a Dx1 switch which will be connected to a receiver. This switch couples the outputs from each port to the receiver, and hence the transponder can be accessed by any port.

The reverse is done for the add side and combiners are used instead of splitters.

Signal Path:

Along the signal path to the transponder, it encounters several lossy components as shown in the Figure 5.10. The gain required of the amplifier would depend on the insertion loss of the various components. The cost of amplification is a function of the gain. We analyze the different cost functions for amplification.

The insertion loss and splitting losses for the different components are outlined below.

Insertion loss for a switch = -7dB. Loss at a splitter is $10\log_{10}N$ where N is the number of ways the signal is split; coupling loss is about -1.5dB.

Let us consider the drop path. The initial signal level is -5.2 dB. The loss at a splitter is $10log_{10}N$, where N is the number of ways the signal is split. In this configuration it is important to note that the power level at B is about -13.5 db. Also it is necessary to maintain the equality

$$N_x * N_y = W_D * \alpha \qquad (5.4)$$

Where

N_x = number of drop outputs at switch X or number of outputs at the splitter X

N_y = number of outputs at the splitter Y

The values of N_x and N_y can be varied to maintain the above equation. However, doing so may result in more losses and hence the need for higher amplification. The cost of amplification of a signal is a function of the power. The aim is to find the best possible value of N_x and N_y to maintain equation (5.1) and also reduce the system cost. The system cost is defined as the cost of amplification and switching/splitting elements. In addition to the system cost, the transmission penalty for each of the architectures should be considered. The signal to noise ratio degradation is the main penalty encountered for all steerable switch architectures; consequently, the rest of the system penalties can be ignored. As all architectures have the same input and output power, the signal to noise ratio will depend on the number of the amplifiers in the path as well as the gain and noise figure of each. Parallel and Cascaded WSS architectures have amplifiers with similar gain and hence similar OSNR. However, for the splitting and combining architecture there is a need for an additional amplifier (relative to the other architectures) in the drop path to compensate for the large insertion losses of the splitters. As a result, the OSNR is reduced by about 3dB.

The cost of a switch is a linear function of the number of ports. The cost of the switch is assumed to be $1500 per port. For amplification, two types of cost functions are used in this study: a) a linear cost function of $660/dB for the amplification, and b) non linear cost function where the cost for amplification <10 dB is $1000. The cost of amplification 10dB <amplification < 20dB is $660/dB, and the cost of amplification > 20dB is $1500. The graph of amplification and switching cost for different switch port and splitter port combinations is shown below in Figure 5.11.

If we consider the cost of amplification as a linear function of the loss then the cost versus amplification graph can be plotted as shown in Figure 5.11(c). As seen in Figure 5.11(a),(b), when the splitting ratio is low, for example 2, the amplification needed is low. This induces a lower cost for amplification. A higher splitting ratio indicates a lower switch size and vice versa to maintain the equality defined in equation 4. Thus, the size of the switch needed in this case will have 32 ports. The cost of such a switch is very high causing the system cost to be high. Equation (5.1) can be maintained by using other combinations as shown. It can be seen that the switch cost decreases more rapidly than the amplification cost due to the splitters. For a linear increase in amplification cost per dB, it can be seen that at higher splitting ratios for the first switch/splitter, i.e. N_x, the system cost reduces. However, the amplification cost is defined by the above cost function. Hence, the lowest system cost is obtained when $N_x = 16$ and $N_y = 4$. The system cost is also influenced by the varying amplification cost. This is shown in Figure 5.11(c). In this graph, we vary the cost of amplification after 20dB from $500 to $2500. It is clear that the system cost is a function of the splitting ratio (which affects the switch size and hence the cost of the switch) and the cost of amplification per dB after 20dB. As the splitting ratio is increased (decrease in switch size) the system cost keeps decreasing. However, as the cost of amplification per dB is increased, the system cost decreases to a minimum and then starts increasing again.

A key point to highlight from this analysis is that there is an optimum choice of switch/splitter combination to achieve the same dimensions for steerability, and this optimum point is dependent on the cost function of the amplification and switch. It can be seen that as the splitting ratio of the splitter is decreased, the cost benefit provided by the reduced amplification cost is offset by the high switching cost. This leads to a concave

curve with a minimum value of achievable system cost that is dependent on the size (number of ports) of the switch and the splitter. After this minimum, the cost of the system starts to increase. The choice of the ports to be used clearly depends on the technology and cost of such technologies.

Another important property of a steerable switch that is of great interest to the network providers is the pay-as-you-grow cost of the switch. In a practical deployment scenario, the network provider does not light up all the channels of the optical fiber. Hence, a network provider would like to deploy as much minimum common equipment as possible, and then scale the switch later as other wavelengths are added. It is clear that it may be a while before all the wavelengths in a long haul network are lit. In this section, the pay-as-you-grow property for the four architectures discussed in the previous section are presented. It is assumed that the transponder costs at the end of the steerable switch are the same for all the switches. Hence, these costs are not taken into consideration in the analysis below.

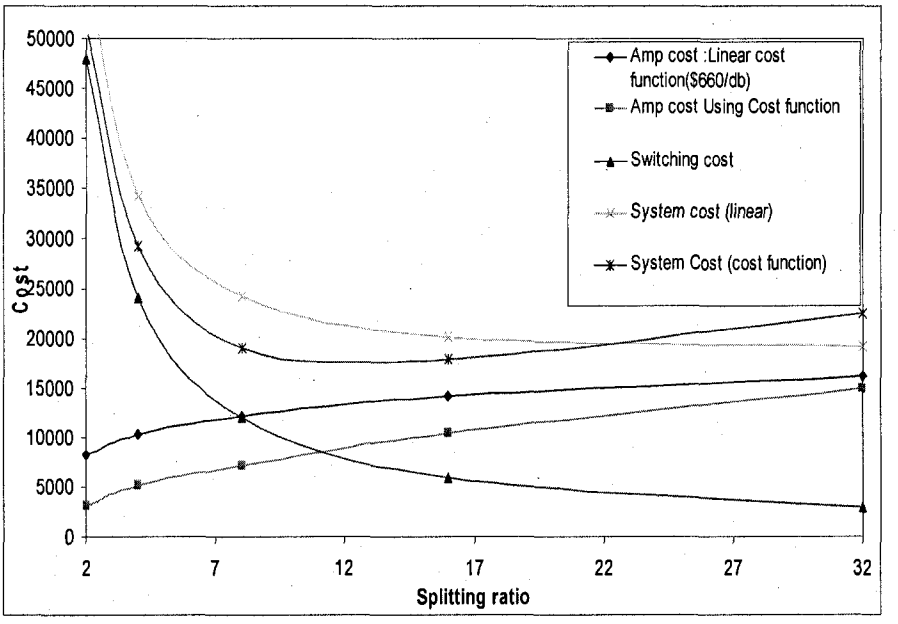

5.11 (a) System Costs with Different Types of Functions.

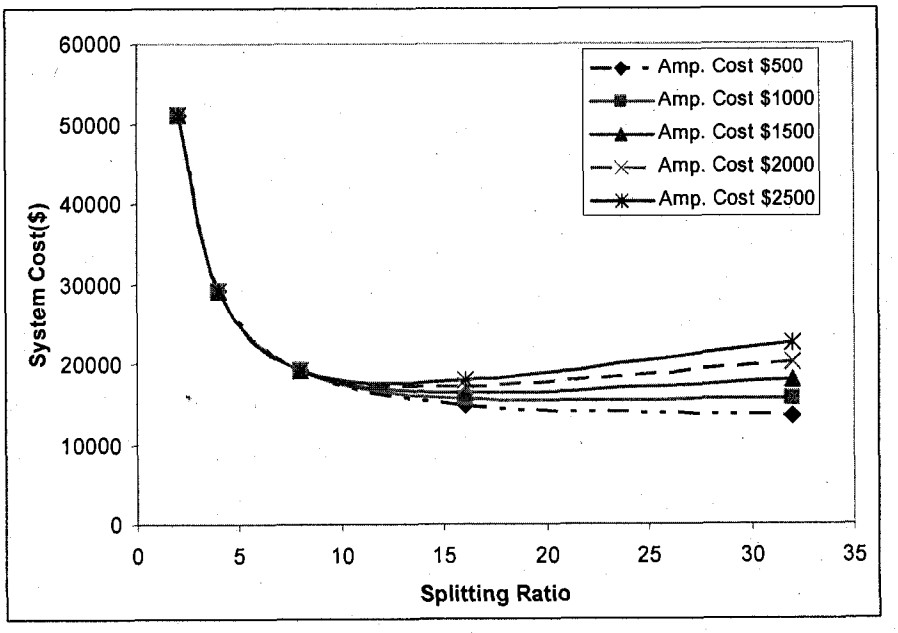

5.11 (b) System Cost with Varying Amplifier Costs

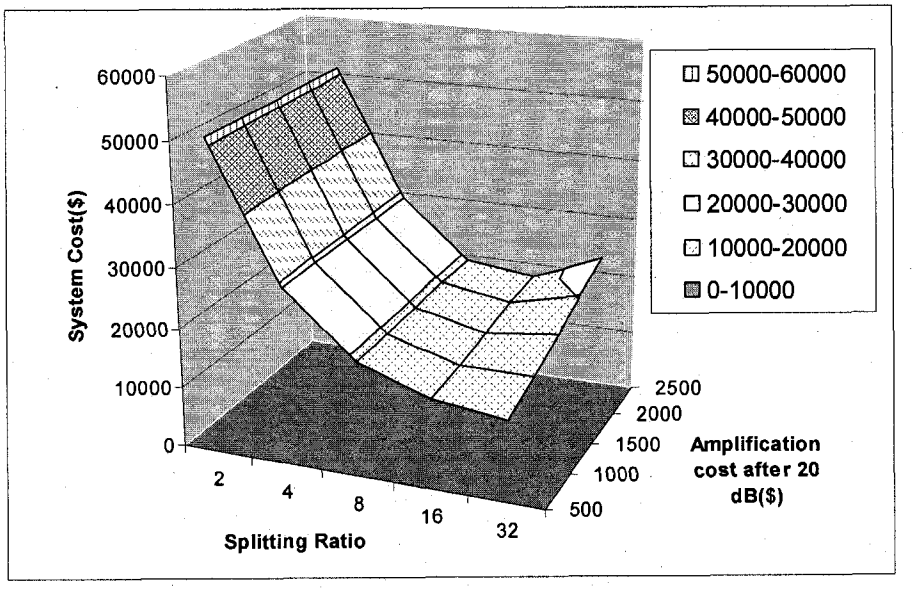

5.11 (c) System Cost with Varying Amplifier Costs after 20 dB

Figure 5.11 Graph of System Cost with Varying Amplification Cost

As shown in Figure 5.3, a node with four port is chosen. Here the steerable switch needs to provide full steerability, i.e., route any wavelength from any port to any of the available transponders. The cost of such a switch for an increment of 8 transponders is shown in Figure 5.12. The startup cost for the splitting and combining method is the

highest compared to the other three architectures. This is because of the high cost of the high power add EDFA and the drop EDFA. The startup cost of the cascaded design is comparatively lower than the other three architectures as for the first wavelength we would need only one WSS at each node for the switch to be functional. For the parallel WSS architectures the startup cost is dominated by the cost of the WSS as there needs to be at least one WSS per port and necessary circulators. Thus for these architectures the system cost is dependant on the cost of the WSS. With better manufacturing techniques and higher demand the cost of the WSS will be reduced and eventually lower the cost of a system using such WSSs. As the number of transponders (assuming 1 transponder per wavelength) increases, it can be observed that the cost of the splitting and combining architecture increases along with the number of transponders added. This is due to the fact that tunable filters and amplifiers need to be added at the add section in order to filter out the ASE noise. The tunable filters and the single channel amplifiers contribute to a significant portion of the cost of the steerable switch. Thus there is a proportional increase in cost per additional transponder. For the cascaded design the increase in cost is proportional to the increase in the number of WSS needed. Here, due to the wavelength selectivity of the WSS, no additional tunable filters are needed at the add side to remove any unwanted ASE noise. This is an additional cost savings on the common equipment compared to the splitting and combining architecture. However, it should be noted that for the cascaded design the WSS cost plays a very important role in the system cost. As seen in Figure 5.12(b), for a high WSS cost (greater than 10k), the cascaded design has the lowest initial deployment cost. However it becomes more expensive than any of the other architectures for a channel count greater than 17. This value shifts more to the left with an increasing WSS cost.

In conclusion, it can be stated that using a wavelength selective switching device to steer the wavelengths leads to a lower cost. Of course, this cost is also a function of the WSS cost and the number of wavelengths in use.

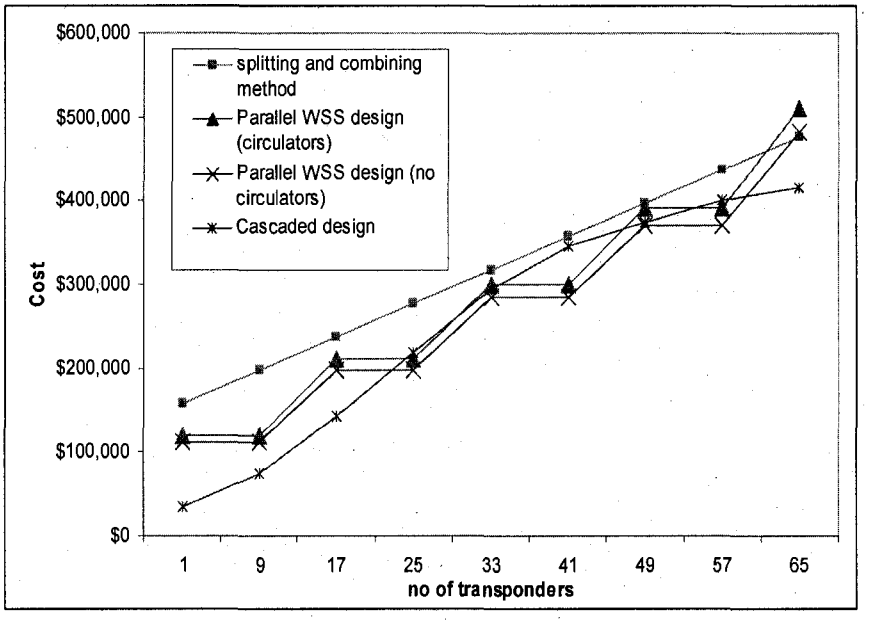

5.12 (a) WSS Cost $6000

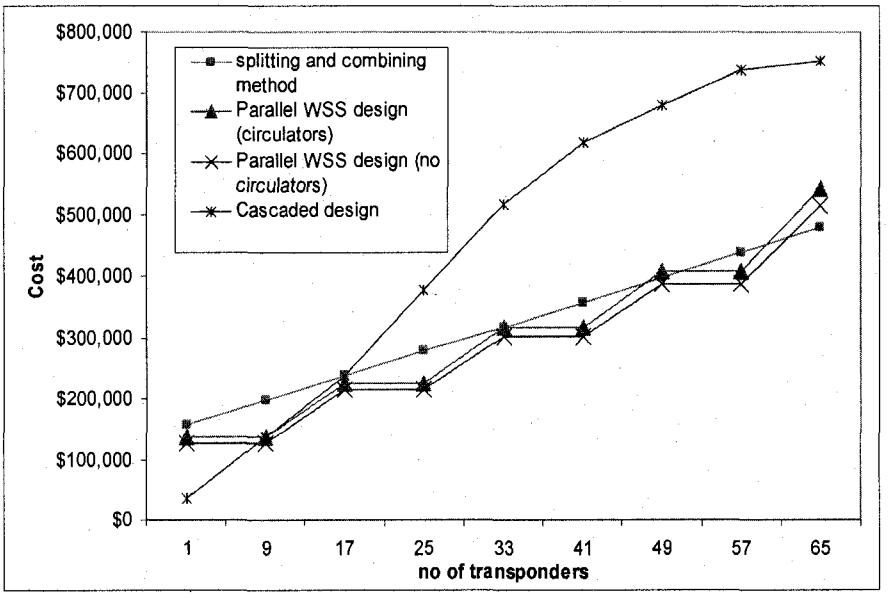

5.13 (b) WSS Cost $10000

Figure 5.12 Common Equipment Cost vs. the Number of Transponders

5.5 Conclusions

In this chapter, three different steerable architectures are presented to transparently and all-optically route wavelengths coming in from any port to any available transponder.

The architectures presented herein have the ability to support 100% steerability and can route any wavelength to any transponder. The optical switch fabric can switch incoming wavelengths to the appropriate out-bound port without the need for electrical signal conversions. Using the scalable architectures presented in this thesis the network provider can resolve resource contention by switching the wavelength to any available transponder. All this is achieved in the optical domain. A comparative analysis of these three architectures was performed to model the cost sensitivities of the node on the various components typically used in the signal path. The cost models incorporated realistic losses incurred in the system, and are thus representative of real-world implementation. Therefore, this analysis provides network operators with a framework to evaluate their architectural options against available technologies and their cost points. This thesis also provides insights for manufacturers of the WSS on price targets that would spur increased deployment and use of these devices. A general conclusion that can be drawn is that the cascaded architecture, which calls for a larger number of WSSs to be used in total, becomes economically attractive at cost points below $10,000 per WSS. On the flip side, an architecture using 1:4 splitters is more cost effective when the WSS cost exceeds $20,000 per device. We have also explored the cost per additional transponder for different price ranges for each of the architectures using WSS. It can also be concluded that there are distinct advantages for choosing different architectures for a steerable switch. The choice of any such architecture, to minimize the cost, would depend on the current price points of the devices being used. At different price points, different architectures become more economically feasible in terms of the cost. We can see that different architectures have advantages in terms of the cost-footprint at different price ranges.

Chapter 6. Optical Reach

6.1 Introduction

Recent advances in transmission technology of ultra long haul (ULH) WDM systems have opened new avenues for pan-continental WDM transport networks. The optical signals can now be transmitted over large distances without any regeneration [SIM-99]. Wavelength division multiplexed (WDM) systems are capable of transmitting 160 channels at 10 Gb/s to distances of about 3000km [PUC-05]. In addition, such systems enable optical bypass, where traffic transiting a node can remain in the optical domain as opposed to undergoing costly optical–electronic–optical (O/E/O) conversion, are being deployed in carrier networks [SIM-99][NOL-00][GHO-03][MUK-00]. Until recently, there was a push in the Optical networking community to provide devices that would allow the signal to remain in the optical domain for as long as possible, i.e., to increase the optical reach of a transmission system. The premise of these ULH WDM systems has been based on the argument that the farther a signal travels, less regeneration is required in the optical network and hence the network becomes more cost effective. However, as the optical reach continues to increase, the cost advantage provided by the longer reach is offset by the cost of using expensive equipment [SIM-05]. Thus a longer optical transmission reach may not necessarily translate to the best optical reach for a transmission network. More recently, the concept of optical reach has been treated as a distance that depends solely on the network topology and the impact of the technology used has never been investigated.

In this research we define the optical reach to be that un-regenerated distance of transmission that will minimize the system cost of the optical network. We show that optical reach for a particular network can vary significantly depending on the technology used. While the optical amplifiers like Erbium Doped Fiber Amplifiers (EDFA) and Raman amplifiers came to make the optical reach longer, now photonic integration [SIM-05][SAR-02][WOS-04][MAS-02] is making transponders cheaper and the answer to achieving the best optical reach is changing. We have investigated the impact of such

changes on the optical reach of the system and show that achieving the best optical reach depends on the type of technology used for amplification and transponders in the system. One of the major costs incurred by an optical network provider is the capital expenditures (CAPEX). In this current depressed market cost reduction and return on investment (ROI) are the key words and there is a critical need to focus and find ways in achieving this objective. It is imperative to achieve the best optical reach by driving down these costs. We also provide solutions and price points as indicators of when and how each technology can contribute to the best optical reach. Moreover, these cost savings due to the increase in optical reach, which were done without technology considerations, have been analyzed only at full fill [PUC-05]. A similar study at low fill is equally important but has never been done. The importance of such a study is that it mimics practical deployments and examines the first-installed cost, along with the scalability in terms of wavelengths for different reach systems for various solutions to achieve the best optical reach. This approach allows fair comparison of the most suitable configurations for different architectures in real network situations.

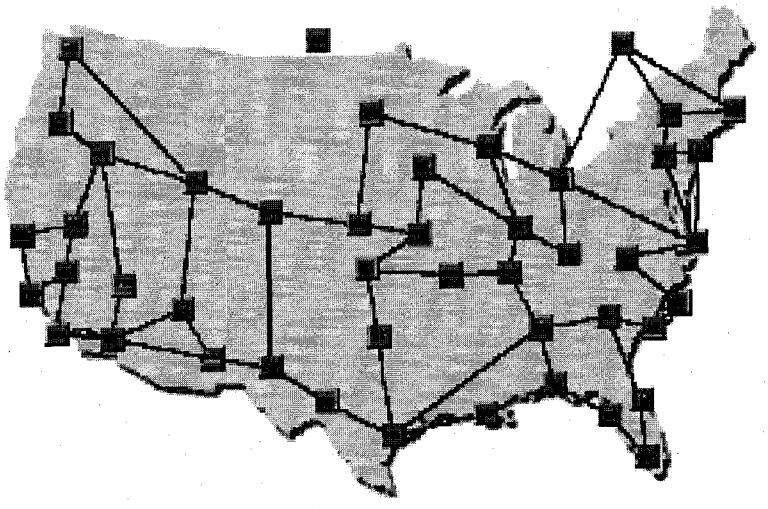

Figure 6.1 45-Node North American Network

6.2 Reference Transport Network under Consideration

The results shown in this research has been observed on a typical 45-Node (average node degree of 2.6) North American Network as shown in Figure 6.1. The total network fiber distance is about 40,000 km, assuming one fiber per link. With a full mesh connectivity

there would be 990 connections. The line amplifiers along the network links are homogenously distributed at distances of 100 km. The maximum number of wavelengths carried by the system is assumed to be 80. Representative traffic data is collected for this network and depicted in Figure 6.2

6.3 Traffic Conditions

In Figure 6.2, we can see that the majority of traffic is flowing to a varied mix of distances ranging from 500 km to about 3000 km. It can be derived from Figure 6.2 that almost 70% of the connections are less than 1500 km. 52% of the wavelength distances are less than 1,000km. Consequently, for such a network, optical equipment vendors typically optimize their optical reach to 1500km to match the distance of the non-regenerated links with the majority of the traffic demands.

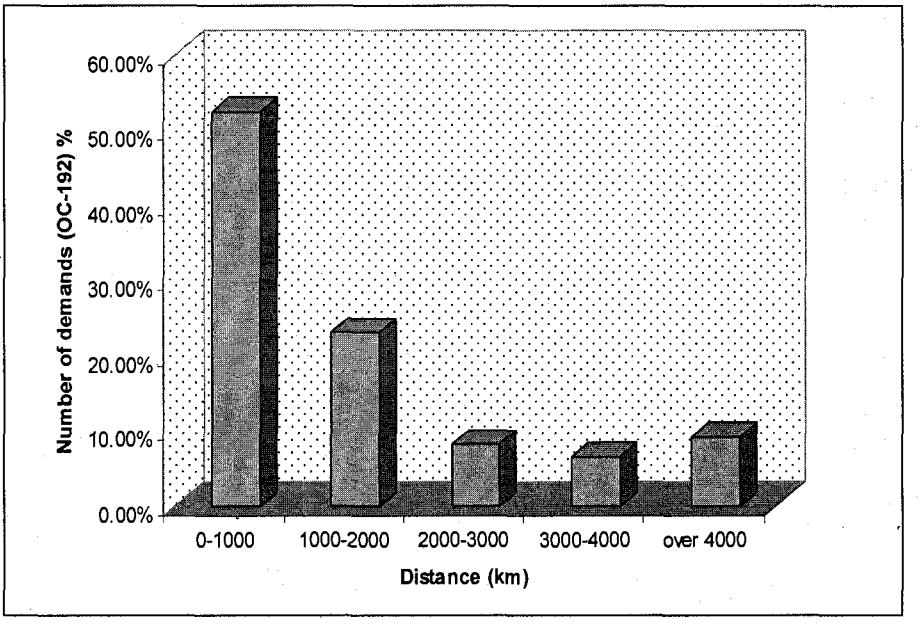

Figure 6.2 Number of Traffic Demands vs. Distance

6.4 Components of an Optical Network System

This section explores the different components that make up an optical network. We quantify the system cost as a summation of the cost of the various components of the network. The total system cost can be represented by the equation

$$TotalSystemCost = Cost_{Amp}\left[\left(\frac{D_t}{L_s}\right)-1\right]+2N_{ch}\left(Cost_{Tm}+\frac{Cost_{cir}}{N_{TC}}\right) \quad (6.1)$$
$$+2*\left\lceil\frac{Cost_{sh}}{N_{CP}}\right\rceil*\left\lceil\frac{N_{ch}}{N_{TC}}\right\rceil+Cost_{OADM},$$

Where $Cost_{Amp}$ = Amplifier Cost, D_t = Total Transmission Distance, L_s= Span length, N_{ch}= Number of Channels, $Cost_{Tm}$ = Transponder Module Cost, $Cost_{cir}$ =Circuit Board Cost, $Cost_{sh}$ = Shelf Cost, $Cost_{OADM}$ = OADM Cost, N_{CP} = number of cards per shelf, N_{TC} = number of Transponders per card. When N_{CP} =1 there is only 1 card per shelf. When N_{TC} =1 there is only 1 transponder per card. The impact of the packing factor on the system cost is discussed in Section 6.5.

It is assumed that the nodes are roughly 500 km apart and hence this system incurs an additional cost from the intermediate optical add-drop multiplexer (OADM) to add and drop the signals.

The total system cost at varying fill levels is plotted in Figure 6.3. It is seen from Figure 6.2 that the majority of the connections are less than 1500 km in length. Hence the total transmission reach of the system is selected to be 1500 without OEO regeneration to encompass a majority of calls. The OADM nodes are 500km apart to represent the average node distance between each node in the given network. The fiber is assumed to be E-LEAF, and the span length, i.e., the distance between each line amplifier, is 100km, with a span loss of 25 dB.

It is visible that the contributions to the system cost are the terminal equipment costs (transponders, shelf costs), and amplifier costs. At very low fills the amplifier and the OADM costs are the major costs encountered by the network provider. This is because the amplifier costs are pro-rated against the number of wavelengths, and hence the cost of amplification per wavelength is higher. As the number of wavelengths increases, the cost of the amplifiers become less significant compared to the shelf and transponders costs. Thus depending on where we are on the fill level curve, the different components of the optical network system impact the cost differently.

Using a 2000 km or a 3000 km transmission system will change the exact percentages of the various system constituents. However, the dominant costs (i.e., amplifier costs at low

fill and transponder costs at high fill) and the overall major trends remain the same as the 1500 km case.

6.5 Optical reach

In this section, we investigate the impact of reach and quantify the impact of the various technologies on the network cost of such a system. In order to study the impact of the various components on the system cost we consider three types of systems with three different optical reaches:

(a) OEO regeneration every 100 km

(b) OEO regeneration every 500 km

(c) OEO regeneration every 1500 km

The choice of the these systems is not mere coincidence. Each of these transport systems represents the methods of signal transmission at different transport levels of an optical network. The 100 km transmission systems are considered in this study, because this is the farthest distance the optical signal can travel without any kind of amplification or regeneration. As distances are short, there is no need for amplifiers and the amplification cost is totally eliminated. As a result, for a lightpath spanning a large geographical distance, many regenerators would be needed at intervals of 100 km. The total system cost in this case would only be a function of the number of channels in the network, and the increased number of the transponders/regeneration equipment that have to be placed every 100 km could offset the cost advantage of eliminating the amplifiers. As a result, there is a need to drive down the cost of transponders.

Case (b) represents equipment that is typically designed to serve the Metro market and the 500km distance is chosen to match the distances of the majority of traffic demands in a typical metro network. While regeneration occurs every 500km, optical amplification occurs every 100km, and amplifier costs become a significant part of the system cost.

Case (c) represents a long haul network, such as the one depicted in Figure 6.2, in which the transponders can send the signal through the optical network for 1500 km without unacceptable degradation in the signal quality. However, just like the 500km case, the signal strength needs to be boosted by amplifiers placed at 100km intervals. In addition,

this system requires optical add and drop capabilities that are assumed to be added roughly 500 kms apart. The size of the bypass would depend on the degree of the node and the number of channels that need to be bypassed without any regeneration. OADMs are devices inserted inline sandwiched between two amplifiers or at the mid-stage of a line amplifier. This enables access to all the wavelengths traversing the amplifier and permits local ingress/egress. While OADMs can be reconfigurable, the additional cost for allowing reconfigurability has not been taken into account in this thesis.

It is seen from Figures 6.3 to 6.6 that for a 1500 km system, at high channel count, many of the cost-reduction opportunities are in the area of terminal equipment (Interface shelves and transponders). However, at lower fills the amplifier cost becomes a significant portion of the total system cost.

We quantify the cost of the various optical network systems described above and compare the costs for varying levels of fill. In order to have a fair comparison between all three systems, the cost is normalized to the dollar amount per Gb per km. In all three cases, it is assumed that the modulation format is non-return-to-zero (NRZ), there is no dynamic gain equalization nor Raman amplification. The three systems are bidirectional systems with different reach. As the signal for the 100 km system needs to propagate for a much shorter distance before regeneration than the two other systems it is assumed that the cost of the 100 km transponder is about 0.2 times the cost of the 500 km transponder. The transponder costs for the 100 km system are assumed to be about $1000 whereas the transponder costs for the 500 km and 1500 km system are assumed to be about $5000 and $8000 per card respectively. The first and last wavelength cost for the three types of reach systems are plotted in Figures 6.7 and 6.8 respectively. It can be seen that for the 100 km reach system, the first wavelength cost per Gb/km is the lowest. This is because the only costs incurred in such a system are the transponder and shelf costs. However, the other two systems (500 km reach and 1500 km reach) have the additional cost of amplifiers every 100 km. Since the amplifiers are usually a cheaper option at a high channel count, the first wavelength cost increases with the increase in optical reach. Moreover, the 1500 km reach system incurs the additional cost of the OADMs every 500km. At full-fill, the situation is different as the cost of amplifiers is shared among many channels and the amplifier cost becomes less significant while the transponder cost

dominates the total system cost. As a result, and as depicted in Figure 6.8, there is a big reduction in cost per Gb/s per km for the 1500 km system, as compared to the 100 km system at full fill. It is worthwhile to note that though the normalized costs are small; they translate into a significant amount when calculated over the whole system cost. For example, a cost reduction of a 0.5Gb/s/km in an 80 channel, 2000 km reach system results in an over a million dollars in savings.

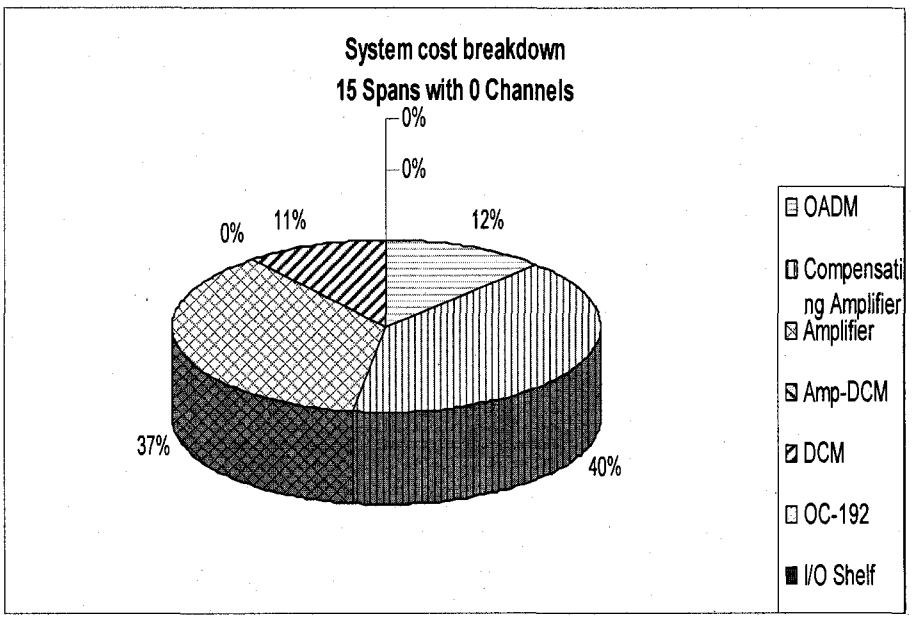

Figure 6.3 System Cost for Zero % Fill

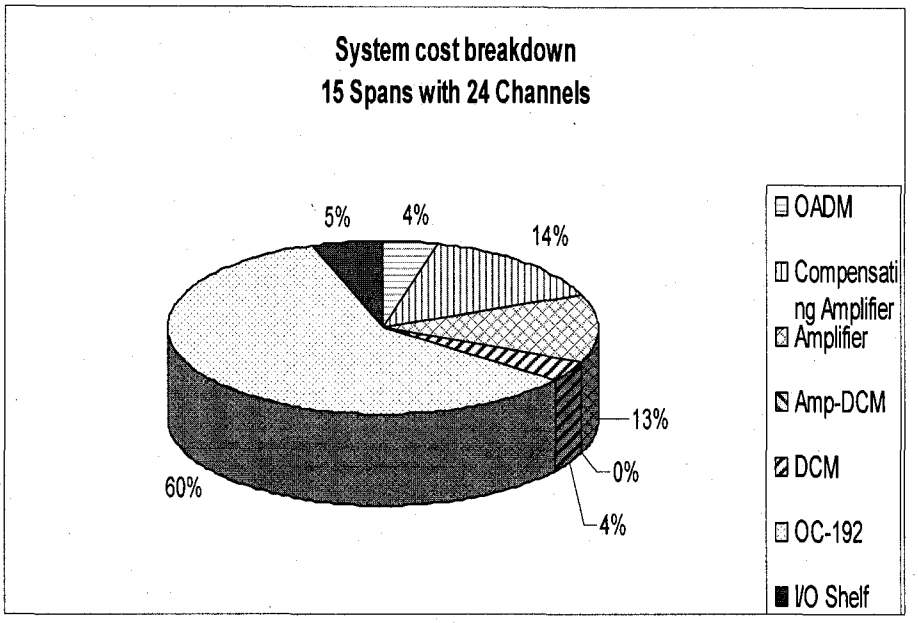

Figure 6.4 System Cost for 25 % Fill

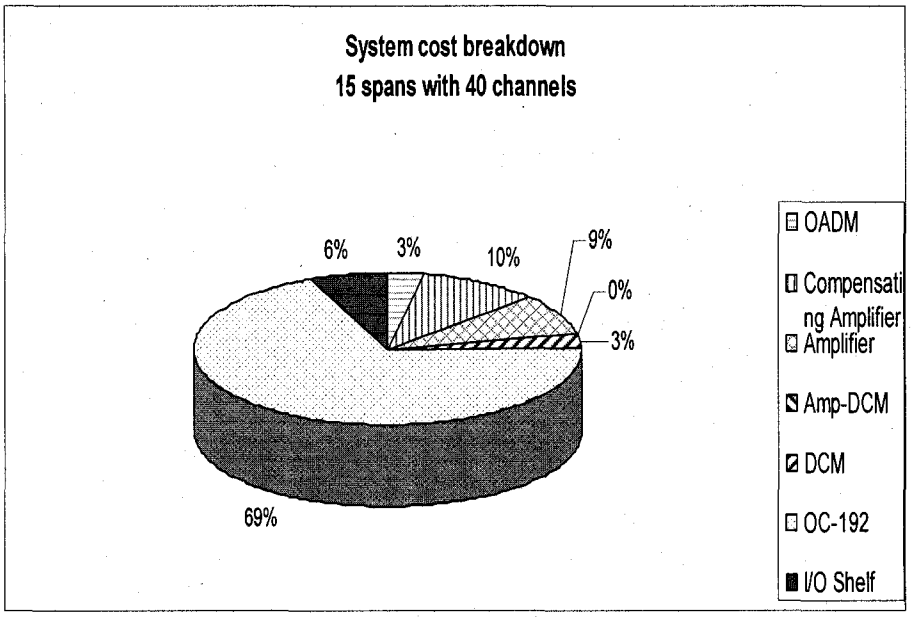

Figure 6.5 System Cost for 50 % Fill

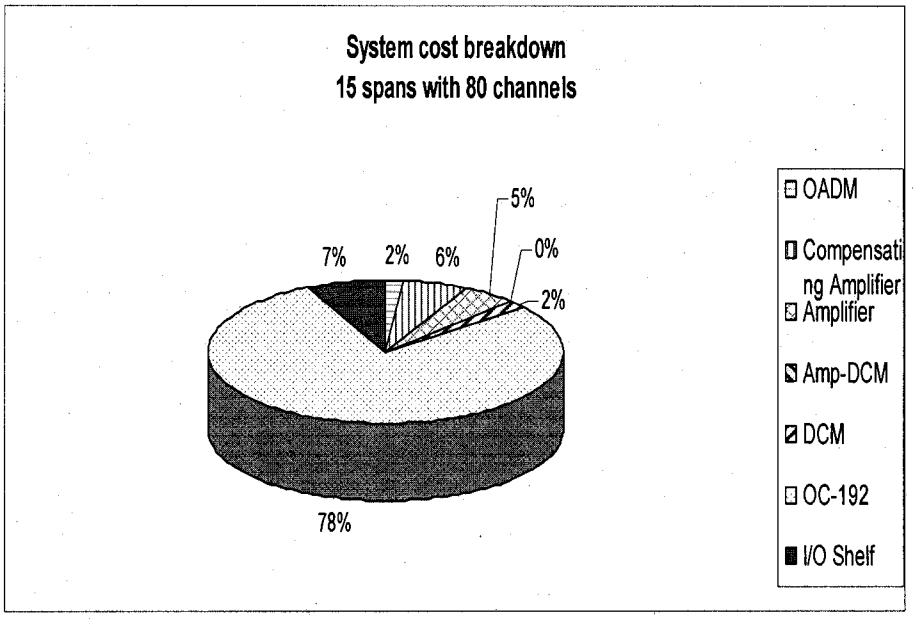

Figure 6.6 System Cost for 100 % Fill

6.6 Optimizing System Cost

From the above discussions, it is evident that the major areas of cost reduction are the amplifier costs, transponder costs and shelf costs. Modularization and vertical integration of components are some key areas that are explored in this section. The impact of using such techniques on the system cost is demonstrated by using normalized costs for various reach systems.

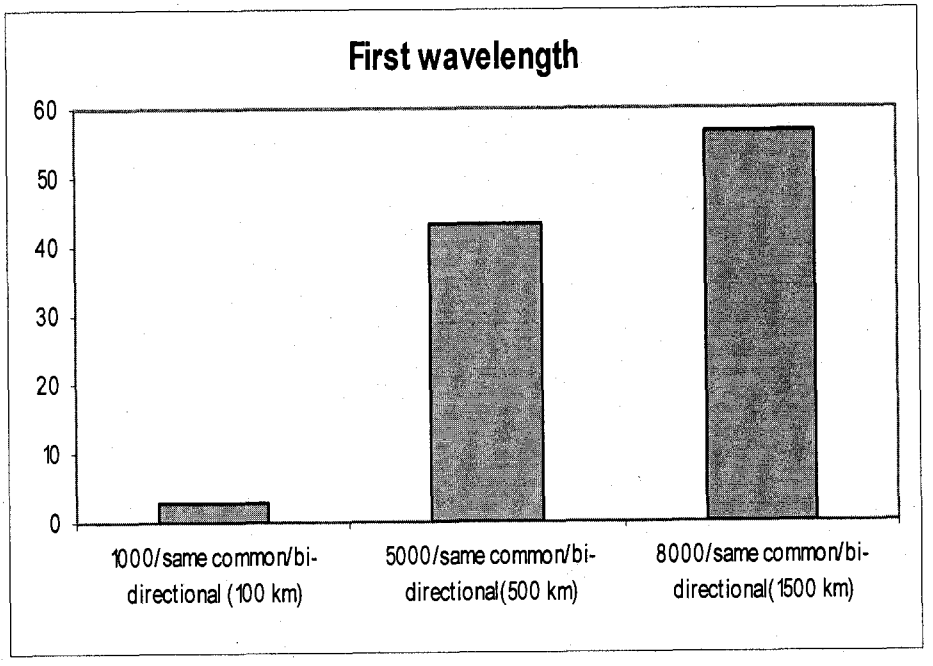

Figure 6.7 Normalized First Wavelength Costs

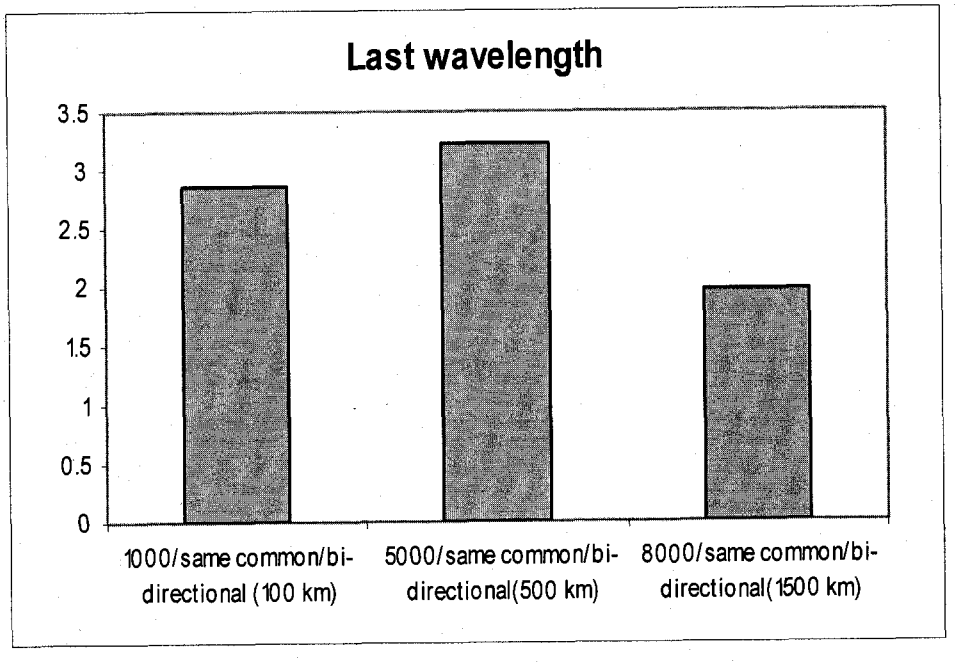

Figure 6.8 Normalized Last Wavelength Costs

6.6.1 Amplifier Costs

EDFAs are designed to amplify light in the C or L band using fiber that is doped with erbium, a rare earth element that has the appropriate energy levels in its atomic structure for amplifying light. EDFAs utilize a 980 nm or 1480nm lasers to pump the doped fiber. These EDFAs are made up of a length of fiber, a pump source and optical filters. The major contributors to the cost of such an amplifier are the pump lasers (used to inject energy into the doped fiber) and the optical filters.

As seen in Section 6.5, the amplifier cost is a major cost at low fill for the 500 km and 1500 km reach systems. This is because amplifiers designed for 80 channels are used to light only a few channels. This would mean that a higher fraction of the cost of the amplifier is shared per wavelength.

The impact of the amplifier costs at low fills can be reduced by adding the pumps modularly or by adding gain blocks as needed to increase the spectral range.

6.6.1.1 Pump Upgrades

In this scheme, the pumps are added modularly as more wavelengths are populated. In order to modularize the amplifier, as shown in Figure 6.10, Pump 1 is deployed initially with splitter ratios optimized to give the right co and counter directional pump powers into each erbium fiber coil. Pump 2 is added to increase available output power. Pumps 3 and 4 are added to further increase available output power for maximized channel count. The advantage of this approach is that the spectral range is not limited but the number of wavelengths that can be amplified is limited by the pump power.

A pump upgrade amplifier offers a scalable pay as-you-grow amplification system that initially requires a single pump to support the transmission of few wavelengths. This mechanism scales modularly and provides a structure that can grow as revenue generating opportunities or capacity exhaust drives expansion of the network.

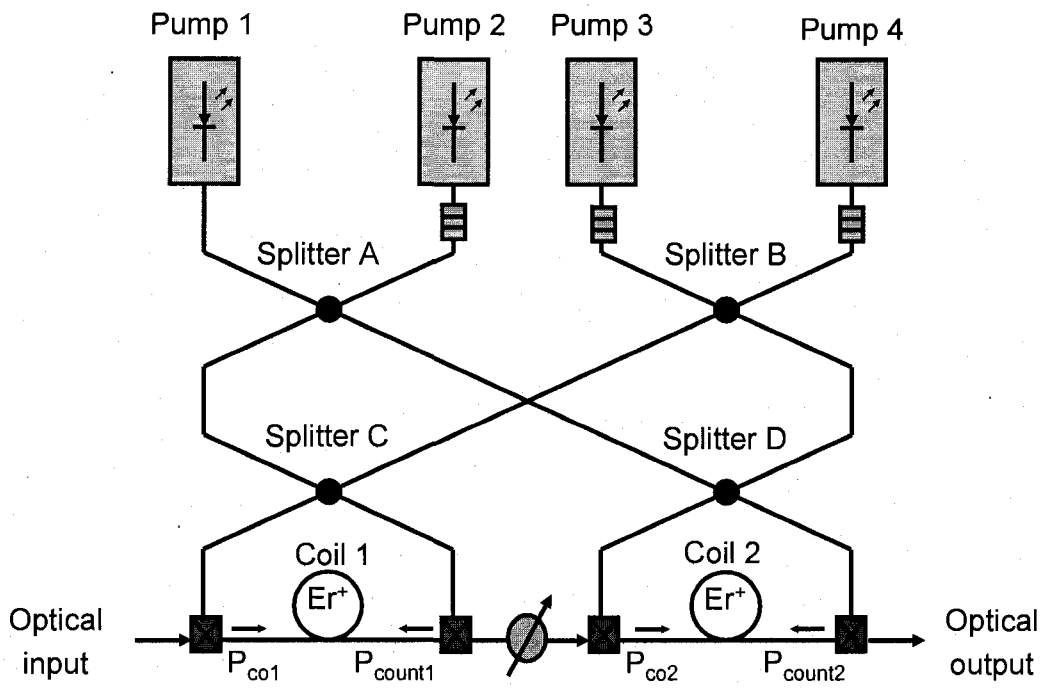

Figure 6.9 Pump Upgrades

6.6.1.2 Spectral Upgrades

Modularization of the amplifiers can also be achieved by spectral upgrades. As the number of wavelengths increase, additional gain blocks are introduced.

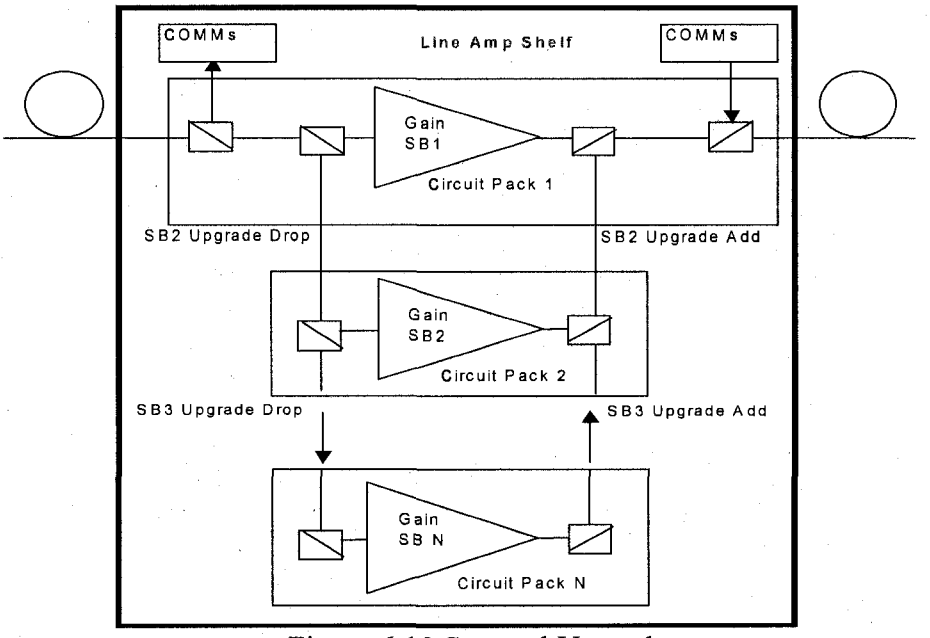

Figure 6.10 Spectral Upgrades

In contrast to the pump upgrade scheme the spectral range is limited in this case, and the spectrum is upgraded by introducing additional circuit packs and the different spectral ranges are isolated by optical filters as shown in Figure 6.11. This is in contrast to the pump upgrades, where there is no limitation on the spectral range.

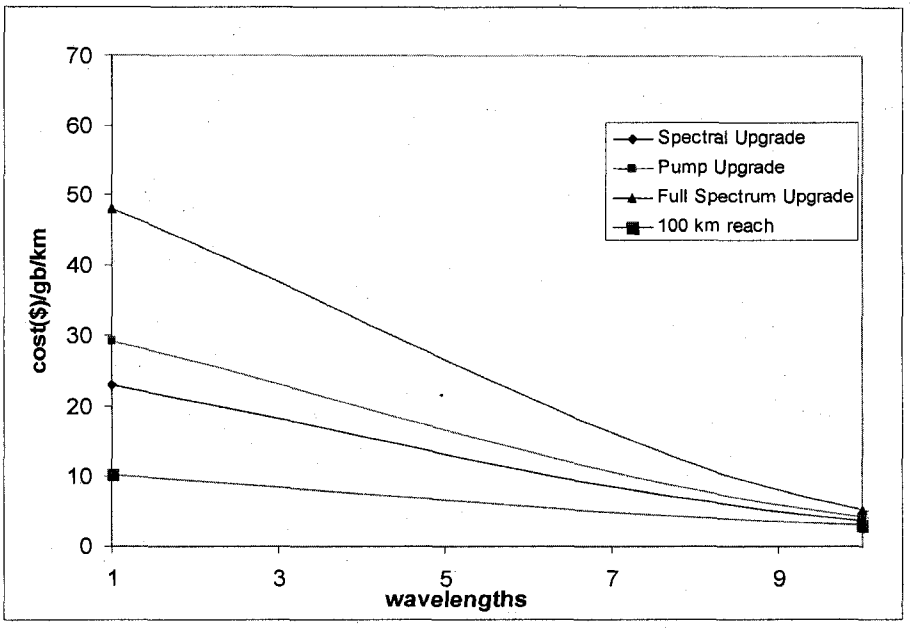

6.11 (a) 500 km reach (low fill)

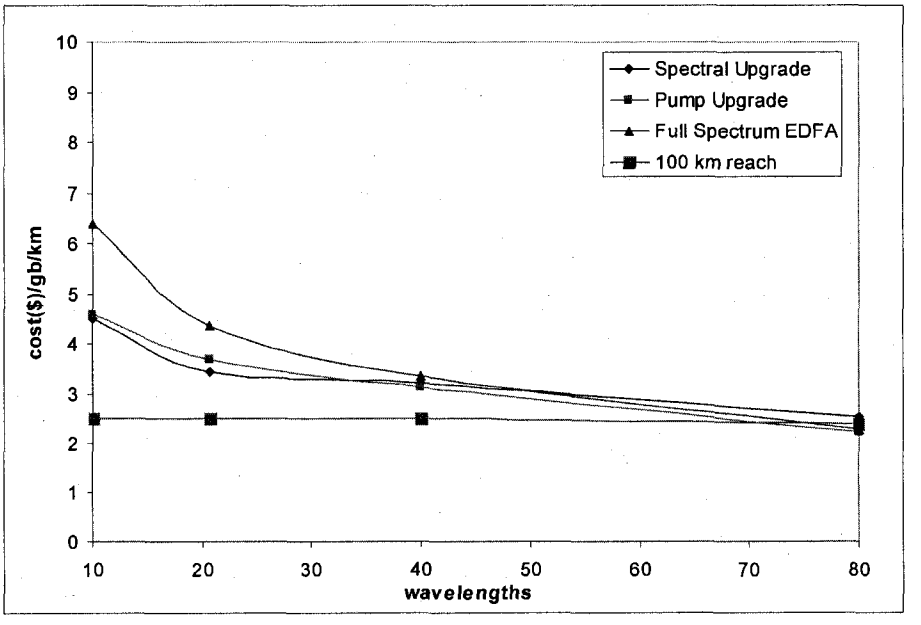

6.11 (b) 500 km reach (high fill)

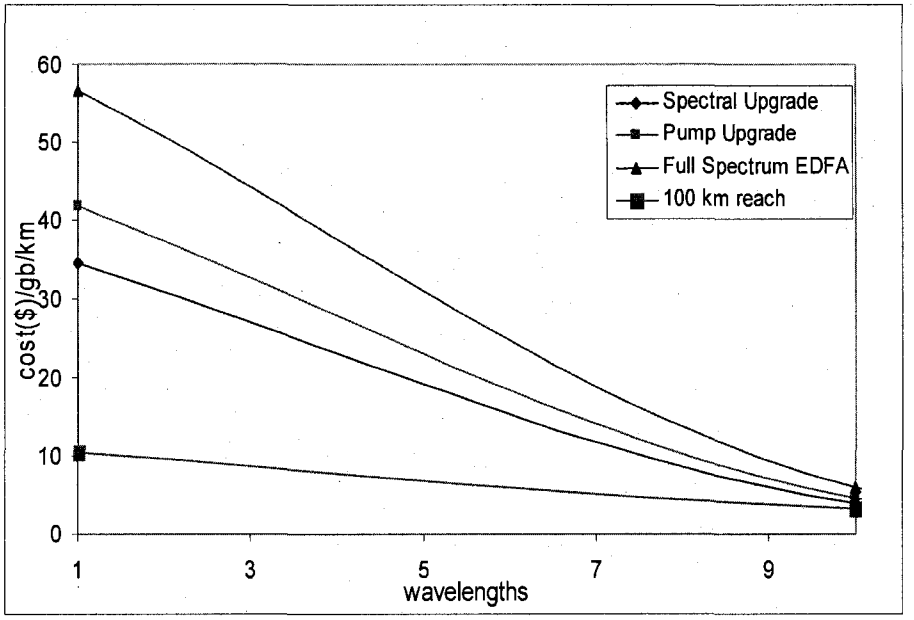

6.11 (c) 1500 km reach (low fill)

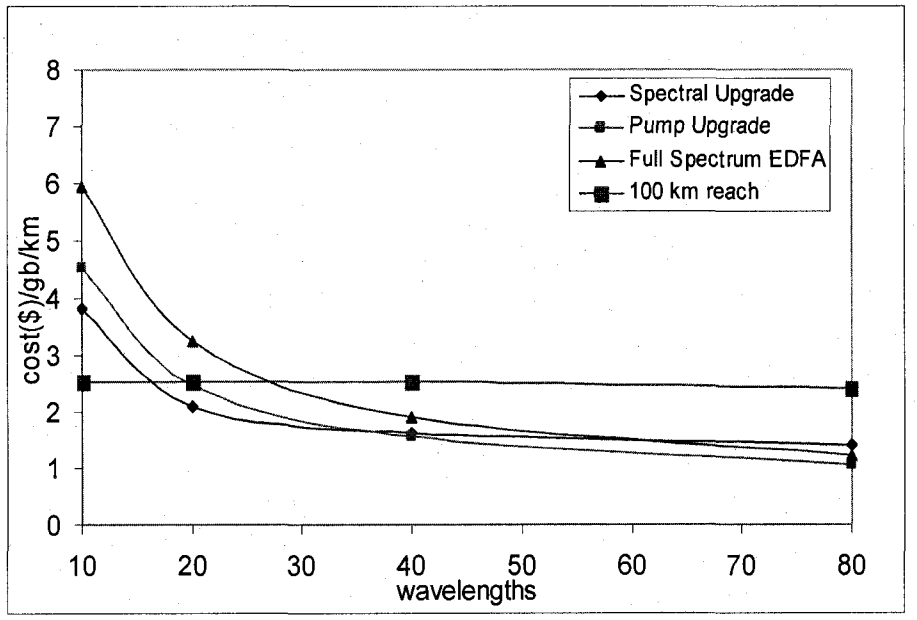

6.11 (d) 1500 km reach (high fill)

Figure 6.11 Impact of Spectral Upgrade and Pump Upgrade on System Cost

The impact of the pump upgrades and spectral upgrades on the normalized cost is plotted in Figure 6.12 for the three systems discussed above. As seen in Figure 6.12 the

horizontal line represents the cost of an optical network in $/Gb/km using an 100 km reach.

Now we examine different scenarios using spectral and pump upgrades. At lower fills, both the pump upgrade and spectral upgrade have a significantly lower normalized cost as compared to a full spectrum amplifier. This makes a strong case for employing such pay-as-you-grow techniques for networks which do not need provisioning of many wavelengths. For both the 500 km reach system and the 1500 km reach system, it is observed that the initial costs of deploying a system with spectral upgrade architecture are cheaper as compared to that of the pump upgrade. This is because in the pump upgrade architecture, the support for the whole spectral band is provided right from day 1 and only modular pumps are added as needed.

In contrast, if a modular spectral up-gradable amplifier is provided then there is support only for 20 wavelengths at a time. This results in a lower initial cost. However at full fill, the situation changes and the pump upgrade architecture is a better choice. It is seen from Figure 6.12(b) that for a 500 km reach after about 50% fill the cost of the pump upgrade becomes lower than the spectral upgrade whereas for a 1500 km reach this is achieved at about 30% fill. Thus, the cost advantage of the spectral upgrade at lower fills becomes lower as the reach increases. In the figures 6.12(a),(b) it can be observed that for a 500 km reach system, regeneration at every 100 km is cheaper than using any other amplification technique. This would, however, be true given the cost assumptions made in the thesis. With a different set of costs for the transponders and amplifiers, these costs would vary significantly. This again shows that optical reach is dependant on the technology used and the different price points for the sub-systems in the network.

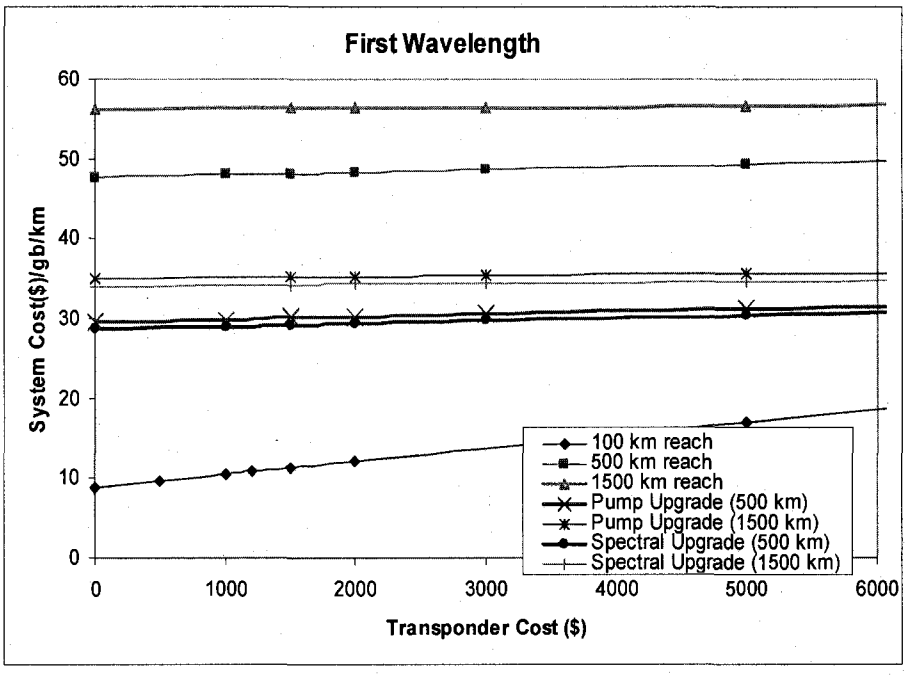

6.12 (a) First Wavelength

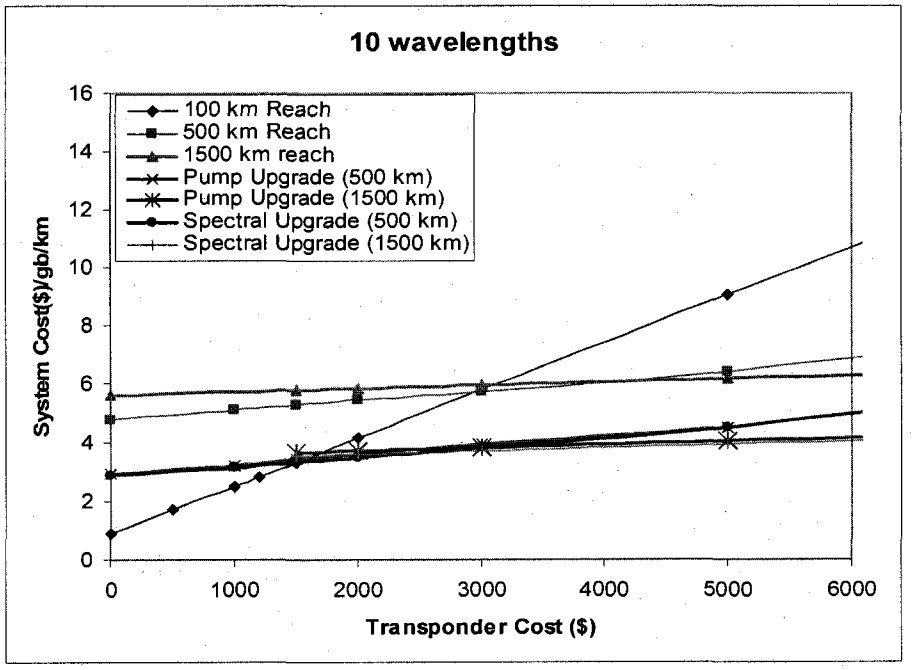

6.12 (b) 10 wavelengths

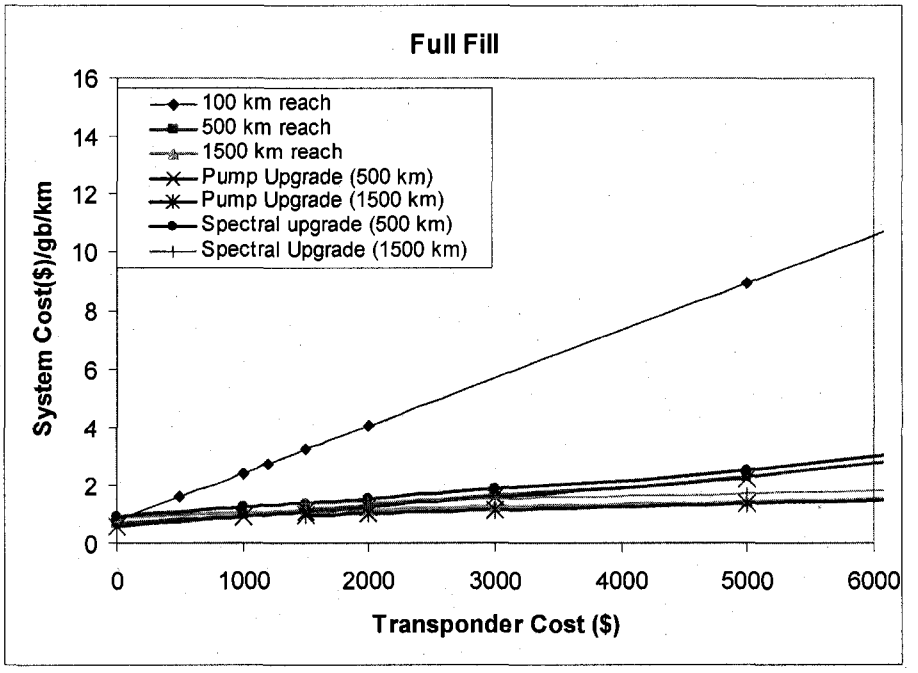

6.12 (c) Last wavelength

Figure 6.12 Cost of 1500km system for varying levels of fills with Transponder Costs from $1000-$8000

6.6.2 Integration

Traditionally the WDM sub-systems are manufactured as discrete modules and are fiber coupled. However, the need to drive down the cost has led to a strong drive in both industry and academia for photonic integration resulting in lower fabrication and packaging cost. Photonic integration leads to combining many devices, both active, and passive, onto single photonic chips [SAR-02][W0S04][MAS-02][NAG-05][SMI-96][SOL-95]. This integration results in lower form factors costs, which result in a significant reduction of the transponder cost. A lower transponder cost translates to a lower system cost and hence a lower cost in ($)/Gb/Km. The system cost for a 100 km reach, 500 km reach and a 1500 km reach system is plotted against a varying transponder cost for each system in Figure 6.13. It is seen that the system cost is proportional to the transponder cost. From Figure 6.13 it can also be observed that for a shorter reach the rate of increase of the system cost for an increase of transponder cost is much higher. Thus for the 100 km reach system the slope of the graph is higher compared to the 1500 km and 1000 km reach systems.

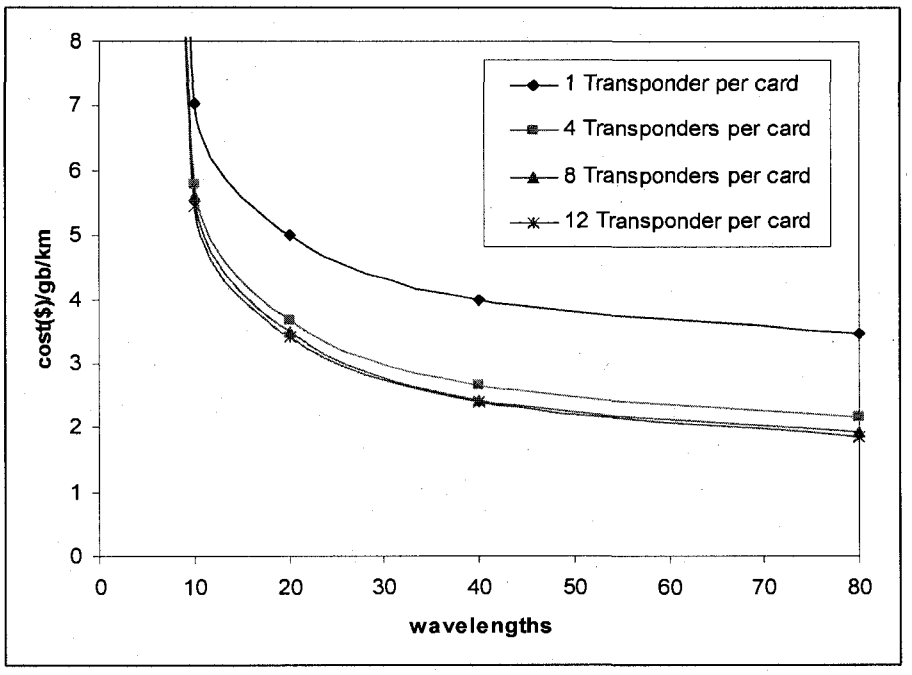

Figure 6.13 System Cost for varying fill levels for P_2 = 1,4,8 and 12 for a 500 km reach system

This is due to the fact that for a lower reach system there are a greater number of transponders per unit distance, and hence there is a higher impact from the transponder cost on the system cost. In Figure 6.13 it can be seen that the system cost for the 500 km reach and 1500 km reach systems for the first wavelength is higher than the 100 km reach system. This is due to the amplification cost and a higher transponder cost that is needed for the 500 and 1500 km reach systems. However, as the number of wavelengths in the system increases, at higher transponder cost levels the 1500 km reach systems become more cost effective. Thus at such price points, shorter reach with regeneration every 500 km is less advantageous compared to a 1500 km reach system. This further highlights the argument that optical reach is dependent on the technology used and the cost of the different components used to build the system. The smaller form factor could be the result of integration of functionalities like the laser and the driver circuits into a single package, or due to the integration of multiple optical functions such as multiplexing, demultiplexing and switching into a single optical module.

6.6.3 Transponder Shelf Packing

The next logical step after the vertical integration of optical subsystems is the transponder packing. From Equation (6.1) it can be seen that the packing density impacts the cost of the optical network system. Such integration would lead to a smaller equipment count and lesser number of shelves. The packing factor N_{CP} represents the number of cards packed per shelf and the packing factor N_{TC} represents the number of transponders packed per card. Higher packing factor (N_{TC}) indicates a higher number of transponders per card. As can be seen in Equation (6.1), packing more transponders per card results in saving on the circuit board cost and leads to a reduced number of transponder cards. This effect is plotted in Figure 6.9. It is observed from the graph that at lower fill levels the impact of transponder packing on the system cost is not as significant as compared to that at higher fills. As shown in Figure 6.14, at a lower fill there is no significant cost savings due to transponder and shelf packing. However, as the number of wavelengths increase the transponder and shelf costs (about 65% of net cost at 25% fill and about 85% of system cost at 100% fill) become very significant and the packing factor plays a significant role in the system cost. Here the packing factor N_{TC} is varied from 1 to 12 transponders per card and there are four cards per shelf. As the dominant system cost is in the amplifiers, the savings amount to about 0.5% to 1% when the packing of transponders is increased from one transponder per card to 4 to 8 to 12 transponders per card. In comparison, at higher fill, as the transponders and shelves contribute to a very significant percentage of the system cost, the system cost reduces by 30% when the number of transponders is increased from one to four per card. However as the number of transponders per card increases beyond 4, the impact of the packing density decreases and there is no significant impact on the total system cost by increasing the number of transponders per card. It can also be seen from Figure 6.14 that by packing more cards per shelf results in a lower system cost. However, as the packing factor increases the net decrease in system cost reduces.

The packing factor (N_{CP}) accounts for the number of transponder cards per shelf. By achieving a high packing density of transponder cards per shelf the number of shelves can be reduced and hence the system cost as well. The impact of integration and packing on

the normalized cost/Gb/km for a 500 km reach system is plotted in Figure 6.15. Here the transponder cost is assumed to be $2000. This graph is plotted for a full fill system. It is evident that the system cost is a function of both N_{CP} and N_{TC}. Also, beyond a certain packing density there is no significant savings in the system cost.

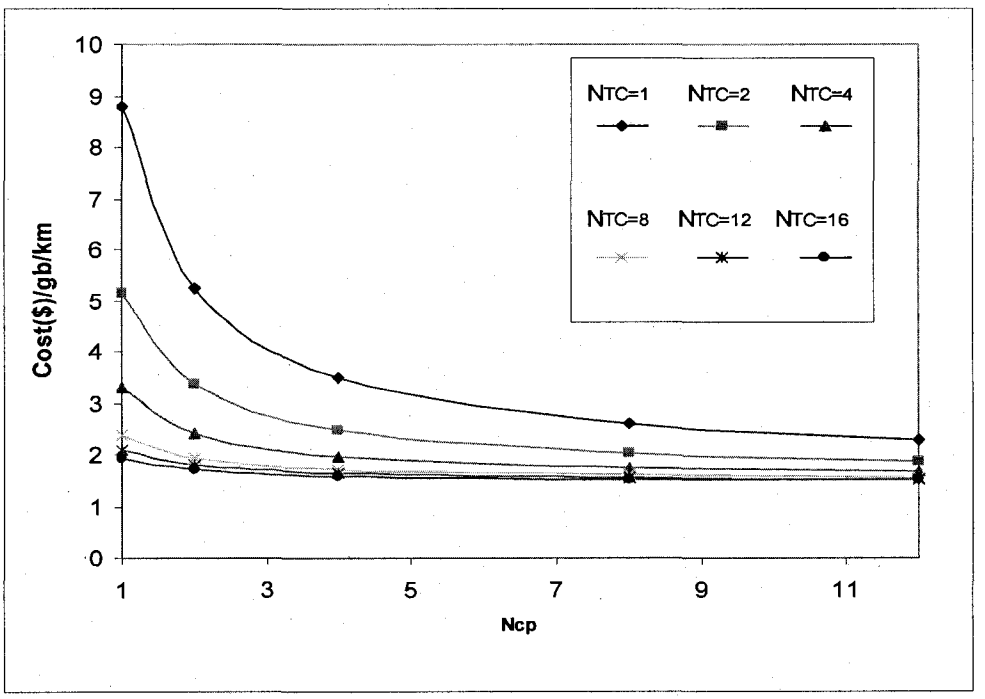

Figure 6.14 System Cost vs. N_{CP} at full fill for N_{TC} = 1,4,8, 12,16 for a 500 km reach system

6.7 Conclusions

In this part of the thesis we explored the concept of optical reach for an optical network. It was shown that extending the optical reach of a system is not necessarily the solution to achieve optical reach. In addition, optimizing the optical reach to match the distance of the non-regenerated links with the majority of the traffic demands might not result in the lowest system cost. It was shown that the optical reach depends on the various technologies used to build the system, given a certain network topology. In addition, we presented techniques like pump and spectral upgrades to achieve lower initial investments costs and a higher ROI for lean networks. The impact of transponder packing and photonic integration on the system cost has been also highlighted in this chapter. It can also be concluded from this study that by using a combination of modularization of

amplifiers, integration and transponder packing techniques the network provider can build a scalable pay-as-you-grow network.

Chapter 7. Conclusions and Future Work

In this thesis we have discussed major design issues in next generation wavelength routed optical networks. The focus of this dissertation has been on developing algorithms and designs to effeciently utilize available resources in the next generation WDM networks. Some of the major issues that need to be addressed in these networks are the provisioning of bandwidth and dimensioning of resources. This will lead to better cost-capacity- reach curves.

7.1 Conclusions

In conclusion through this research we have

- Shown that through proper selection of the waveband size and criticality levels it is possible to reduce the global degradation of blocking probability induced due to reservation of wavebands.
- Shown that the tunable-dense regenerator-placement scheme can achieve similar or equivalent performance to the fixed-sparse scheme, with, however, a much smaller total number of transponders in the network. Therefore, the tunable-dense regenerator-placement scheme is more cost-effective than the prevailing fixed-dense regenerator-placement scheme.
- Quantified the impact of transmission impairments on the routing algorithms. These algorithms provide signal quality guaranteed connections which reduces the impact of the physical impairments.
- Examined the availability of resources being one of the major factors affecting the blocking probability and presented a mechanism to maximize the utilization of TR pairs, and keep the blocking probability at acceptable limits.
- Presented a sharable architecture to maintain the QoS and acceptable blocking probabilities for add-drop calls and regeneration calls.

- Developed a novel architecture to achieve maximal sharing amongst transponder cards. By adding a small switch between the transmit and receive interfaces of a transponder card, we were able to make it function as an add-drop and regenerator card. Thus, when traffic was bursty for certain time periods, the additional transponders needed to handle the bursty load could be borrowed from the regeneration section. This allowed maximal sharing of transponder cards during periods of non-conformance of traffic.
- Presented three different steerable architectures to transparently and all-optically route wavelengths coming in from any direction to any available transponder. The architectures presented herein have the ability to support 100% steerability and can route any wavelength to any transponder. It can also be concluded that there are distinct advantages to choosing different architectures for a steering switch. The choice of any such architecture, to minimize the cost, would depend on the current price points of the devices being used. At different price points different architectures become more economically feasible in terms of the cost.
- Introduced the concept of optical reach. In this dissertation, we have shown that optical reach for a particular network varies depending on total cost of ownership and can vary significantly depending on the technology used. We also discussed the CAPEX and OPEX involved in achieving optical reach, and provided solutions and price points as indicators to when and how each technology can contribute to the optical reach. More importantly we have shown that the answer to achieving optical reach is changing and that achieving the best optical reach really depends on the type of technology used.

7.2 Future Research

This dissertation focused on the design and architecture of the next-generation optical network. We highlighted the areas of efficient resource utilization, and provided mechanisms and techniques to achieve them. Some of the areas of future research that can be undertaken are as follows:

- This research modeled the fairness problem in multi-hop WDM optical networks. This research through simulation and through mathematical modeling of a link showed that the traffic classification mechanism was a way to lower the impact of unfairness. An area of further research is to provide an accurate network-wide mathematical model to evaluate the impact of fairness and to model the different wavelength assignment schemes presented in this thesis.
- The impact of using a sharing mechanism to efficiently utilize all the available transponders was proposed in this research. An impairment aware algorithm which routes the traffic using the best available path using the smallest number of regenerators was also proposed. Extension of this proposed algorithm to be aware of the sharable transceivers available to make use of the sharing mechanism is an area of interest for further research.
- There is also an interest in using the Traffic classification algorithms in combination with impairment aware routing algorithms in order to optimize the utilization of wavelengths and provision signal quality guaranteed connections.
- The concept of optical reach has been explored in this thesis. It has been shown that optical reach for a particular network varies depending on total cost of ownership and can vary significantly depending on the technology used. However, more research is needed to analyze the impact of reach on a network-wide scale, using realistic traffic.

Appendix A Physical Layer Impairments

In lightwave communication systems, optical signal loss is a phenomenon associated due to the physical composition of the fiber. Hence, optical signal loss is the main factor to limit the transmission distance, also limited by fiber dispersion. In order to overcome the fiber loss, optical regeneration has been applied to amplify the optical signal. The process of regeneration is cumbersome and complicated especially in multichannel lightwave systems where each wavelength needs to be regenerated separately. Therefore, optical amplifiers have been developed to amplify directly the optical signal and have become a very important component in lightwave systems.

A.1 Attenuation

Attenuation is one of the most fundamental impairments that affect an optical signal when it propagates through the fiber. It is a property of the fiber, and is a result of various material, structural, and modular impairments in the fiber. The attenuation in a fiber is characterized by the attenuation coefficient α and is expressed in dB per km. It represents the loss of signal power in dB per kilometer.

It can be expressed as

$$\frac{dP}{dz} = -\alpha P \tag{A.1}$$

Here $\frac{dP}{dz}$ is the change in power with respect to length. It should be noted that the direction of propagation of the signal is in the z-direction.

If the input power is P and L is the total length of the fiber we can express the output power and the end of the fiber with

$$P_2 = P_1 e^{-\alpha L} \tag{A..2}$$

Thus the value of α can be derived as

$$\alpha = -\frac{10}{L}\log_{10}\left(\frac{P_2}{P_1}\right) \tag{A.3}$$

The unit of α is dB/km.

Generally the values for a single mode fiber α are about .25db/km in the 1550 nm range and .5db/km in the 1310 nm range.

A.2 Noise

In a multiwavelength optical network one of the main sources of noise is Amplified Spontaneous Emission (ASE) caused by the optical amplifiers present in the network. An optical amplifier is an essential component in building Wavelength Division Multiplexing (WDM) all optical networks because of the capability to amplify multiple channels simultaneously without converting the optical signal into the electrical domain. By compensating the signal loss along the fiber link, the optical amplifier considerably increases the optical reach making the All-Optical Network possible. In such an optical amplifier multiple channels share a common pool of photons for amplification. The gain of the Optical Amplifier is defined as the ratio of output to input signal power.

$$G = P_{out} / P_{in} \tag{A.4}$$

However the Optical amplifier also has a downside to its use. It degrades the OSNR by adding noise contributed by spontaneous emission.

The spontaneous noise for a given bandwidth B is given by

$$P_{ase} = hfBF(G-1) \tag{A.5}$$

Where , F is the Noise Figure, h is Plancks constant, B Bandwidth and f is the frequency. When N such amplifiers are cascaded as in a lightwave system [GIL-91], each of these amplifiers would add some amount of spontaneous noise power resulting in the degradation of the OSNR hence Bit-Error-Rate (BER) along the fiber optic link. During the transmission of the data through an optical channel, the receiver should be able to detect the individual bits without errors. Errors can occur when the receiver fails to detect an incoming bit correctly. Causes for the errors generally stem from the impairments that are associated with the transmission channel. In this case it is the ASE. A receiver fails to detect a bit correctly when it detects a 1 instead of a 0 and vice versa. For different rates the receiver has different magnitudes of errors and hence the BER is a figure of quality of an optical network. Typically the optical network systems should have a BER of 10^{-9} – 10^{-12} . Mathematically the BER is the sum of probabilities, such that when a 0 bit in

transmitted, a 1 is received and vice versa. The summation of these conditional probabilities gives the BER of the system.

In a cascaded amplifier system at each amplifier not only the signal but the ASE noise is also amplified. As the signal travels down the cascade of amplifiers, ASE grows linearly with the number of amplifiers giving rise to the reduction of OSNR and hence an increase in BER.

The total ASE noise power and signal power at the output of the n^{th} amplifier is given by

$$P_{ASE,n}^{TOT} = LG_n P_{ASE,n-1}^{TOT} + n_{sp} hf (G_n - 1) B_0 \tag{A.6}$$

$$P_{sig,n} = LG_n P_{sig,n-1}$$

With $P_{ASE,0}^{TOT} = 0$ and $P_{sig,0}$ is the transmitted signal power.

A.3 Crosstalk

In a wavelength routed optical network spanning a larger geographical area and many hops an optical signal will pass through a large number of intermediate nodes. At each of these intermediate nodes some noise may be added due to the presence of crosstalk in the switching element. This crosstalk is accumulative as the signal travels through intermediate nodes in the network. A detailed analysis of this crosstalk has been done in [SHE-99]. The crosstalk can be broadly classified as Intraband and Interband crosstalk [SHE-99]. Hetrodyne crosstalk is also called intraband crosstalk and occurs between signals at different wavelengths. Hetrodyne crosstalk can be suppressed by filtering. On the other hand, homodyne crosstalk originates from the signals at the same wavelength. Homodyne crosstalk cannot be eliminated by filtering and so it will beat with the signal and generate new noise.

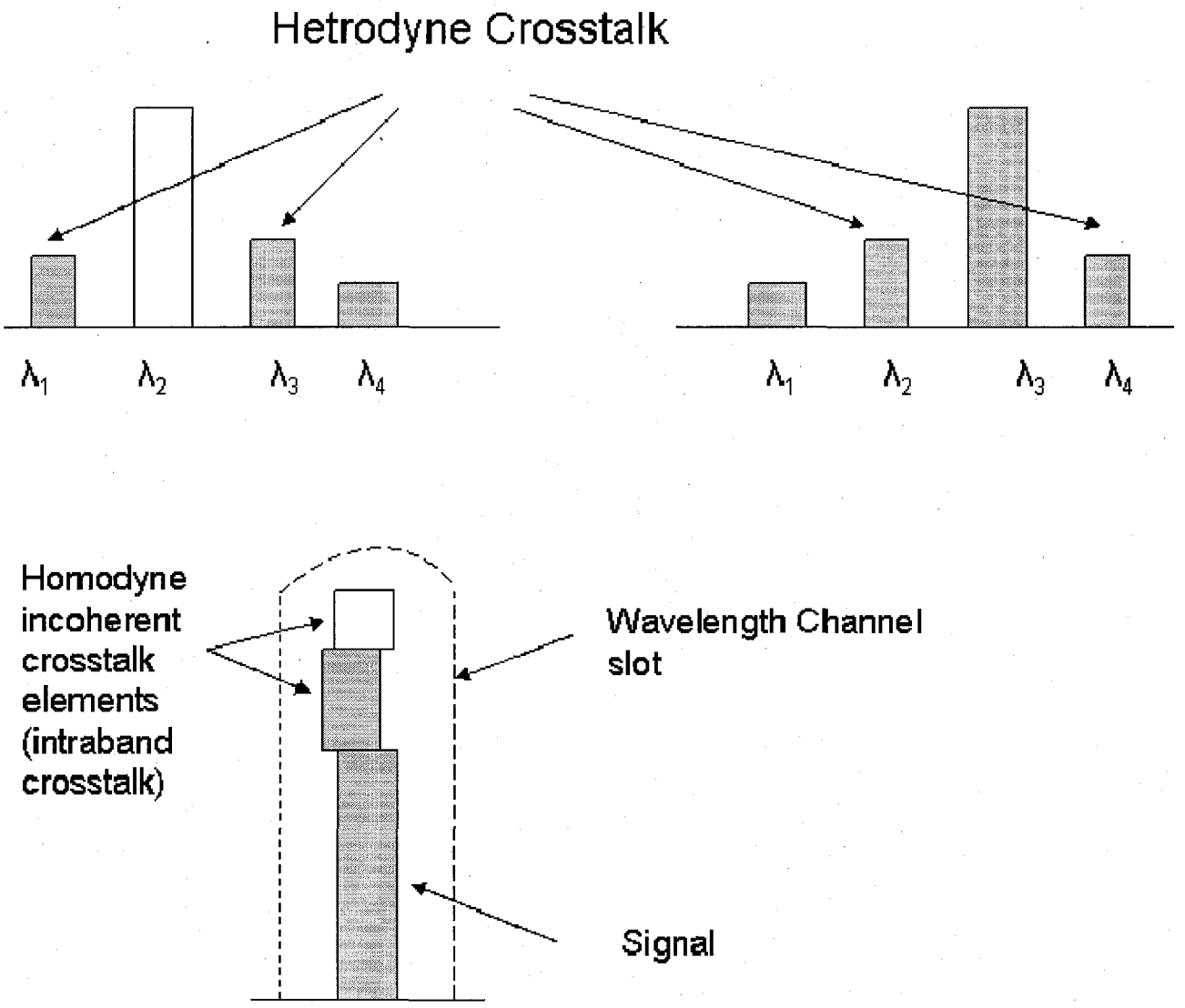

Figure A.1 Crosstalk

Interband crosstalk is situated in the wavelengths outside the channel slot. Interband crosstalk can be removed with narrow-band filters and it produces no beating during detection so it is less harmful. Also such crosstalk is non accumulative with multiple node traversing. In comparison the Intraband crosstalk is more harmful. This crosstalk is caused due to interference in the same wavelength slot. It cannot be removed by an optical filter and hence it accumulates throughout the network. The Intraband crosstalk for a given lightpath at an $N_P x N_P$ OXC is induced by N_P-1 lightpaths carried over the same wavelengths due to imperfections in the switch construction.

The Intraband crosstalk between interfering optical channels has been identified as one of the major limitations in diameter and performance of the wavelength switched optical network. When the number of switching elements are large, the Intraband crosstalk accumulates linearly over the optical path and becomes a cause for signal degradation and therefore becomes a constraint for the maximum number of nodes the signal can travel without regeneration

Due to the insertion loss and crosstalk induced in the switch due to the imperfections in the switch architecture additional power is required to offset the effects of these impairments. This is measured in terms of the power penalty. The power penalty is defined as the additional signal power required to maintain a specified BER in the presence of a particular impairment.

It can be given as

$$\text{Power Penalty} = 10\log_{10}\left[\frac{Power\,\text{Re}\,quiredWithimpairment}{Power\,\text{Re}\,quiredWithoutimpairment}\right] \qquad \text{(A.7)}$$

It has been shown in [SHE-99] that the probability function for the power penalties is of the Gaussian form and can be given as

$$\text{Power Penalty} = -5\log[1-4q^2 10^{(E_{db}/10)}] \qquad \text{(A.8)}$$

where $E_{db} = 10\log_E$ which is the component crosstalk in db.

q is the Q-factor corresponding to the reference BER (q=5.9 for a BER of 10^9)

There is an error floor corresponding to the BER at $4q^2 10^{(E_{db}/10)}=1$, where power penalty tends to be infinity. It is impossible to achieve a BER smaller than the error floor because of the nature of the crosstalk.

The OXC is an N_PxN_P switch with N_P input and N_P output ports. Each input/output fiber is assumed to have M wavelengths. There are hence M optical switch elements with N_P inputs and N_P outputs. In order to multiplex/demultiplex the signals there are N_P multiplexers and demultiplexers. The worst case of crosstalk occurs when the switch is fully loaded. In this case signal passing through the switch will be interfered by N_P-1

crosstalk elements from the switch and M-1 elements from the multiplexer/demultiplexer pair. Thus the total number of cross talk elements is $M+N_P-2$.

A.4 Dispersion

Another important characteristic affecting the signal is dispersion in the fiber. The effect of dispersion is the broadening of the light pulse as it travels down the length of the fiber. There are three main types of dispersion which are caused for different reasons

1. Intermodal dispersion
2. Chromatic dispersion
3. Polarization mode dispersion (PMD)

Intermodal Dispersion

When light propagates through a fiber, it follows many trajectories or modes. The number of modes by which the light can propagate down the fiber can be given by the expression

$$M = (Fr)^2/2 \qquad \text{(A.9)}$$

where Fr is the normalized frequency. Thus if Fr is very large, many modes will propagate. This results in the broadening of the pulse after traveling some distance as shown in Figure. At the receiving end, the energy from the different modes arrives somewhat delayed in time in relation to the principle mode resulting in the broadening of a given light pulse. This causes a problem in signal detection. The effects of such dispersion can be eliminated by using a single mode fiber.

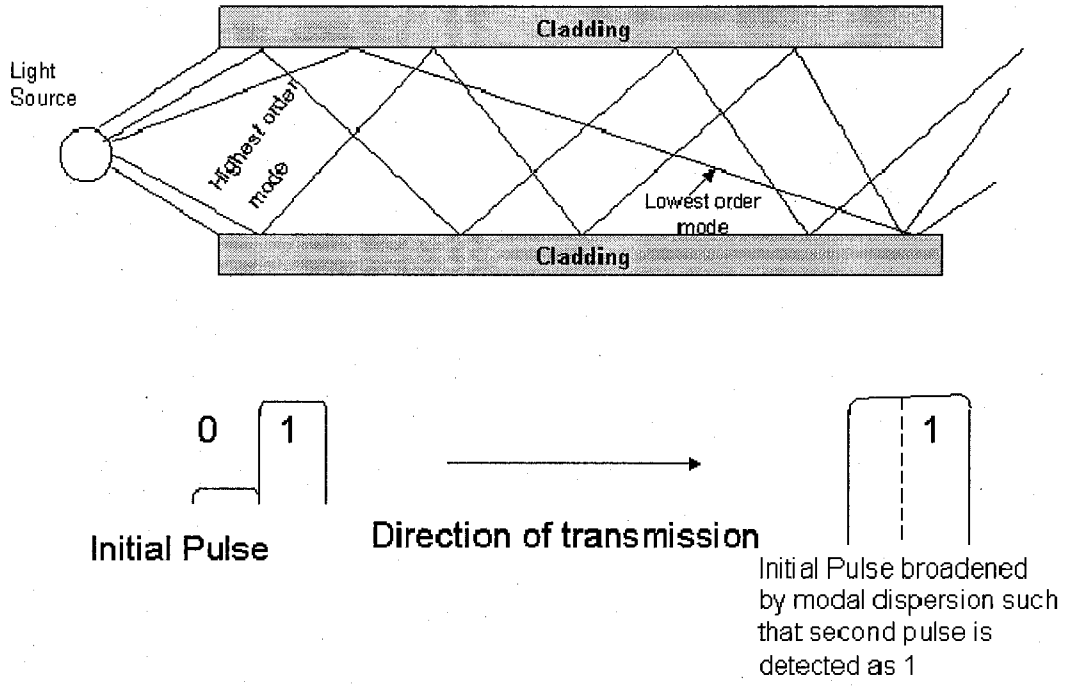

Figure A.2 Impact of Dispersion on a Pulse

Chromatic Dispersion

Chromatic Dispersion is a combination of two effects: Material Dispersion (D_M) and Waveguide Dispersion (D_W). Waveguide Dispersion is caused by the fact that when a single-mode fiber is drawn fro glass, the geometric form and refractive index profile contribute significantly to the wavelength dependence of the velocity of propagation of the pulses traveling in the fiber. The Material Dispersion (D_M) is caused by the fact that different wavelengths passing through certain materials at different velocities. Chromatic Dispersion, which is the sum of the above mentioned dispersions, is cumulative with the distance. Thus the broadening of the pulse due to the chromatic dispersion impairs system performance resulting in intersymbol interference imposing a limitation on the transmission distance.

Dispersion parameter, D_p, is of the form [AGG-95]

$$D_p = \frac{2\pi c}{\lambda^2}\beta_2 \qquad \text{(A.10)}$$

Where c is the speed of light, λ is the wavelength, and β_2 is the second order Group velocity dispersion. D_p is measured in units of ps/nm/km, indicates the amount of broadening in picoseconds when a pulse of one nanometer bandwidth propagates through one km of fiber.

It is also sensitive to the number of links in tandem and the link lengths. It is also very sensitive to the increase in bit-rate. The effects of such dispersion can be reduced with a decrease in the fiber's chromatic dispersion and by using dispersion compensation.

Polarization Mode Dispersion

In a single mode fiber, only one mode is present. However, from the viewpoint of polarization two modes are launched into the fiber. These polarization modes are orthogonal to each other. For an ideal fiber, the cross section of the fiber is circular and the speed of each of the orthogonal modes is identical. However, due to the imperfections in the manufacturing process, it is difficult to achieve a "perfect fiber". Stresses are induced onto the fiber during the manufacturing process. Also, the mechanical action of winding fiber on mandrels causes asymmetrical strains. When the cable is installed further stresses are induced. Such stresses deform the fibers' circularity and concentricity resulting in elongation. This results in a change in the propagation speed of the different modes. This difference in speeds between the different modes results in statistical spreading of the pulse over time. This is PMD. PMD is measured in picoseconds for a particular span of fiber.

Appendix B Ergodic Markov Chains

The foundation of Markov chain theory is the Ergodicity Theorem. It establishes the conditions under which a Markov chain can be analyzed to determine its steady state behavior. Ergodicity is an important property of a system possessing statistical equilibrium. Ergodicity simply means that in the realization of process, the proportion of the time interval *(0,x)* that the system spends in state E_j converges to the equilibrium probability P_j as $x \to \infty$.

A Markov chain can be characterized by the properties of its states. A Markov chain is

- Transient if all of its states are transient
- Recurrent non-null if all of its states are recurrent non-null
- Periodic if all of its states are periodic
- Aperiodic if all of its states are aperiodic

An irreducible Markov chain is one in which all states are reachable from all other states (i.e., all states communicate - see below).

An irreducible Markov chain is one of the following:

- Transient
- Recurrent non-null
- Recurrent null and if it is recurrent, then it is either periodic or aperiodic.

An ergodic Markov chain is

- Irreducible,
- Recurrent non-null, and
- Aperiodic

Most of the systems in which we are interested are modeled with ergodic Markov chains, because this corresponds to a well-defined steady state behavior.

Let $\pi = \{\pi_1 \pi_2 ..... \pi_k\}$ be the limiting distribution for the state probabilities (the number of states may be infinite). That is,

$\pi_i = \lim_{n \to \infty} p_i(n)$, $p_i(n)$ is the probability of being in state i at time n, n=0,1,2,...

B.1 Ergodicity Theorem

If a Markov chain is ergodic, then a unique steady state distribution π exists, independent of the initial state $p(0) = \{p_1(0)\ p_2(0) \ldots p_k(0)\}$.

Although we will not prove this theorem, ergodicity comes into play roughly as follows:

- aperiodic and recurrent non-null -> π exists
- irreducible π is unique and independent of $p(0)$

Some shortcuts exist for helping to determine when a Markov chain is ergodic.

1. A Markov chain with a finite number of states has only transient and recurrent non-null states (in other words, only a Markov chain with an infinite number of states can be recurrent null).
2. A sufficient test for a state to be aperiodic is that it has a "self-loop" (that is, the probability that the next state is the same as the current state is non-zero) or that it communicates with an aperiodic state. Two states i and j communicate if i is reachable from j and vice versa.
3. In an irreducible, finite state Markov chain, the presence of one aperiodic state guarantees ergodicity.

Appendix C Transceiver Sharing for different load levels

Sharing of transponders results in a lower blocking probability for the number of calls added or dropped at a node. Thus in order to achieve a given blocking probability the sharing scheme results in a lower number of transponders. This is shown in Figures shown below. The graph of the load vs. Number of Transponders for varying blocking probability levels is plotted. It is seen that a sharing scheme outperforms the no-sharing scheme in terms of the number of transponders needed.

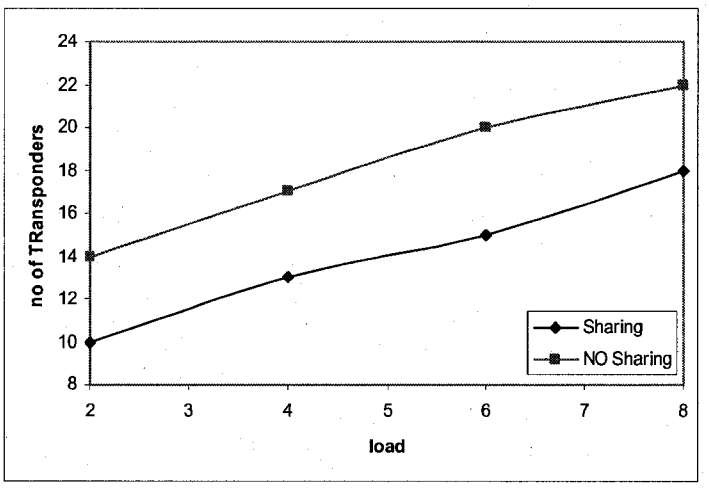

Figure c.1 Regeneration Load = 2, to maintain a BP = 0.01 for the regeneration section and add-drop section

Percentage savings on the number of transponders using sharing mechanism=28%

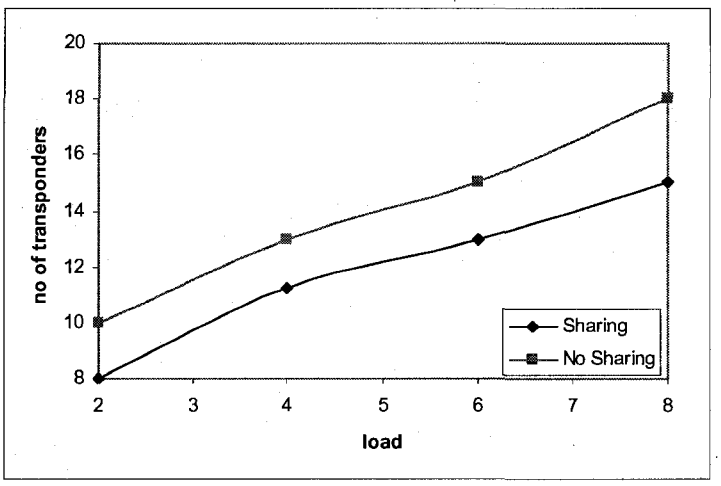

Figure c.2 Regeneration Load = 2, to maintain a BP = 0.05 for the regeneration section and add-drop section

Percentage savings on the number of transponders using sharing mechanism=20%

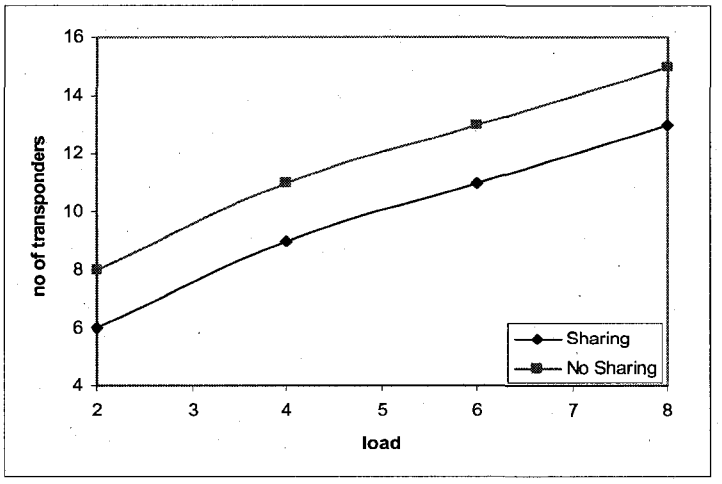

Figure c.3 Regeneration Load = 2, to maintain a BP = 0.1 for the regeneration section and add-drop section

Percentage savings on the number of transponders using sharing mechanism=25%

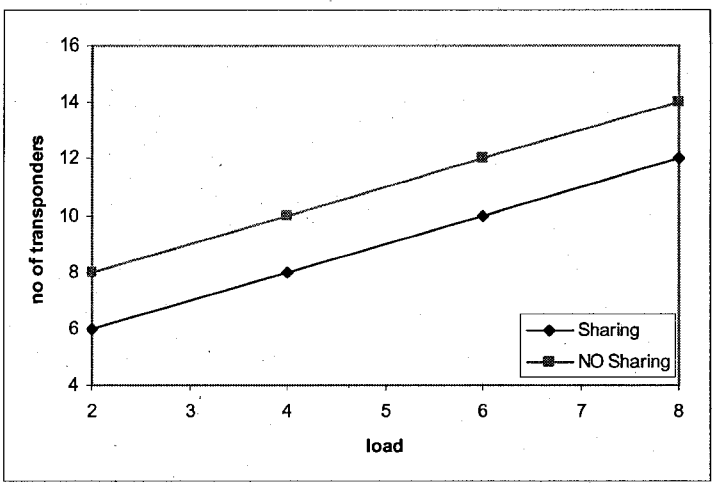

Figure c.4. Regeneration Load = 2, to maintain a BP = 0.15 for the regeneration section and add-drop section

Percentage savings on the number of transponders using sharing mechanism=25%

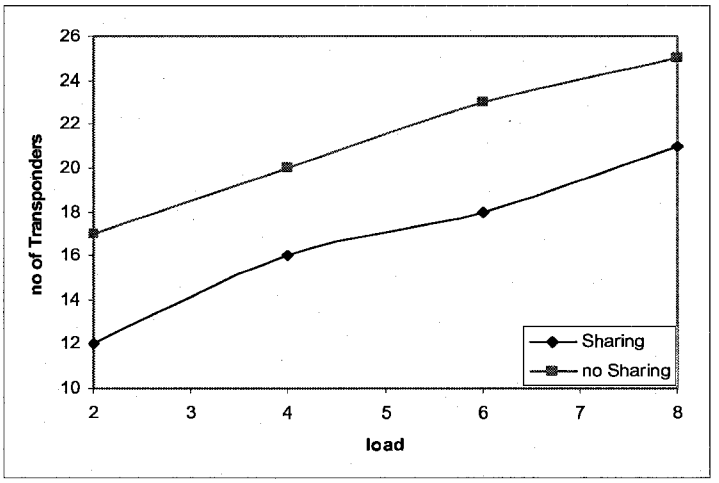

Figure c.5 Regeneration Load = 4, to maintain a BP = 0.01 for the regeneration section and add-drop section

Percentage savings on the number of transponders using sharing mechanism=30%

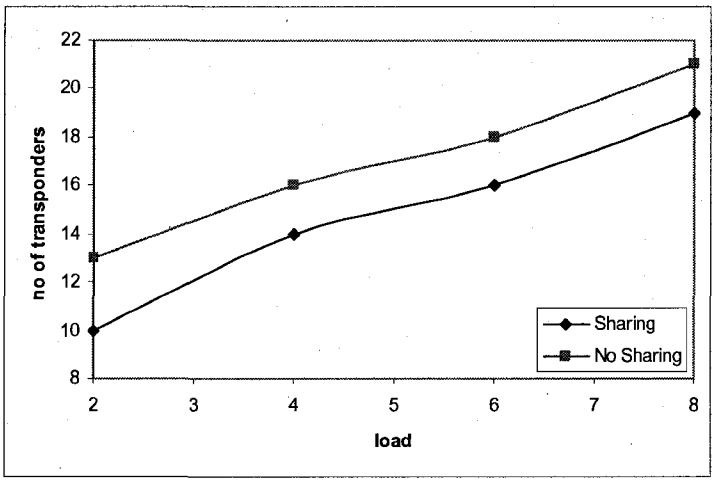

Figure c.6 Regeneration Load = 4, to maintain a BP = 0.05 for the regeneration section and add-drop section

Percentage savings on the number of transponders using sharing mechanism=23%

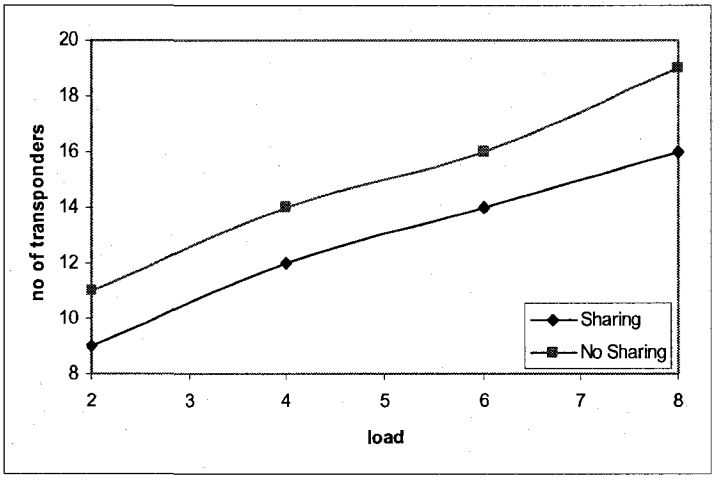

Figure c.7 Regeneration Load = 4, to maintain a BP = 0.1 for the regeneration section and add-drop section

Percentage savings on the number of transponders using sharing mechanism=18%

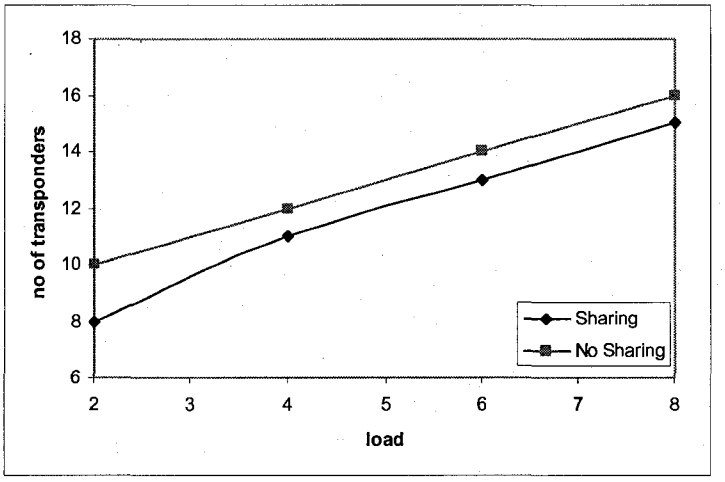

Figure c.8 Regeneration Load = 4, to maintain a BP = 0.15 for the regeneration section and add-drop section

Percentage savings on the number of transponders using sharing mechanism=20%

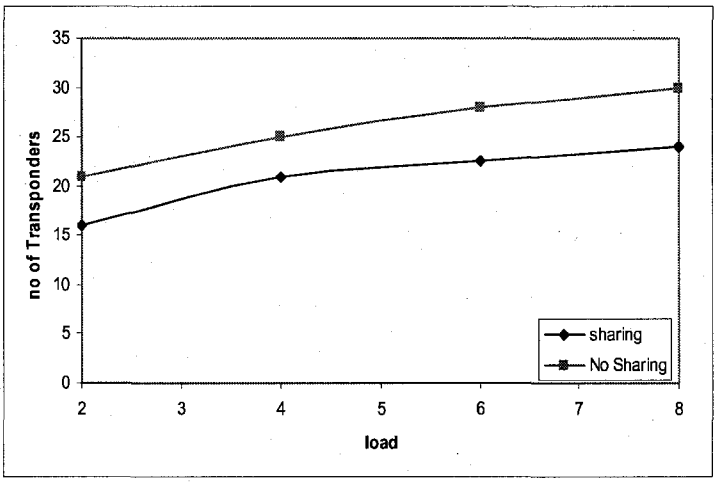

Figure c.9 Regeneration Load = 8, to maintain a BP = 0.01 for the regeneration section and add-drop section

Percentage savings on the number of transponders using sharing mechanism=23%

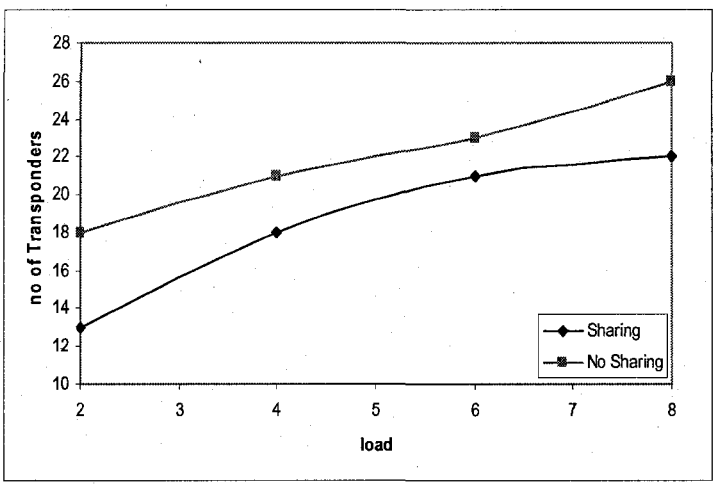

Figure c.10 Regeneration Load = 8, to maintain a BP = 0.05 for the regeneration section and add-drop section

Percentage savings on the number of transponders using sharing mechanism=25%

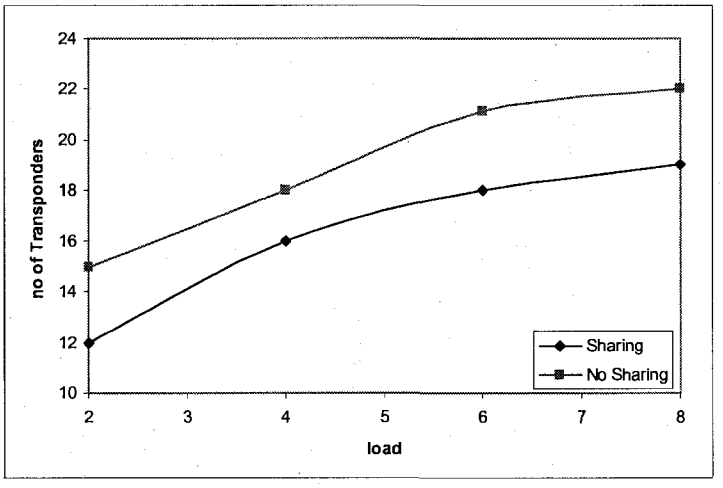

Figure c.11 Regeneration Load = 8, to maintain a BP = 0.05 for the regeneration section and add-drop section

Percentage savings on the number of transponders using sharing mechanism=20%

Appendix D Wavelength Selective Switch

A wavelength Selective Switch(WSS) is a low-loss, compact integrated-optics modular device with high switching flexibility. The Wavelength Selective Switch comes in many configurations like 1x5 or 1x9 WSS. At a WSS any channel can be dropped at any port resulting in truly reconfigurable add-drop.

The Wavelength Selective Switch is an K-port module composed of a hermetically sealed optics block (as shown in Figure D.1) and control electronics. The optics block is based on the highly successful free space optics platform.

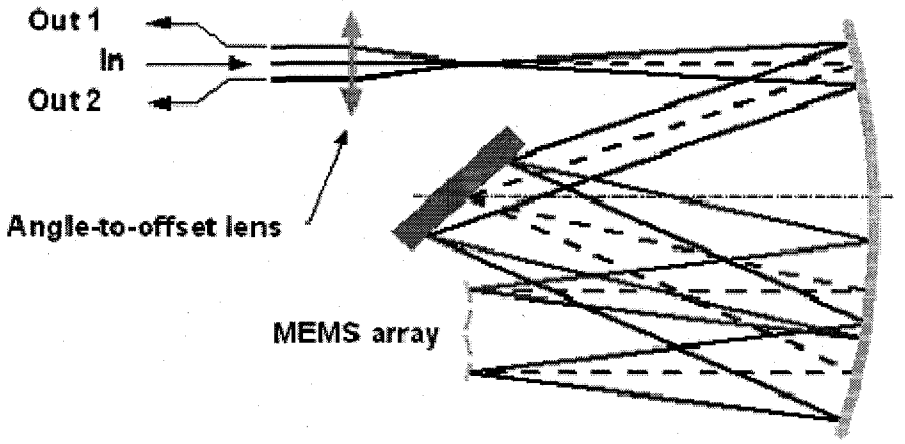

Figure D.1: Wavelength Selective Switch using MEMS (source JDS Uniphase)

The WSS is used to dynamically attenuate, block switch and route wavelengths independently. Any wavelength/wavelengths can be routed from any port/ports to any other port/ports in any order, resulting in a colorless solution, that is highly flexible and requires no pre-planning.

Some of the key features are (Source www.jdsu.com)

- 50 GHz 5x1
- Free space optics and MEMS technology

- Equalize, attenuate, block, switch/route any or all wavelengths
- Flat wide pass bands, low dispersion- cascadability
- Colorless solution

Appendix E Confidence Intervals

Any set of simulated values (in our case blocking probability) are measured by taking a very large number of simulation runs. Each of these are simulated may times to produce a sets of uncorrelated results. These runs are identical and independent from each other by nature of the different values of the seeds chosen during each simulation run. Let us assume a set of n independent runs to obtain blocking probabilities for a given optical network. Let this set of blocking probabilities be represented by $B_1, B_2, B_3, ...B_n$. Let the average blocking probability be B_k for the k^{th} simulation run.

The mean value of all these values can be given as

$$\overline{B} = \frac{1}{n}\sum_{k=1}^{n} B_k$$

This mean however, gives us only one value for the estimate of the expected value $E[B] = \mu$. In order to get a sense of how good the estimate for $\overline{B}$ is we would need to compute the variance V_b^2

The variance is given by

$$V_b^2 = \frac{1}{b}\sum_{k=1}^{n} (B_k - \overline{B})^2$$

A small value of variance would indicate that the results obtained from the simulation are clustered around the mean value and we can say with confidence the mean is close to the expected value. On the other hand, a large variance indicates that the results are not clustered around B and we cannot say with confidence that the mean value lies around the expected value.

Now, instead of specifying a single value to estimate the mean $E[B] = \mu$ we will specify an interval of values that is highly likely to contain the true value of the parameter. This is done by specifying some high probability, say $1-\alpha$; we then find an interval $[L(B), U(B)]$ such that:

The probability $P[L(B) \leq \mu \leq U(B)] = 1-\alpha$

The interval contains the true value of the parameter in question with a probability of $1-\alpha$. Such an interval is a $(1-\alpha)$ X100 % confidence interval. Using the standard deviation and the t distribution table, the lower and upper limits of the 95% confidence interval can be calculated as follows:

$$\text{Lower Limit } L(B) = \overline{B} - \frac{\sigma t_{[1-\frac{\alpha}{2},n-1]}}{\sqrt{2}}$$

$$\text{Upper Limit } U(B) = \overline{B} - \frac{\sigma t_{[1-\frac{\alpha}{2},n-1]}}{\sqrt{2}}$$

Where

α=0.05

n = number of observations

$\overline{B}$ = sample average

σ = sample standard deviation

Thus, the confidence interval means that 95% of the simulation results fall within that interval. In this work the confidence interval is computed based on 5 independent runs. It was observed that 95% of the results were within the calculated confidence interval for each experiment. These calculated confidence intervals were very small and hence were not plotted in the figures. A sample confidence interval calculation is shown below.

Table E.1 Example of Confidence Interval calculations

Load	Simulation run Averages								
(erlang)	B_1	B_2	B_3	B_4	B_5	$\overline{B}$	σ	L(B)	U(B)
1	8E-6	1E-5	2E-5	8E-6	3E-6	8E-6	6E-6	0	2E-5
2	8E-4	6E-4	8E-4	6E-4	6E-4	7E-4	1E-4	5E-4	9E-4
3	0.0114	0.0114	0.0123	0.0113	0.0112	.0115	4E-4	.0108	0.0122
4	0.0502	0.0514	0.0522	0.0527	0.0530	0.0517	2E-3	0.0482	0.0552
5	0.1021	0.1032	0.1017	0.1023	0.1019	0.1022	7E-4	0.101	0.1034

The probabilities of 5 independent runs are shown together with the calculated average $\overline{B}$, the lower and upper values of the interval L(B) and U(B). Therefore it can be concluded that the simulation results in this thesis have 95% confidence intervals.

References

[AGG-94] A. Aggarwal, A. Bar-Noy, D. Coppersmith, R. Ramaswami, B. Schieber, and M. Sudan, "Efficient Routing and Scheduling Algorithms for Optical Networks", Proceedings of 5th Annual ACM-SIAM symposium on Discrete Algorithms, pp. 412-429, Jan. 1994.

[AGG-95] G.P. Agrawal, "Non-Linear Fiber Optics," 1995.

[AGG-97] G.P. Agrawal, "Fiber-Optic Communication Systems," 1997.

[AL-F-04] A. I. Al-Fuqaha, G. M. Chaudhry, M. Guizani, and M. A. Labrador, "Routing Framework for All-optical DWDM Metro and Long-haul Transport Networks with Sparse Wavelength Conversion Capabilities," IEEE Journal on Selected Areas in Communication, Vol. 22, no. 8, pp. 1443–1459, Oct. 2004.

[ALI-99] M. Ali, B. Ramamurthy and J.S. Deodun, "Routing and Wavelength Assignment with Power Considerations in All-Optical Wavelength-Routed Networks", Proceedings of IEEE GLOBECOM 99, Rio de Janeiro, pp. 1433-1437, Dec. 1999.

[ATM-99] ATM Forum, "PNNI Augmented Routing (PAR) Version 1.0," af-ra-0104, January 1999.

[BAL-97] K. Bala and E. Bouillet, "The Benefits of Wavelength Interchange in WDM Rings", Proceedings of IEEE International Conference on Communciations, Montreal, Canada, pp. 411-415, June 1997.

[BAN-95] D. Banerjee and B. Mukherjee, "A Practical Approach for Routing and Wavelength Assignment in Large Wavelength-routed Optical Networks,"

IEEE Journal on Selected Areas in Communications, Vol. 14, No. 5, pp. 903-908, Jun 1996.

[BAR-95] R. Barry and D. Marquis, "An improved Model of Blocking Probability in All-Optical Mesh Networks with Wavelength Changers," LEOS Summer Topical Meetings, San-Francisco, pp. 43-44, Aug. 1995.

[BAR-96] R.A. Barry and P.A..Humblet, "Models of Blocking Probability in All-optical Networks with and without Wavelength Interchangers", IEEE Journal on Selected Areas in Communication, Vol. 14, No. 5, pp. 858-867, June 1996.

[BEL-06] M. P. Belanger and M. Cavallari, "Network Cost Impact of Solutions for Mitigating Optical Impairments: Comparison of Methods, Techniques, and Practical Deployments Constraints," IEEE Journal of Lightwave Technology, Vol. 24, Issue 1, pp 150-163, Jan. 2006.

[BIR-95] A. Birman and A. Kershenbaum, "Routing and Wavelength Assignment Methods in Single-hop All-optical Networks with Blocking," Proceedings of IEEE INFOCOM '95, Boston, pp. 431- 438, Apr. 1995.

[BIR-96] A. Birman, "Computing Approximate Blocking Probabilities for a Class of Optical Networks", IEEE Journal of Lightwave Technology: Special Issue on Optical Networks, Vol. 14, No. 5, pp. 852-857, May 1996.

[BOR-98] S. Borst and D. Mitra, "Virtual Partitioning for Robust Resource Sharing: Computational Techniques for Heterogeneous Traffic ", IEEE Journal on Selected Areas in Communications, Vol. 16, No. 5, pp. 668-678, June 1998.

[BUU-06] J. Bus and E. J. Murphy, "Tunable Lasers in Optical Networks," Journal of Lightwave Technology, Vol. 24, Issue 1, pp. 5-10 Jan 2006.

[CHL-89] I. Chlamtac, A. Ganz, and G. Karmi, "Purely Optical Networks for Terabit Communication," Proceedings of the Eighth Annual Joint Conference of the IEEE Computer and Communications Societies, IEEE INFOCOM '89, Ottawa, Canada, Vol.3, pp.3887 - 896 April 1989.

[CHL-92] I. Chlamtac, A. Ganz, and G. Karmi, "Lightpath Communications: An Approach to High Bandwidth Optical WAN's," IEEE Transactions on Communications, Vol. 40, No. 7, pp. 1171-1182, July 1992.

[CHL-96] I. Chlamtac, A. Farago, and T. Zhang, "Lightpath (Wavelength) Routing in Large WDM Networks," IEEE Journal on Selected Areas in Communications, Vol. 14, No. 5, pp 909-913, June 1996.

[CHO-00] J. S. Choi, N. Golmie, F. Lapeyrere, F. Mouveaux, and D. Su, "A Functional Classification of Routing and Wavelength Assignment Schemes in DWDM Networks: Static Case," Proceedings of 7th International Conference on Optical Communication and Networks, Toronto, pp 401-408, Jan. 2000.

[CHR-90] A.R. Chraplyvy, "Limitations on Lightwave Communications Imposed by Optical-fiber Nonlinearities" IEEE Journal of Lightwave Technology, Vol. 8, Issue 10, pp.1548 – 1557, Oct. 1990.

[CHU-02] X.W. Chu, B. Li, and I. Chlamtac, "On the Wavelength Converter Placement for Different RWA Algorithms in Wavelength-routed All-optical Networks," Proceedings of SPIE Opticomm'02, Boston, MA, pp. 186–197, July 2002.

[CHU-03] X. Chu, B. Li, and I. Chlamtac, "Wavelength Converter Placement Under Different RWA Algorithms in Wavelength-Routed All-Optical Networks", IEEE Transactions on Communications, Vol. 51, No. 4, pp. 607-617, Apr. 2003.

[DOD-97] S. D. Dods, J. P. R. Lacey, and Rodney S. Tucker, " Homodyne Crosstalk in WDM Ring and Bus Networks", IEEE Photonics Technology Letters, Vol. 9, No. 9, pp. 1285-1287, 1997.

[DOD-99] S. D. Dods, J. P. R. Lacey, and Rodney S. Tucker, " Performance of WDM Ring and Bus Networks in the Presence of Homodyne Crosstalk", Journal of Lightwave Technology, Vol. 17, No. 3, pp. 388-396, 1997.

[DOE-02] C. R. Doerr, L. W. Stulz, D. S. Levy, M. Cappuzzo, E. Chen, L. Gomez, E. Laskowski, A. Wong-Foy, and T. Murphy, "Silica-waveguide 1 x 9 Wavelength-Selective Cross Connect," Optical Fiber Communication Conference, Anaheim, CA, postdeadline paper FA3, 2002.

[DOS-01] B. Doshi, et al, "Transparent Cross-Connect and Ultra-Long-Reach Transmission Systems: Complementary Technologies", in Technical Proceedings of NFOEC 2001, Baltimore,MA, July 2001.

[DUC-02] T. Ducellier et al., "The MWS 1 × 4: A High Performance Wavelength Switching Building Block," Proceedings of European. Conference on Optical Communication (ECOC), Copenhagen, Denmark, session 2.3.1., Sept. 2002.

[DWI-00] A. Dwivedi et all, "Value of Reach Extension in Long-Distance Networks", Proceedings of NFOEC 2000, Denver, August 2000.

[EAR-03] M.P Earnshaw, J.B.D Soole, M. Cappuzzo, L. Gomez, E. Laskowski, and A. Paunescu, "8x8 Optical Switch Matrix using Generalized Mach-Zehnder Interferometers", IEEE Photonic Technology Letters, Vol. 15, pp. 810-812 March 2003.

[GHO-03] P. Ghobril, S. Tohme, "Towards a dynamic hierarchical cross-connecting without wavelength conversion in multi-fiber WDM networks", Proceedings

of 5th International Conference on Transparent Optical Networks, Barcelona, Spain, pp. 51 – 54, May 2003.

[KOV-96] M. Kovacevic and A. Acampora, "Benefits of Wavelength Translation in All-optical Clear-channel Networks," IEEE Journal of Selected Areas on Communications, Vol. 14, pp. 868–880, June 1996.

[ELL-01] G. Ellinas, "Wavelength Assignment Algorithms for WDM Ring Architectures", Optical Networks Recent Advances, pp. 19-45, Kluver Academic Publications, 2001.

[FAN-03] F.Fang, X.Zheng and H.Zhang, "Performance Study of Distributed Wavelength Reservation Protocols Within both Single and Multi-Fiber WDM Networks," Photonic Network Communications, Vol. 6, No. 2, pp. 95-103, Sep 2003.

[FRE-97] R.J. Freeman, "Fiber Optic Systems Communication", Wiley Press, 1997.

[GIL-91] C.R. Giles, E. Desurvire "Propagation of Signal and Noise in Concatenated Erbium-Doped Fiber Optical amplifiers" IEEE Journal of Lightwave Technology, Vol. 9, Issue 2, pp. 147 – 154, Feb. 1991.

[GIR-85] A. Girard, "Blocking Probability of Noninteger Groups with Trunk Reservation", in IEEE Transactions on Communications, Vol. 2, No. 33, pp. 113-120, Feb. 1985

[GOL-94] E. L. Goldstein, L. Eskildsem, and A. F. Elrefai, "Performance Implication of Component Crosstalk in Transparent Lightwave Networks," IEEE Photonics Technology Letters, Vol. 6, pp. 657-670, May 1994.

[GOL-00] N. Golmie, T. Ndousse and D. Su, "A Differentiated Optical Services Model for WDM Networks," IEEE Communications Magazine, Vol. 38, No. 2, pp. 68-73, Feb. 2000.

[GOP-81] G. J. Foschini, B. Gopinath, and J. F. Hayes, "Optimum Allocation of Servers to Two Types of Competing Customers", IEEE Transactions on Communications, Vol. 29, No. 7, pp. 1051-1055, July 1981.

[GUR-01] C.Murthy and M.Gurusamy, "WDM Optical Networks, Concepts, Design and Algorithms", Prentice Hall, 2001, pp. 67-69.

[HAH-02] D. Hah, S. Huang, H. Nguyen, H. Chang, H. Toshiyoshi, and M. C. Wu, "A Low Voltage, Large Scan Angle MEMS Micro-mirror Array with Hidden Vertical Comb-drive Actuators for WDM Routers," Proceedings of Optical Fiber Communication (OFC), Anaheim, CA, 2002, pp. 92–93. March 2002.

[HAH-02B] D. Hah, S. Huang, H. Nguyen, H. Chang, J. C. Tsai, and M. C. Wu, "Low voltage MEMS Analog Micro-mirror Arrays with Hidden Vertical Comb-drive Actuators," Proceedings of Solid-State Sensor, Actuator, and Microsystems Workshop, Hilton Head Island, SC, pp. 11–14, Jun. 2002.

[HAH-04] D. Hah, S. T. Y. Huang, J. C. Tsai, H. Toshiyoshi, and M. C. Wu, "Low voltage, Large-scan Angle MEMS Analog Micro-mirror Arrays with Hidden Vertical Comb-drive Actuators," IEEE Journal of Microelectromechanical. Systems., Vol. 13, No. 2, pp. 279–289, Apr. 2004.

[HUA-02] S. Huang, J. C. Tsai, D. Hah, H. Toshiyoshi, and M. C. Wu, "Open Loop Operation of MEMS WDM Routers with Analog Micromirror Array," Proceedings of IEEE/LEOS Optical MEMS Conference, Lugano, Switzerland, pp. 179–180, May 2002.

[HUA-03] Y. Huang, W. Wen, J.P. Heritage and B. Mukherjee, "Signal-Quality Consideration for Dynamic Connection Provisioning in All-Optical Wavelength-Routed Networks", Proceedings SPIE Optical Networking and Communications conference (OptiComm),Dallas, TX, pp. 163-173, Oct. 2003.

[KAU-81] J.S. Kaufman, "Blocking in a Shared Resource Environment", IEEE Transactions on Communications Vol. 29, No. 10, pp. 1474-1481, Oct 1981.

[KAM-97] I. P. Kaminow, T. L. Koch, Optical Fiber Telecommunications *IIIA*, San Diego, Academic Press, 1997.

[KAR-98] E.Karasan and E.Ayanoglu, "Effects of Wavelength Routing and Selection Algorithm on Wavelength Conversion Gain in WDM Optical Networks", IEEE/ACM Transactions on Networking., Vol.6, No.2, pp.186-196, Apr 1998.

[KAZ-96] L. Kazovsky, S. Benedetto, A. Willner, Optical Fiber Communication Systems, Boston, Artech House, 1996.

[KOG-96] M. Koga et al, "Design and Performance of an Optical Path Crossconnect System Based on the Wavelength Path Concept", IEEE Journal of Lightwave Technology, Vol. 14, No. 6, pp. 1106-1118, June 1996.

[KOV-95] M. Kovacevic and A. Acampora, "On Wavelength Translation in All-optical Networks", in Proceedings of the Fourteenth Annual Joint Conference of the IEEE Computer and Communication Societies, Boston, MA, Vol. 2 pp. 413-422, April 1995.

[KRI-99] S. Krishnan and A. K. Choudhury, and F. M. Chiussi, "Dynamic Partitioning: A Mechanism for Shared-Memory Management", Proceedings IEEE INFOCOM 99, New York, pp. 144-152, Mar. 1999.

[KUZ-92] A.Kuczura, "A Method of moments for the Analysis of a Switched Communication Networks Performance", IEEE transactions on Communications, Vol. Com-25, pp. 185-193, June 1992

[LI-03] Y.Li, M.J. Francisco , I. Lambadaris and D. Huang, "Traffic Classification and Service in Wavelength Router all-optical Networks", IEEE International Conference on Communications (ICC 03), Ottawa, Canada, Vol. 2, pp. 1375-1380, May 2003.

[LU-05] K.Lu, G.Xiao and I.Chlamtac, "Analysis of Blocking Probabilities for Distributed Lightpath establishment in WDM Optical Networks", IEEE/ACM Transactions Networking., Vol.13, no.1, pp. 187-197, Feb, 2005.

[MAR-02] D. M. Marom et al., "Wavelength-selective 1 × 4 switch for 128 WDM Channels at 50 GHz Spacing," in Proceedings Optical Fiber Communication (OFC), Anaheim, CA, 2002, pp. FB7-1–FB7-3.

[MAR-03] D. M. Marom et al., "Wavelength Selective 4 × 1 Switch with High Spectral Efficiency, 10 dB Dynamic Equalization Range and Internal Blocking Capability," in Proceedings of European Conference on Optical Communication (ECOC), Rimini, Italy, Sept. 2003.

[MAS-02] B.Mason, A. Ougazzaden, C. Lentz, L. Ketelsen, "Integrated Photonic Devices for Fiber Optic Communication Systems" in The 15th Annual Meeting of the IEEE Lasers and Electro-Optics Society, 2002. LEOS 2002. Glasgow, Scotland, Vol. 2, pp. 443- 444, Nov. 2002.

[MOK-04] A. Mokhtar, L. Benmohammad, M. Bortz "OXC port Dimensioning Strategies in Optical Networks- A nodal perspective", IEEE Communications Letters, Vol. 8, No. 5, pp. 283-285, May 2004.

[MIT-96] D. Mitra and I. Zeidins "Virtual Partitioning by Dynamic Priorities: Fair and Efficient Resource-Sharing by Several Services", Proceedings of the 1996 International Zurich Seminar on Digital Communications: Broadband Communications, Zurich, Switzerland, pp. 173-185, Feb. 1996.

[NAG-05] R. Nagarajan, C.H. Joyner,R.P. Schneider, et. al "Large-scale Photonic Integrated circuits" IEEE Journal of Selected Topics in Quantum Electronics, Vol. 11, Issue 1, pp.50 - 65 Jan. 2005.

[OKA-96] S. Okamoto, A. Watanabe, K. Sato, "Optical path Crossconnect Node Architecture for Photonic Transport Networks", IEEE Journal of Lightwave Technology, Vol. 14, no. 6, pp. 1410-1422, June 1996.

[OU-04] Y. Qu, P. Verma, J.Y. Cheung ,"Enhancing Carrying Capacity of a DWDM Network" Proceedings Optical Networks Control and Management (ONCM) Workshop in conjunction with ICPP 04, Montreal, Canada, pp 415-421, August 2004.

[PAP-01] D Papadimnitriou, et al, "Non-Linear Routing impairments in Wavelength Switched Optical Networks", Internet-Draft, Nov 01 (expired May 2002).

[PUC-05] A.Puc, G. Grosso, P.Gavrilovic, H.Fevrier, A.Kaminski, S.Burtsev,D. Chang, M.Foster, W. Pelouch and P.Perrier, "Ultra-wideband 10.7 Gb/s NRZ terrestrial Transmission Beyond 3000 km using All-Raman Amplifiers" in Proceedings of 31st European Conference on Optical Communication, 2005. ECOC 2005, Glasgow Scotland, pp. 17 – 18, Vol.1, Sept. 2005.

[RAM-97] R. Ramaswami and G. Sasaki, "Multiwavelength Optical Networks with Limited Wavelength Conversion," Proceedings IEEE INFOCOM 97, Kobe, Japan, pp. 489-498, April 1997.

[RAM-97] R. Ramaswami and A. Segall, "Distributed network control for optical networks", IEEE/ACM Transactions on Networking., Vol. 5, No. 6, pp. 936–943, Dec. 1997.

[RAM-99] B. Ramamurthy, D. Datta, H. Feng, J.P. Heritage and B. Mukherjee, "Impact of Transmission Impairments on the Teletraffic Performance of Wavelength-routed Optical Networks", IEEE Journal of Lightwave Technology, Vol. 17, No. 10 , pp. 1713-1723, Oct 1999.

[RAM-01] B. Ramamurthy, S. Yaragorla, and X. Yang, "Translucent Optical WDM Networks for Next-generation Backbone Networks", Proceedings of IEEE GLOBECOM, New York, pp. 60-64, Nov. 2001.

[RAM-95] R. Ramaswami and K.N. Sivarajan, "Routing and Wavelength Assignment in All-Optical Networks", IEEE/ACM Transactions on Networking, Vol. 3, pp. 459-500, Oct. 1995.

[RAM-02] R. Ramaswami and K. N. Sivarajan, Optical Networks - A Practical Perspective, 2002.

[RAP-65] Y. Rapp, "Planning of Junction Network in a Multi-exchange Area", Ericsson Technics 1965, Vol. 2, pp. 187-240.

[SAB-98] R. Sabella, E. Iannone, M. Listanti, M. Berdusco and S. Binetti ,"Impact of Transmission Performance on Path Routing in All-Optical Transport Networks", IEEE Journal of Lightwave Technology, Vol.16, No. 11, pp. 1965-1972 Nov. 1998.

[SAR-02] E.H Sargent, "Multifunctional Photonic Integration for the Agile Optical Network", Internet Proceedings of 39th Design Automation Conference, 2002, pp.231 – 234, June 2002.

[SEN-02] S. Sengupta, D. Saha, and S. Chaudhuri, "Analysis of Enhanced OSPF for Routing Lightpaths in Optical Mesh Networks," in Proceedings of IEEE International Conference on Communications (ICC), New York, Vol. 5, pp. 2865–2869, Apr. 2002.

[SHE-99] Y.Shen, K. Lu and W. Gu, "Coherent and Incoherent and Incoherent Crosstalk in WDM Optical Networks", IEEE Journal of Lightwave Technology, Vol 17., No. 5, pp 759-764, May 1999.

[SHE-00] G. Shen, T. H. Cheng, S. K. Bose, Chao Lu, and T. Y. Chai, "The Impact of Number of Transceivers and their Tunabilities on WDM Network Performance," IEEE Communications Letters, Vol. 4, No. 11, pp. 366-368, Nov. 2000.

[SHE-03] G. Shen, S.K. Bose, T.H.C. Chao Lu and T.Y.Chai, "Impact of the Number of Add/drop Ports in Wavelength routed Optical Networks", SPIE Optical Networks Magazine, Vol. 10, pp. 112-122, Oct. 2003.

[SHE-06] S. Shen, G. Xiao, and T. H. Cheng, "A Novel Method of Link-State Update in Wavelength-Routed Networks," IEEE Journal of Lightwave Technology Vol. **24**, no. 3, pp. 1112-1120 March. 2006.

[SIM-99] J.M. Simmons, A.A. Saleh "The value of optical bypass in reducing router size in gigabit networks" Simmons, Proceedings of IEEE International Conference on Communications, Vancouver, Canada, pp. 591 – 596, June 1999

[SIM-05] Simmons,J.M. "On Determining the Optimal Optical Reach for a Long-haul Network" IEEE Journal of Lightwave Technology, Volume 23, No. 3, pp.1039-1048, March 2005.

[SOL-02] A. Solheim, "Agile Photonic Networking", World Markets Series: Global Optical Communications World Markets Whitepaper, July 2002.

[SOL-95] L.B. Soldano and E.C.M. Pennings, "Optical Multi-Mode Interference Devices Based on Selfimaging: Principles and Applications", IEEE Journal of Lightwave Technology, Vol. 13, June 1995, pp. 615-627.

[SRI-03] K.Sriram, D. Griffith, R. Su, and N. Golmie, "Static vs. Dynamic Regenerator Assignement in optical switches", Proceedings for Workshop on High Performance Switching and Routing (HPSR 2004), Phoenix, Arizona, April 8-21, 2004

[STA-99] A. Stavdas1, H. Avramopoulos1, E. N. Protonotarios1, J. E. Midwinter, "An OXC Architecture Suitable for High Density WDM Wavelength Routed Networks", Photonic Network Communications, Vol.1, pp.77-88, 1999.

[STR-01] J. Strand, A.L. Chiu and R. Tkach, "Issues for Routing in the Optical Layer", IEEE Communications Magazine, No. 2, pp. 81-87, February 2001.

[SUB-96] S. Subramaniam, M. Azizoglu and A. Somani, "Connectivity and Sparse wavelength Conversion in Wavelength-Routing Networks," Proceedings of IEEE INFOCOM, San Francisco, CA, pp. 148-155, March 1996.

[TES-98] Mitsuhiro Teshima, Takeshi Kawai, Norio Sakaida, Hiroshi Yasaka, Hiroyuki Ishii, and Masafumi Koga, "Virtual Wavelength Path Cross-Connect Based on Optoelectronic Wavelength Conversion" Journal of IEEE Lightwave Technology, Vol. 16, No. 9, Sept. 1998.

[TSA-04] J. C. Tsai, S. Huang, D. Hah, H. Toshiyoshi, and M. C. Wu, "Open-loop Operation of MEMS-based 1 × N Wavelength-selective Switch with Long

Term Stability and Repeatability," IEEE Photonics Technology Letters, Vol. 16, No. 4, pp. 1041–1043, Apr. 2004.

[TSA-06] J. C. Tsai, S. T. -Y. Huang, D. Hah, and M. C. Wu, "1 × N^2 Wavelength-Selective Switch With Two Cross-Scanning One-Axis Analog Micromirror Arrays in a 4-f Optical System," IEEE Journal of Lightwave Technology. Vol. 24, Issue 1, pp. 897- 903, Jan.2006.

[WAL-92] J.F.E. Wallin and B. Sanders, "The Calculation of Overflow Moments in Loss Systems with Selective Trunk Reservation," Performance Evaluation, Vol. 15, Issue 3 Sept. 1992.

[WAU-96] N. Wauters ad P. Demeester, "Is Wavelength Translation Required" Proceedings of IEEE International Conference on Communications (ICC 96), Workshop on WDM Network Management, Dallas, TX, June 1996.

[WAU-97] N. Wauters and P. Demeester, "Wavelength Translation in Optical Multi-wavelength Multi-fibre Transport Networks," International Journal of Optoelectronics, Vol. 11, No. 1, pp. 53-70, Jan. 1997.

[WOS-01] L. Wosinska, L. Thylen, and R. P. Holmstrom "Large-Capacity Strictly Nonblocking Optical Cross-Connects Based on Microelectrooptomechanical Systems (MEOMS) Switch Matrices: Reliability Performance Analysis" IEEE Journal of Lightwave Technology Vol. 19, No. 8, pp. 1065-1075, Aug. 2001.

[WOS-04] L. Wosinska, "Silica-on-silicon Technology for Photonic Integrated Devices" Proceedings of 2004 6th International Conference on Transparent Optical Networks, 2004. Vol. 2, pp-274 - 279 Vol.2 , July 2004.

[YAN-02] X. Yang and B. Ramamurthy, "Dynamic Routing in Translucent WDM Optical Networks," Proceedings of IEEE International Conference on Communications (ICC) 2002, New York, NY, pp. 2796-2802, Apr. 2002.

[YOU-99] J.Y. Youe and S. Seo, "An Algorithm for Virtual Topology Design in WDM Optical Networks under Physical Constraints", Proceedings of IEEE International Conference on Communications, Vancouver, Canada, pp.1234-5678, Jun. 1999.

[ZAN-00] H.Zang, J.P.Jue and B.Mukheriee, "A review of Routing and Wavelength Assignment Approaches for Wavelength-routed Optical WDM Networks", Optical Networks Magazine, Vol. 1, no. 1, Jan. 2000.

[ZAN-01] H.Zang, J. P. Jue, L. Sahasrabuddhe, R. Ramamurthy and B.Mukherjee, "Dynamic Lightpath Establishment in Wavelength-routed WDM Networks", IEEE Communications Magazine, pp.100-108, Sep 2001.

[ZAN-99] H. Zang, L. Sahasrabuddhe, J. P. Jue, S. Ramamurthy, and B. Mukherjee, "Connection Management for Wavelength-routed WDM networks", Proceedings IEEE GLOBECOM '99, Rio de Janeiro, Brazil, Vol. 2, pp.1428-1432, Dec 1999.

[ZHO-00] Y. Zho, G.N. Rouskas, H.G. Perros, "A Path Decomposition Algorithm for Computing Blocking Probabilities in Wavelength Routing Networks", IEEE/ACM Transactions of Networking, Vol. 8 pp. 747–762, Aug. 2000.